# DIPOLE EXCITATION
# AND
# FRAGMENTATION
# OF
# $H_2$, $HD$, $D_2$, and $CH_4$

## C. BACKX

# DIPOLE EXCITATION
# AND
# FRAGMENTATION
# OF
# $H_2$, HD, $D_2$, and $CH_4$

# DIPOLE EXCITATION
# AND
# FRAGMENTATION
# OF
# $H_2$, HD, $D_2$ and $CH_4$

PROEFSCHRIFT

TER VERKRIJGING VAN DE GRAAD VAN DOCTOR
IN DE WISKUNDE EN NATUURWETENSCHAPPEN
AAN DE RIJKSUNIVERSITEIT TE LEIDEN,
OP GEZAG VAN DE RECTOR MAGNIFICUS DR. A.E. COHEN,
HOOGLERAAR IN DE FACULTEIT DER LETTEREN,
VOLGENS BESLUIT VAN HET COLLEGE VAN DEKANEN
TE VERDEDIGEN OP WOENSDAG 12 NOVEMBER 1975
TE KLOKKE 16.15 UUR

door

# CORNELIS BACKX

geboren te Rotterdam in 1946

PROMOTOR:    Prof.Dr. J. Los

This work has been done under supervision of
Dr. M.J. van der Wiel

*Aan mijn ouders*

*Aan Wil, Merijn en Floris*

CONTENTS

# INTRODUCTION

## 1. GENERAL

Electron impact experiments are widely recognized as providing physical information that is complementary to that obtained by photon impact. Best known is the study of optically forbidden and electron exchange transitions. Perhaps less well known is the possibility of obtaining optical quantities, i.e. dipole oscillator strengths or spectral averages thereof, by means of electron impact. This possibility was pointed out already as early as 1930 by Bethe. The first experimental work to show this quantitative relation between photon and electron impact concerned a study of the energy dependence of total cross sections at high impact energy by Miller and Platzmann (1957). Later, more direct evidence came from differential scattering experiments, in which context the pioneering work of Lassettre and his group (1964) should be mentioned.

The ability of fast electron scattering experiments to produce optical data may be visualized as follows. When only electrons scattered over a small angle are detected, the observed processes are the result of distant collisions (i.e. large impact parameter). The target experiences the passage of an electron as an essentially uniform electric field sharply pulsed in time. The Fourier transform of such a δ-function like pulsed field will be a spectrum that is constant over a large range of frequencies of the electric field. This range will be larger when the velocity of the electron is higher. In other words the glancing collisions generate a spectrum of "white light" for the target. The probability for the absorption of a light quantum from this spectrum is proportional to the photoabsorption properties of the target, while the energy of the quantum absorbed is given by the energy loss of the scattered electron. The quantitative relation will be discussed in section 2 of this introduction.

The aim of the work described in this thesis is to get insight in the processes connected with the absorption of photons by molecules, making use of the optical characteristic of the scattering of fast electrons. By correlating (i.e. measuring in coincidence) the electron energy losses with the products of the energy transfer (e.g. ions, electrons, photons), a comprehensive picture of photon energy degradation in molecules emerges.

The various coincidence techniques developed for this purpose are indicated in section 3, in which also a parallel has been drawn between the electron impact coincidence measurements and the analogous photon experiments. The techniques described provide the gross spectral features of the optical oscillator strengths for the following processes:

- Absorption
- Ionization
- Ionization, partial with respect to the various ionic fragments
- Formation of threshold electrons (< 0.2 eV)
- Photofluorescence

The first chapter deals with a study of the He atom, which in the context of this thesis can be seen as a test case of the method used to extract optical quantities from electron scattering intensities. For this atom accurate calculations were available in literature with which the experimental results could be compared. An investigation of the molecules $H_2$, $D_2$ and HD is described in chapter IV and $CH_4$ in chapter II and III.

Apart from detailed information on continuum wave functions, the dipole oscillator strengths of these molecules give information on the following physical properties in particular:

- the existence of discrete states having an energy higher than the lowest ionization potential, so-called superexcited states (Platzman 1962). These states can decay by autoionization, dissociation or fluorescence. The last two decay routes give rise to final products that are neutral, the first process to ionic species. Evidence for the existence of superexcited states and their decay has been found for all molecules studied.

- The probability for ionization into the various electronic continua separately, which correspond to the different excited states of the ion. The various continua could be extracted from the measurements by assuming the validity of the Born-Oppenheimer approximation. In the case of $H_2$ and its isotopes information is obtained on the Franck-Condon factors for the formation of the molecular ion in its ground state.

## 2. DERIVATION OF OPTICAL QUANTITIES FROM ELECTRON IMPACT

When the projectile electrons have velocities far in excess of the velocities of the target electrons involved in the collision, the differential scattering cross section is given by the Bethe theory (1930, revised by Inokuti 1971):

$$\frac{d^2\sigma}{d\theta dE} = \frac{2}{E}\frac{k_n}{k_o}\frac{1}{K^2}\, f(K,E) \tag{1}$$

where E is the energy loss, $k_o$ and $k_n$ are the magnitudes of the incident and scattered momenta and K the magnitude of the momentum transfer. $f(K,E)$, the generalized oscillator strength is defined as,

$$f(K,E) = 2E\, \left| \frac{1}{K} < \psi_f \right|\, e^{i\vec{K}\vec{r}}\, \left| \psi_i > \right|^2 \tag{2}$$

When the operator $e^{iKr}$ is expanded in a power series of K at K=0, it is obvious that $f(K,E)$ tends to the dipole term $f^{(0)}(E)$ in the limit of $K \to 0$ and higher terms in the expansion,

$$f(K,E) = f^{(0)}(E) + f^{(1)}(E)K^2 + f^{(2)}(E)k^4 + \ldots \tag{3}$$

vanish. The dipole term $f^{(0)}(E)$ is a quantity directly proportional to the cross section for photoabsorption, $\sigma(E)$:

$$f^{(0)}(E) = 2E\, \left| <\psi_f |r| \psi_i > \right|^2 = \frac{mc}{\pi e^2 h}\, \sigma(E) \tag{4}$$

From the arguments given above it is clear that optical quantities can be obtained by making use of the characteristics of the scattering of fast electrons.

Experimentally, one has two alternatives for obtaining $f^{(0)}(E)$. The first is the measurements of $f(K,E)$ over a range of $K^2$ and extrapolation to $K^2 = 0$. This method was used by Lassettre et al. (1964) and by several other groups. The second alternative (see Van der Wiel 1973 for a review) makes use of the fact that although $K^2_{min.}$ (i.e. K at zero scattering angle) never vanishes, it can be made arbitrarily small by a proper choice of the experimental conditions. Since for small scattering angles the momentum transfer squared, $K^2$, is given by,

$$K^2 = 2E_o(\frac{E^2}{4E_o^2} + \theta^2) \qquad (5)$$

a large impact energy, $E_o$, and a small scattering angle, $\theta$, will be the proper conditions.

A combination of the two methods has been used in chapter I, in which the optical oscillator strength, $f^{(0)}(E)$, of He has been obtained with a systematic error due to the neglectance of higher terms in the expansion (eq.3) of less than .5%. Moreover a fair estimate could be obtained for the second term in eq. 3, $f^{(1)}(E)$. From this term it was concluded that $f(K,E)$ resulting from forward scattering intensities deviated less than 2% from the optical value $f^{(0)}(E)$. Since no general rule can be given as to the value of $K^2$ for which the dipole approximation is applicable (i.e. neglect of terms of a higher order than $f^{(0)}(E)$ in eq. 3) this procedure has been applied for the absorption oscillator strengths of the molecules investigated. The coincidence measurements were then performed using the second method, knowing that the contribution of higher order terms was small.

When integrating eq. 1 to obtain a total cross section, the relation with the optical oscillator strength is retained. The total cross section for e.g. ionization is then given by,

$$\sigma_i(E_o) = \frac{\ln c \, E_o}{E_o} \int_{I.P.}^{\infty} \frac{R}{E} \, \eta_i(E) \, f^{(0)}(E)dE,$$

where R is the Rydberg energy, c is a constant depending on terms of a higher order than $f^{(0)}(E)$ in eq. 3 and $\eta_i(E)$ is the photoionization efficiency, that is the probability that absorption of a photon results in ionization. This relation has been used in chapter III, to check the consistency of the ion mass spectra and the oscillator strength distribution of the ionic fragments of $CH_4$.

## 3. ELECTRON IMPACT COINCIDENCE EXPERIMENTS AND THEIR ANALOGY WITH PHOTON IMPACT

In figure 1 a parallel has been drawn between the electron impact coincidence experiments at small momentum transfer used in this thesis and photon impact.

1. In a photon impact experiment the oscillator strength for absorption is obtained by measuring the attenuation of a photon beam traversing a target gas as a function of wavelength. The analogous electron impact experiment consists of recording an energy loss spectrum at small momentum transfers of the scattered electrons. This spectrum is then converted to an oscillator strength spectrum in the way described in section 2.

2. In a photon impact experiment the oscillator strength for ionization is obtained by a measurement of the total number of ions or electrons created by the ionization processes. In the analogous electron impact experiments, the electrons ejected in the ionization process or the total number of ions formed are measured in coincidence with the scattered projectile electron. In order to do this an electric field was applied across the collision centre to extract the charged particles towards the detector.

3. The electron impact analogue of photoionization mass spectrometry consists of a measurement of the mass selected ions in coincidence with the energy loss selected electrons. Mass analysis was provided in two ways, by using a mass spectrometer or by a time of flight analysis of the ions from the collision centre to the detector. The last method had the advantage that in this mode of operation it was possible to design ion optics that were able to transport the ions to the detector independent of their recoil energy. This method of mass selection was therefore used for all measurements on ions resulting from dissociative processes.

4. By lowering the extraction field across the collision chamber it was possible to extract essentially only electrons with energies < 0.2 eV. A measurement of these electrons in coincidence with the scattered projectile electrons as a function of energy loss provided the ionization

| photon impact | electron impact equivalent (small K) |
|---|---|
| hν | e⁻ (E₀)  E' coincidence |
| photoabs. product | collision product |
| analysis | analysis |

| | |
|---|---|
| 1. photoabsorption | energy loss |
| 2. photoioniz. (total) | el - el coinc. (total) |
| 3 Photoioniz. mass. sp. | el - ion coinc. |
| 4. threshold photoel. sp. | threshold el - el coinc. |
| 5 photofluorescence | el - photon coinc. |

Fig. 1. A parallel between the electron impact coincidence experiments
at small momentum transfer used in this thesis and the
analogous photon impact experiments.

potentials and Franck Condon distributions of the various ionic
states of $CH_4$, the analogous photon impact experiment being threshold
photoelectron spectroscopy (Stockbauer and Inghram 1971).

5. The oscillator strength for photofluorescence is provided by a
measurement of photons emitted from the target in coincidence
with the electron energy loss. An interference filter selects
the wavelength of interest. Electron-photon coincidence measure-
ments are not included in this thesis, although electron-ion-
photon triple coincidence measurements have been performed in
the course of the research (Backx et al. 1973).

REFERENCES

- C. Backx, M. Klewer and M.J. Van der Wiel, 1973, Chem.Phys. Letters
  20 100.
- H. Bethe, 1930, Ann.Physik 5 325.
- M. Inokuti, 1971, Rev.Mod.Phys. 43 297.
- E.N. Lassettre and co-workers, 1964, J.Chem.Phys. 40 1208-1275.
- W.F. Miller and R.L. Platzman, 1957, Proc.Phys.Soc. (London) 70 299.
- R.L. Platzman, 1962, The Vortex, Vol. XXII 8.
- R. Stockbauer and M.G. Inghram, 1971, J.Chem.Phys. 54 2242.
- M.J. Van der Wiel, 1973, The Physics of Electronic and Atomic Collisions
  Invited lectures and Progress Reports, VIII ICPEAC (Beograd) Edts.
  B.C. Cobić and M.V. Kurepa, 417.

<p align="center">C H A P T E R   I</p>

# DIPOLE TERM AND FIRST DERIVATIVE AT K = 0 OF THE GENERALIZED OSCILLATOR STRENGTH OF He BY keV ELECTRON IMPACT

C. Backx, R.R. Tol, G.R. Wight and M.J. Van der Wiel

*An approximate method is described for obtaining the derivative to $K^2$ of the generalized oscillator strength for keV electron scattering at zero momentum transfer, over a large range of energy losses. The measured data enable us to reduce the systematical uncertainty in the derivation of optical oscillator strengths to below 1% level. Results are presented for He over the spectral range of 19 to 65 eV. The data for the derivative are in satisfactory agreement with earlier electron scattering results at lower impact energy and extend over a sufficient range to allow the application of a sum rule for this term of the generalized oscillator strength.*

## 1. INTRODUCTION

In a series of papers over the last few years (for a review see Backx and Van der Wiel 1974) we have reported optical oscillator strengths derived from inelastic electron scattering intensities at small momentum transfers. The procedure was to convert measured scattering intensities into generalized oscillator strengths, f(K,E), by the use of Bethe theory for the scattering of high energy electrons (Bethe 1930). The impact energy and collision geometry were chosen such that at all values of the energy transfer, E, the momentum transfer, K, was small, and therefore higher terms in the expansion of f(K,E) at K = 0 (Inokuti and Platzman 1965):

$$f(K,E) = \sum_{\lambda=0}^{\infty} \frac{K^{2\lambda}}{\lambda!} f^{(\lambda)}(E) \tag{1}$$

were neglected. The generalized oscillator strength was then directly

approximated by the dipole oscillator strength. The magnitude
of the systematic error made in neglecting multipole terms could be
estimated only for H and He (Van der Wiel and Wiebes 1971 a) to be
of the order of at most 10%, using other sources (Inokuti 1966;
Silverman and Lassettre 1964). For other systems no information
was available except from spot checks of the angular behaviour of
$\sigma(K,E)$, which invariably showed that the multipole contribution did
not exceed the statistical uncertainty. We have recently improved
the experimental arrangement used in our previous work (Van der Wiel
and Wiebes 1971 b). The statistical uncertainty of the data has now
been reduced to such and extent, that in addition to accurate dipole
measurements, it has also become feasible to make routine determina-
tion of the contribution from multipole terms to the scattered
intensity.

## 2.  APPARATUS

A simplified scheme of the apparatus is given in fig. 1. In
principle the apparatus is the same as that described in earlier
publications (Van der Wiel and Wiebes 1971 b; Backx et al. 1973)
and therefore only essential changes will be discussed.

The gas jet with its poorly defined distribution of target
gas was replaced by a short collision chamber, which improved
the ratio of scattering inside and outside the actual scattering
region by a factor of twenty. This diminishes the number of
accidental coincidences by the same factor. Moreover, a coincidence
measurement of the projectile electron and a collision product
(e.g. an ion) is no longer required in order to define the actual
collision volume and therefore we are able to determine oscillator
strengths also for absorption.

A voltage is applied across the collision chamber to extract
ions (or ejected electrons). In order to maintain a homogeneous
field in as short a collision chamber as possible, fringe field
problems were minimized by covering the walls of the collision
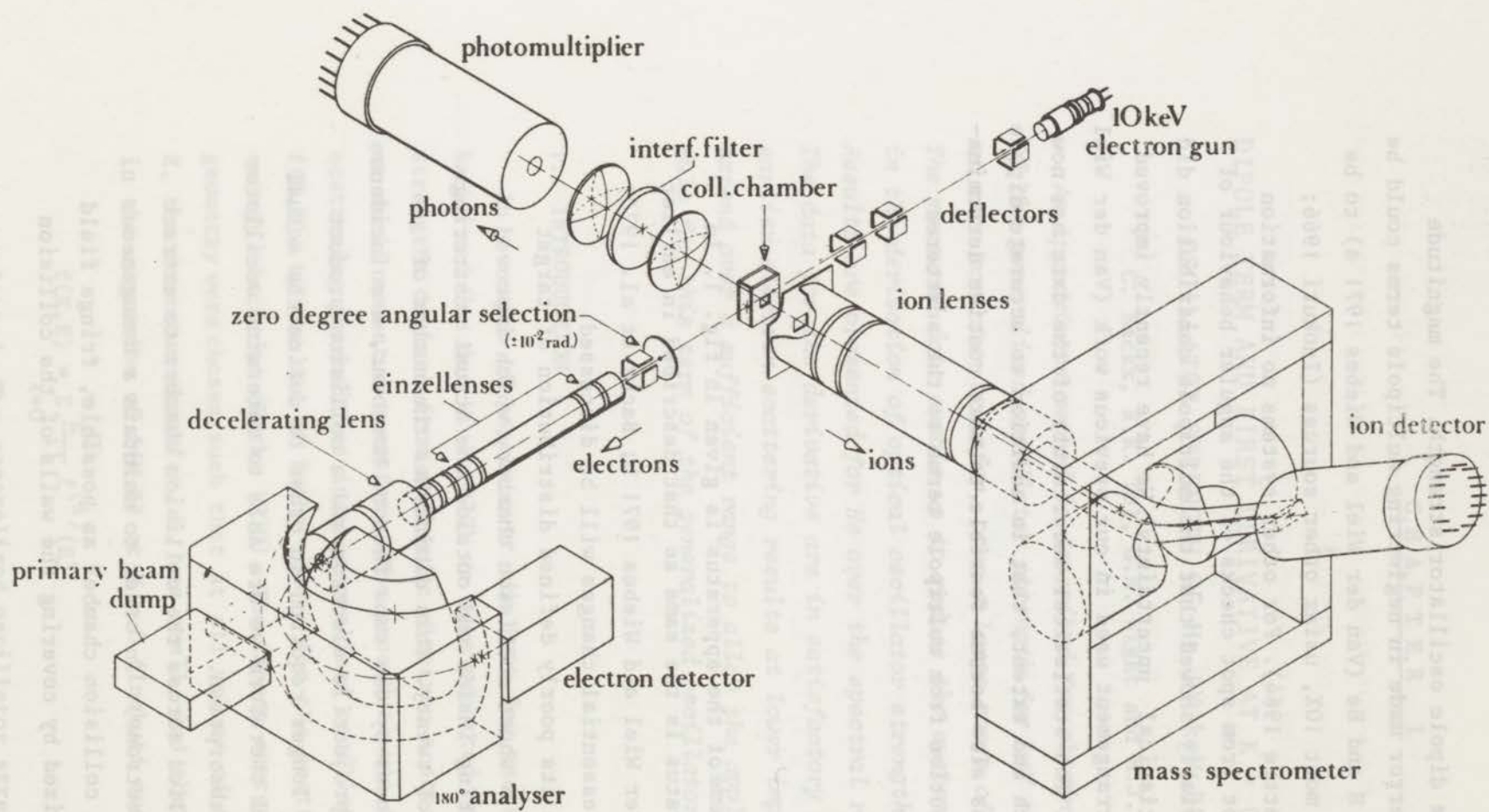
**ELECTRON-ION-PHOTON COINCIDENCE EXPERIMENT**

1. - Schematic diagram of the apparatus.

chamber parallel to the field direction with resistance material[*].
The improvements of the ion extraction system are not essential
here and will be discussed in a subsequent article. The solid angle,
accepted by the scattered electron channel was increased from
$2 \times 10^{-5}$ to $1.4 \times 10^{-4}$ sterad (an aperture of 1 mm diam. at a
distance of 75 mm from the interaction region). The first lens in
the scattered electron channel is an einzel lens, which makes an
image of the collision chamber at a second einzel lens, which can
be any of the four cylinders in front of the decelerating lens.
This feature of having a moveable field lens makes it possible to
vary the final magnification at the entrance of the analyzer; the
focal power of the field lens can be adjusted such that the beam
angle is zero after deceleration. The potentials of the einzel
lenses are referenced with respect to the mean potential of the
energy analyzer, such that the focal properties of the lens system
are constant over the entire energy loss spectrum. The change in
voltage ratio across the decelerating lens is small and has a
negligible effect on the focal properties over the energy loss
range.

In view of the increased opening angle, we now use a hemispherical
electrostatic analyzer (radius 6 cm, gap 2 cm). The electron
multiplier is operated at a constant impact energy and a constant
voltage across the multiplier at all energy losses.

For an accurate measurement of the scattering intensity it is
essential that electrons scattered into the angular selection
aperture are transmitted completely, independent of where they
enter it. This is tested in the following way: we adjust the
energy loss selector to transmit the primary beam, which is then

f$^{(0)}$(E) (eV$^{-1}$)

energy loss (eV)
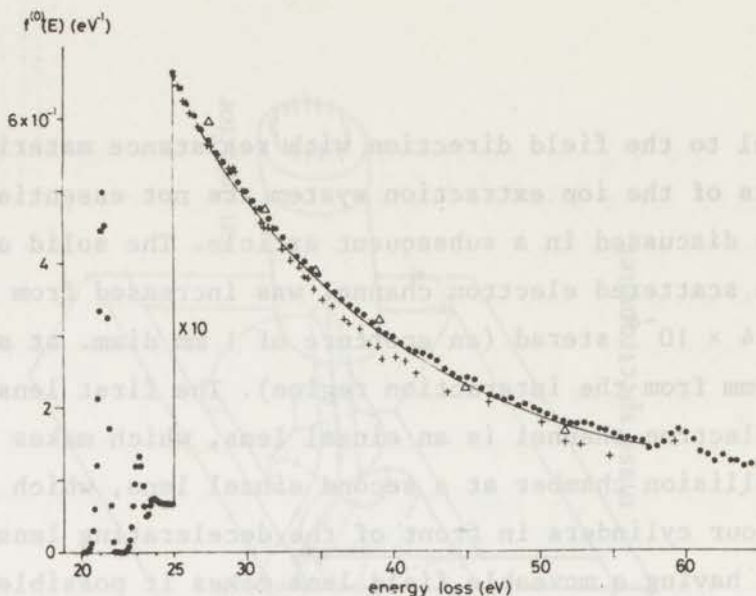
2. – Optical oscillator strengths of He. ● – This work (normalized on the 1s-2p transition, see 4); + – Samson (1966), photoabsorption; Δ – Lowry et al. (1965), photoabsorption; —— – Burke and McVicar (1965), dipole length approximation.



f$^{(1)}$(E) (eV$^{-1}$)

energy loss (eV)
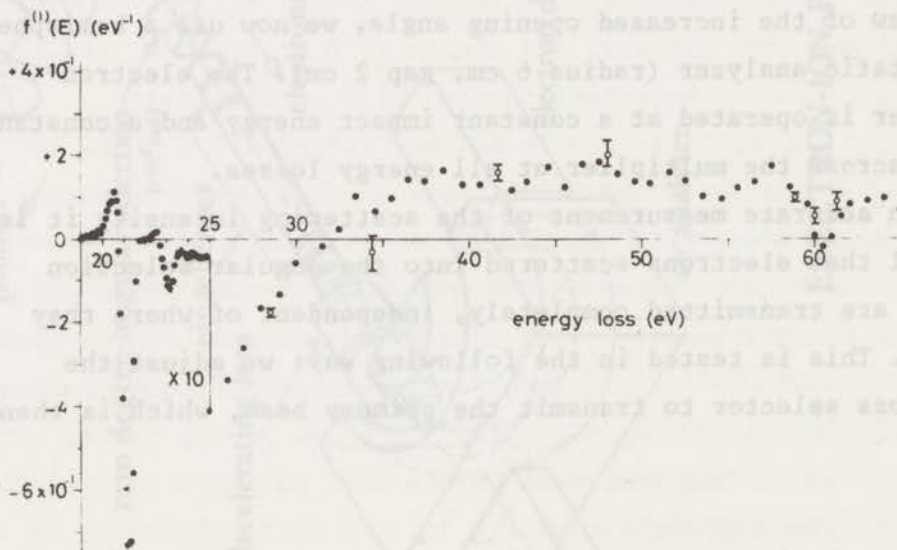
3. – Derivative to K$^2$ (a.u.) of the generalized oscillator strength at K = 0. ● – This work; φ – From an extrapolation of data by Silverman and Lassettre (1964).

measured as a DC current on the first dynode of the electron multiplier.
We observe a constant signal, when scanning the primary beam (cross
section 0.2 mm) over the entire area of the angular aperture. A slot
(4 mm wide and extending over $90^{\circ}$) was made in the backsphere of
the energy loss analyzer in order to prevent the primary beam from
colliding with the backsphere. This makes it possible to measure
at zero degree scattering angle and results in an increased signal
at smaller momentum transfers then in our previous experiments.

## 3. PROCEDURE OF ANALYSIS

We restrict ourselves to a range of small momentum transfers, such
that one can reasonably approximate $f(K,E)$ by $f^{(0)} + K^2 f^{(1)}$ (see
eq. 1). The object is to obtain increased accuracy for the dipole
term $f^{(0)}$ and a quite reasonable approximation of the first
derivative at $K = 0$, $f^{(1)}$.

In order to limit the amount of data that have to be taken, and
being interested in only two terms of $f(K,E)$, we have adopted the
procedure to record energy loss spectra (if required in coincidence
with ions, ejected electrons or photons) at only two angles, i.e.
at two different ranges of momentum transfers. Taking only the
first two terms of the expansion of $f(K,E)$, we can write for the
differential scattering cross section, $\sigma(K,E)$ (Bethe 1930):

$$\sigma(K,E) = \frac{2}{E} \frac{k_n}{k_0} \{\frac{1}{K^2} f^{(0)}(E) + f^{(1)}(E)\} \qquad \text{(a.u.)} \qquad (2)$$

where $k_0$ and $k_n$ are the magnitudes of the momenta of the projectile
electron before and after the collision respectively. The two
quantities $f^{(0)}(E)$ and $f^{(1)}(E)$ are derived from the scattering inten-
sities as follows:

$$I_{sc}(\theta,E) = \int_{\Omega} \sigma(K,E)d\Omega = \frac{2}{E} \frac{k_n}{k_0} \left[ f^{(0)}(E) \int_{\Omega} \frac{1}{K^2(\theta,E)} d\Omega + f^{(1)}(E)\Delta\Omega \right] \qquad (3)$$

where the integration of $1/K^2$ is made over the cross section of the
electron beam and the angular selection aperture (see Appendix).

TABLE I

Dipole oscillator strengths, $f_n^{(0)}$, and the first derivative of the generalized oscillator strengths at K = 0, $f_n^{(1)}$, for discrete transitions in He.

| State | $f_n^{(0)}$ | | $f_n^{(1)}$ | | |
| --- | --- | --- | --- | --- | --- |
| | Theory | This work | Theory | This work | Expected value[*] |
| $2^1S$ | – | – | +0.0836[b] | +0.070 | +0.062[b] |
| $2^1P$ | 0.27616[a] | (0.276)[+] | −0.4502[b] | −0.36 | −0.37[b] |
| $3^1P$ | 0.0734[a] | 0.073 | −0.0925[b] | −0.078 | +0.081[b] |
| I.P. $\sum\limits_o f_n^{(0)}$ | 0.427[c] | 0.421 | – | – | – |

a: Schiff and Pekeris (1964)

b: Kim and Inokuti (1968)

c: Bell and Kingston (1967); Pekeris (1959); Schiff and Pekeris (1964)

* The expected result of our analysis, when using in our straight-line approximation of f(K,E) the values of Kim and Inokuti at the same two average momentum transfers as in the experiment.

+ By normalization

A measurement of $I_{sc}(\theta,E)$ at two angles leads to a solution of the
two unknowns $f^{(0)}(E)$ and $f^{(1)}(E)$ in eq. 3 on the same relative
scale. Spectra recorded at two angles are normalized on each other
by means of an accurate determination of the scattering intensity
ratio at one energy. The angular ranges chosen are $0 < \theta_1 < 6.6 * 10^{-3}$
("forward" scattering) and $13.3 < \theta_2 < 26.7 * 10^{-3}$. At $\theta_2$, $\overline{K^2}$ is
larger by a factor of 20 to 40 (depending on E) than $\overline{K^2}$ at $\theta_1$,
such that $f^{(1)}(E)$ contributes about 10% to the scattering intensity
at $\theta_2$ at an energy loss of 40 eV.

## 4. RESULTS

### 4.1 Dipole Oscillator Strengths

Using the procedure described in 3, we obtained results for the
optical oscillator strengths, $f^{(0)}(E)$, of He for energy losses from
19 to 65 eV. In the 19-30 eV region energy loss spectra were recorded
with a resolution of 0.5 eV and steps of 0.1 eV. From 26-65 eV, the
scattered electrons were measured (resolution 1 eV) in coincidence
with the He$^+$ ions extracted from the collision chamber. The oscillator
strength distribution is normalized on a value of 0.276 for the
1s → 2p transition (Schiff and Pekeris 1964). A three-point average
of the measurements is given in fig. 2. The data of the ionization
continuum are listed in Table II. The systematic error due
to higher terms of the multipole expansion is estimated to be smaller
than 0.3%; this estimate is based on the accuracy, with which $f^{(1)}(E)$
is determined (see 4.2). The largest contribution of $f^{(1)}(E)$ to
$f(K,E)$ amounts to 1.5% for a zero degree spectrum. In fig. 2 we
have also plotted the experimental results of Samson (1966) and
Lowry et al. (1965). Samson's data agree to within 1% with our
results up to 30 eV. However, above 30 eV Samson's results become
progressively lower than ours and there is a 10% discrepancy with
our data at 55 eV. We do not expect that our data contain a systematic
deviation of such magnitude, since this would lead to a considerable
error in the $f^{(1)}(E)$ results. In section 4.2 we present evidence

## TABLE II

### Optical Oscillator Strengths of Helium ($10^{-2}$ $eV^{-1}$)

| E(eV) | $f^{(0)}(E)$ | E(eV) | $f^{(0)}(E)$ | E(eV) | $f^{(0)}(E)$ |
|-------|--------------|-------|--------------|-------|--------------|
| 25    | 6.61         | 39    | 3.08         | 53    | 1.77         |
| 26    | 6.22         | 40    | 2.98         | 54    | 1.71         |
| 27    | 5.84         | 41    | 2.81         | 55    | 1.62         |
| 28    | 5.53         | 42    | 2.75         | 56    | 1.56         |
| 29    | 5.25         | 43    | 2.63         | 57    | 1.52         |
| 30    | 4.98         | 44    | 2.44         | 58    | 1.44         |
| 31    | 4.76         | 45    | 2.40         | 59    | 1.62         |
| 32    | 4.55         | 46    | 2.25         | 60    | 1.65         |
| 33    | 4.23         | 47    | 2.15         | 61    | 1.36         |
| 34    | 4.02         | 48    | 2.11         | 62    | 1.26         |
| 35    | 3.85         | 49    | 2.05         | 63    | 1.23         |
| 36    | 3.60         | 50    | 1.93         | 64    | 1.17         |
| 37    | 3.42         | 51    | 1.84         | 65    | 1.17         |
| 38    | 3.29         | 52    | 1.77         |       |              |

that the $f^{(1)}(E)$ obtained in this work, agree quite satisfactory
with earlier measurements and with calculated values.

We compared our results with calculations of oscillator strengths
for the discrete transitions (see Table I). There is good agreement
both for the 1s → 3p excitation and for the entire discrete part of
the spectrum. The theoretical value for the discrete spectrum,
evaluated by Bell and Kingston (1967) from calculations of Pekeris
(1959) and Schiff and Pekeris (1964), amounts to 0.427, while our
results yield a value of 0.421. The calculations of Burke and McVicar
(1965) (the dipole velocity and length approximations differ less
than 3% over the whole energy range) are in excellent agreement with
our oscillator strength spectrum.

Finally, we tested our results with the Thomas-Reiche-Kuhn (Inokuti
1971) sum rule, i.e. $\int_0^\infty f^{(0)}(E)dE = 2$ for He. The integral of our spectrum
from 19 to 65 eV is equal to 1.60. The contribution of the integral from
65 eV to infinity is 0.46 on the basis of the calculation of Bell and
Kingston (1967). The total spectrum then yields a value of 2.06, i.e.
only 3% higher than the exact value of 2.

## 4.2 *Derivative of f(K,E) at K = 0*

Figure 3 shows the absolute $f^{(1)}(E)$ (based on the same normalization
as $f^{(0)}(E)$) as obtained through the procedure described in section 3
and compares it with earlier work of Silverman and Lassettre (1964).
They measured $f(K,E)$ as a function of $K^2$, at a number of continuum
energy losses, down to values of $K^2$ of the order of 0.1 a.u.$^2$. By
extrapolating their data to $K^2$ equal to zero, we were able to estimate
the derivative of $f(K,E)$. There is good agreement between the two
sets of data over the whole continuum. The data point of Silverman
and Lassettre at 34.5 eV, which is the only one to deviate signifi-
cantly from our curve, is slightly uncertain, as the extrapolated
$f(K,E)$ at this energy is the only one to show an appreciable discre-
pancy with the optical value. For the three discrete transitions
which can be separated with our resolving power of 0.5 eV, results

for $f^{(1)}(E)$ are given in Table I, and compared with the calculated values of Kim and Inokuti (1968). The last column of Table I lists the expected experimental value, when using a linear approximation of $f(K,E)$ (Kim and Inikuti) over our experimental K range, i.e. the same approximation as made in section 3. From the agreement between the last two columns of this table it can be concluded, that the relatively small (< 20%) deviation between theory (third data column) and the experimental values presented here, does arise from terms in $f(K,E)$ higher than $f^{(1)}(E)$. As regards the continuum, the $f(K,E)$ data of Silverman and Lassettre lack the accuracy to derive more than an average derivative at small K.

Since our measuring technique permits a determination of $f^{(1)}(E)$ over a wide and continuous energy range, it is interesting to check the validity of the data against the contraints given by the sum rule for $f(K,E)$ (Inokuti 1971):

$$\int_0^\infty \frac{d}{dK^2} f(K,E)dE = 0 \text{ at any fixed K.}$$

We are now in a position to apply this sum rule at $K = 0$. i.e.

$$\int_0^\infty f^{(1)}(E)dE = 0 \tag{4}$$

This integral over the region shown in figure 3, including the discrete region (in which, due to the limited resolution, we derive an average value of $f^{(1)}(E)$ over the discrete states above 22 eV) yields a value of $-0.134$, which should be compared with the analogous integration of $|f^{(1)}(E)|$, having a value of 1.03. Our result for the energy range up to 65 eV is quite satisfactory already; it is still slightly negative, since the part of the spectrum beyond 65 eV (which contains 25% of the optical oscillator strength) can be expected to yield a positive contribution.

It appears that the 2s 2p resonance at 60 eV, well-known from optical spectra (Madden and Codling 1965), has a pronounced effect on $f^{(1)}(E)$; the value even changes sign at the peak of the resonance.

## 5. CONCLUSION

It has been shown that by measuring the scattering intensities of fast electrons at two different, small (average) momentum transfers it is possible to obtain highly accurate optical oscillator strengths and a reasonable approximation of the first derivative of the generalized oscillator strength at K = 0. The systematic error in $f^{(0)}(E)$ and $f^{(1)}(E)$ due to contributions from multipole terms in $f(K,E)$ are estimated for He to be at most 0.3% and 20% for the two quantities respectively. Our $f^{(0)}(E)$ are the first experimental data with which reliable calculations show an extremely good agreement. Our data on $f^{(1)}(E)$ are in good agreement with values that can be derived from earlier work by Silverman and Lassettre. Moreover, our method produces $f^{(1)}(E)$ over such a large continuous range that the first time the sum rule for the first derivative of the generalized oscillator strength could be applied.

APPENDIX

$K^2$ is approximated by $2E_o\left[\frac{1}{4}(\frac{E}{E_o})^2 + \theta^2\right]$, where $E_o$ is the primary energy and $\theta$ the scattering angle. The integration of $1/K^2$ over the angular selection aperture for any arbitrary point in the collision volume can be done analytically. The integration over

the scattering length and the electron beam cross section is performed numerically. Note that it is not necessary to assume that the electron beam is parallel; only its diameter at the aperture has to be known. The diameter is determined from a scan of the beam across the known diameter of the angular selection aperture, and is found to be 0.2 mm. The scattering length is taken as 12 mm for the absorption measurements (the length of the collision chamber) and as 5 mm (the extraction length) for the coincidence measurements. The difference in length has a negligible effect on the dependence of the integral on E.

## REFERENCES

- C. Backx and M.J. Van der Wiel, 1974 Proceedings of the IV International Conference on Vacuum Ultraviolet Radiation Physics, Hamburg, Eds. E.E. Koch, R.H. Haensel and C. Kunz, p. 137.
- C. Backx, M. Klewer and M.J. Van der Wiel, 1973, Chem.Phys.Letters 20 100.
- K.L. Bell and A.E. Kingston, 1967, Proc.Phys.Soc. 90 31.
- H. Bethe, 1930, Ann.Physik, 5 325.
- P.G. Burke and D.D. McVicar, 1965, Proc.Phys.Soc., 86 989.
- M. Inokuti and R.L. Platzman, 1965, Proceedings of IV ICPEAC (Science Bookcrafters, New York), p. 408.
- M. Inokuti, 1966, Argonne Nat. Labor., Report 7220.
- M. Inokuti, 1971, Rev.Mod.Phys., 43 297.
- Y.K. Kim and M. Inokuti, 1968, Phys.Rev. 175 176.
- J.F. Lowry, D.H. Tomboulian and D.L. Ederer, 1965, Phys.Rev. 137 A 1054.
- R.P. Madden and K. Codling, 1965, Astrophys.J. 141 364.
- C.R. Pekeris, 1959, Phys.Rev., 115 1216.
- J.A.R. Samson, 1966, Adv. in Atomic and Molec. Physics, Vol. 2, Academic Press, New York, 177.
- B. Schiff and C.L. Pekeris, 1964, Phys.Rev. 134A 638.
- S.M. Silverman and E.N. Lassettre, 1964, J.Chem.Phys., 40 1265.
- M.J. Van der Wiel and G. Wiebes, 1971 a, Physica, 54 411.
- M.J. Van der Wiel and G. Wiebes, 1971 b, Physica, 53 225.

# C H A P T E R   II

# ELECTRON-ELECTRON COINCIDENCE MEASUREMENTS FOR $CH_4$

## C. Backx, G.R. Wight, R.R. Tol and M.J. Van der Wiel

*We report a measurement of fast electron scattering in $CH_4$ at low momentum transfers, in coincidene with the ejected electrons. A complete collection is made of ionization electrons ejected over the entire solid angle with kinetic energies up to 20 eV and a novel method has been developed for testing the transmission of the extraction system as a function of the initial kinetic energy of the electrons. The results are presented as optical data, i.e. relative dipole oscillator strengths for absorption (0 to 90 eV) and ionization (I.P. up to 27.5 eV) and the absolute photoionization efficiency. In order to extract optical data from the electron scattering intensities, we measured the scattering at two average momentum transfers (K) and extrapolated to K = 0. The contribution of non-dipole terms to the generalized oscillator strength is presented as an average derivative over our momentum transfer range. The absorption results have been normalized to earlier absolute measurements. Our ionization efficiency is in good agreement with earlier work, which was limited to energy transfers of up to 22 eV.*

*We have also made coincidence measurements of energy loss electrons and essentially zero energy ejected electrons. These threshold electron data show the existence of a third (two-electron) excited ion state at 29 eV, in addition to the two one-electron states of $CH_4^+$, and give the relative intensities of the threshold oscillator strengths of the three states.*

## 1. INTRODUCTION

The electron energy loss method, at high impact energy and small momentum transfers, has been used to obtain results equivalent to that of photoabsorption (i.e. the oscillator strength for absorption), while the oscillator strength for ionization was obtained by measuring either the ejected electrons or the ions formed in coincidence with the scattered projectile electrons. Earlier measurements on the noble gases, $N_2$, CO, $NH_3$ (for a review see Van der Wiel 1973) and $H_2O$ (Branton and Brion 1974) have demonstrated the capability of this method to produce optical data. The systematic error in these earlier measurements, due to terms higher than the dipole term in the expansion of the generalized oscillator strength (GOS) around K = 0. was estimated to be at most 10%.

Recently, our experimental set-up was considerably improved (Backx et al 1975). The resulting improvement in counting statistics allows us to record such accurate spectra at two scattering angles $(\overline{\theta}_1 = 0, \overline{\theta}_2 = 2 \times 10^{-2}$ rad), that in addition to the dipole term, also the derivative of the GOS w.r.t. $K^2$ can be determined over a large spectral range. (The method and its application to He has been recently described by Backx et al. 1975). Therefore, the systematic error in the extraction of the dipole term due to higher multipoles is now reduced to the much smaller effect of the uncertainty in the derivative of the GOS at K = 0. The derivative may also be of use for other experimentalists to check the validity of their procedure of extracting optical data from electron scattering intensities at small momentum transfers. The electron-electron coincidence measurements were performed by extracting the ionization electrons with a high extraction field, without energy analysis, and detecting them in coincidence with the energy loss electrons. A somewhat similar experiment, but without an extraction field and having energy analysis of the electrons ejected at $90^{\circ}$, was reported earlier (Van der Wiel and Brion, 1973 a and b). In our arrangement, it is possible to extract electrons ejected over the entire solid angle having kinetic energy up to 20 eV. Therefore changes in the anisotropy of ejected electrons do not affect our measurements up to 20 eV above the

lowest ionization threshold. By this method an accurate photoionization efficiency curve has been obtained, with an energy resolution of 0.5 eV over a continuous energy range from the I.P. up to 27 eV energy loss.

We have also been able to lower the extraction field to such an extent, that essentially only zero energy electrons contribute to the coincidence signal. This leads to the equivalent of threshold photo-electron spectroscopy (Stockbauer and Inghram 1971).

## 2. EXPERIMENTAL

### 2.1 *Apparatus*

With the exception of the extraction system, the apparatus has already been described in a previous publication (Backx et al. 1975). Briefly, the inelastic scattering of 4-8 keV electrons in a target gas is observed at small angle (see figure 1). Detection is made in coincidence with the ions or electrons ejected in the collision. For the measurement of the oscillator strength for total ionization it was essential to make a total collection of all electrons ejected from the target, even those with considerable kinetic energy (and also of dissociation fragments, see subsequent paper on electron-ion coincidence). This was achieved by extracting particles from the target with a homogeneous field of 400 V/cm across the collision chamber (see figure 2). Perpendicular to the electron beam, the height of the extraction slit is such, that particles with 'transverse' energies up to 20 eV are transmitted completely. In the direction of the electron beam no discrimination can take place because the interaction region is **sufficiently** longer than the slit width. The homogeneous extraction field is immediately followed by a lens system, consisting of an immersion lens followed by an einzel lens (forming a flight tube) for a proper transport of the particles to the detector. The length of the tube is such that when ions are extracted, time-of-flight analysis can be performed with a mass resolving power of 50, by measuring the ions in coincidence with the scattered projectile electron (see subsequent paper on electron-ion coincidence). For the case of a complete collection of the ejected electrons having
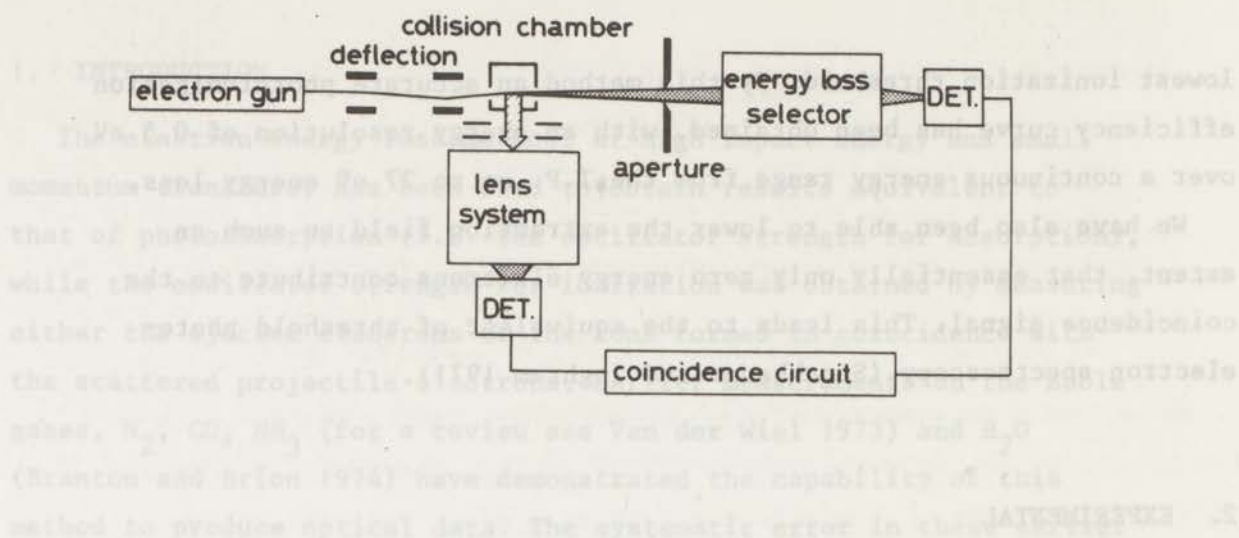
Fig. 1 - Schematic diagram of the electron-electron and electron-ion
coincidence apparatus. The aperture has a diameter of 1 mm
at a distance of 75 mm from the collision chamber. The lens
system is shown in more detail in figure 2.
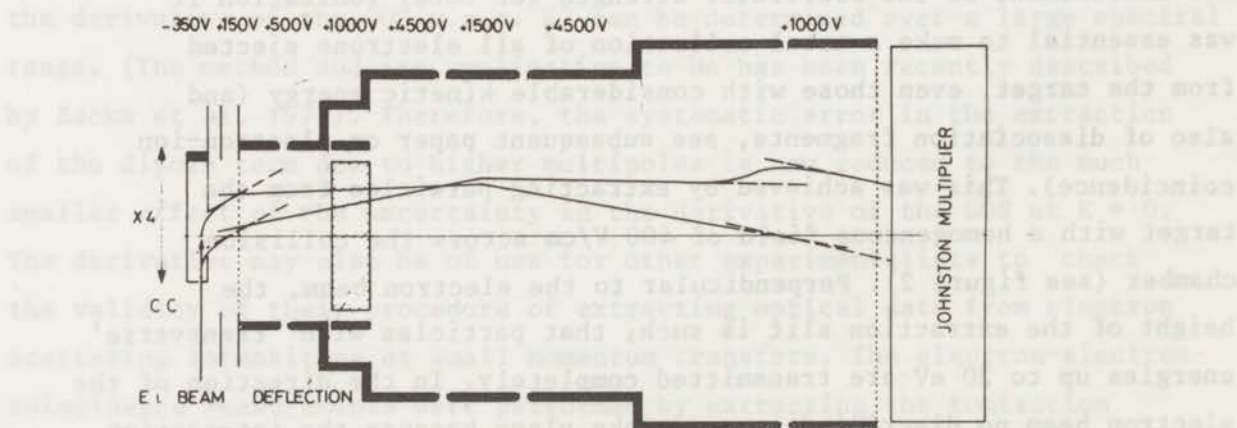


Fig. 2 - Cross section of extraction system (vertical scale multiplied
by a factor of four; length = 50 cm). The interaction region
has been drawn in two planes: through the electron beam
(below the axis) and perpendicular to it (above the axis).
Beyond the first grid the system consists of cylinders.
Extreme trajectories of particles with initial kinetic energy
of 20 eV are shown in the two planes. The voltages refer to
electron extraction in the case of a total ionization measure-
ment.

kinetic energies < 20 eV, the voltages applied to the lenses are given in figure 2. The trajectories shown in this figure have been contructed using first-order lens parameters (Read et al. 1971; Adams and Read 1972).

In the measurement of threshold electrons all voltages are lowered by a factor of 1000, which results in a high transmission for very low energy electrons (< 0.2 eV) and a rapidly decreasing transmission for electrons having higher energies.

## 2.2 *Test of extraction system*

In our instrument, the possibility of measuring either ions or ejected electrons in coincidence with scattered projectile electrons enables us to test the transmission differentially as a function of the 'transverse' energy with respect to the direction of extraction. We used electron ejection from the He atom as a source of charged particles of variable energy. Their energy $\varepsilon$ is selected by measuring these electrons in coincidence with the energy loss E, since $\varepsilon = E - I.P.$ As a standard for complete transmission we used the He$^+$ ions which have only thermal kinetic energies. The actual procedure is:
- Firstly we extract the He$^+$ ions formed by 4 keV electron impact and make a relative measurement of the number of electron-ion coincidences as a function of the energy loss at zero degree scattering angle. In this measurement no change of transmission can take place for He$^+$ coincident with different energy losses. From this measurement we obtain a relative differential cross section, $\sigma(\theta,E)$, for ionization of He for energy transfers from the I.P. up to 60 eV.
- Secondly we extract the ejected electrons by reversal of the extraction field and the lens voltages and make a relative measurement of the number of electron-electron coincidences as a function of energy loss from the I.P. up to 60 eV. In this measurement the transmission of the extraction system may change with the energy of the ejected electron. Thus we obtain a relative differential cross section for ionization times the
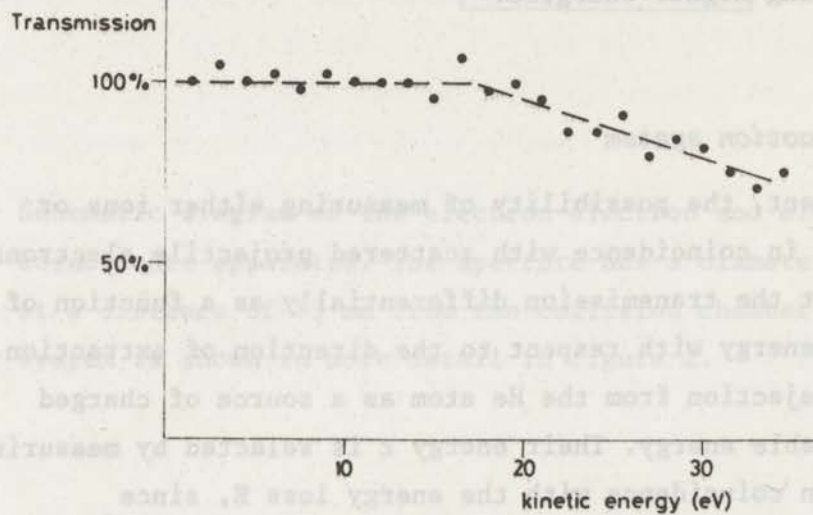
Fig. 3 - Transmission of extracted particles as a function of initial kinetic energy, obtained by the method described in section 2.2.

transmission function, $\sigma(\theta,E) \times T (E-I.P.)$.

The ratio of these two measurements, normalized to 100% close above threshold, provides the transmission function. From figure 3 it is evident that the transmission is 100% for kinetic energies up to 20 eV and slowly decreases for higher energies.

## 3. MODES OF OPERATION AND ANALYSIS

The apparatus has been used for the determination of four different quantities: The relative dipole oscillator strength for absorption, the derivative of the generalized oscillator strength at $K = 0$ on the same relative scale, the absolute ionization efficiency and the relative oscillator strength for the formation of zero energy electrons.

In the determination of the relative oscillator strength for absorption and the first derivative of the generalized oscillator strength at $K = 0$ we followed the procedure described by Backx et al. (1975). Briefly, the scattered intensity of 8 keV electrons is measured at two different angles, i.e. (average) momentum transfers ($\bar{K}$). We than approximate the GOS by the dipole term plus a second term proportional to $K^2$. This enables us to derive the relative dipole oscillator strength spectrum, while the second term gives a fair estimate of the derivative w.r.t. $K^2$ of the generalized oscillator strength, $f^{(1)}(E)$, at $K = 0$.

The relative oscillator strength for ionization was obtained by measuring the ejected electrons in coincidence with the scattered projectiles in the way described in 2.1. In order to diminish the amount of data taking, the contribution from non-dipole terms was neglected and only a zero angle scan was made. It is known from the absorption measurements (section 4.1) that this contribution is smaller than 1% for an electron impact energy of 4 keV. Therefore the generalized oscillator strength obtained from forward scattering intensities was taken equal to the dipole oscillator strength.

The absolute ionization efficiency is determined as follows. The ratio $F(E)$ of the electron-electron coincidence signal $I_{coinc.}(E)$ and the energy loss signal $I_{sc}(E)$,

$$F(E) = I_{coinc.}(E)/I_{sc}(E) \tag{1}$$

contains the ionization efficiency in the following fashion:

$$F(E) = \eta_i(E) \times \text{App}(E).$$

App $(E)$ is an apparatus function which takes into account the difference in scattering length in the two modes of operation (energy loss and coincidence) and the detection efficiency of the ejected electron detector. App $(E)$ can be obtained using He, since for an atom $\eta_i(E)$ equals unity above the first ionization potential.

To avoid a possible change of the detection efficiency of the ejected electron detector when changing the target gas from $CH_4$ to He, we measured the energy loss and coincidence spectra of a mixture of $CH_4$ and He from 10 - 27.5 eV. In these two spectra the He contributions (for which we know $\eta_i(E) = 1$) give us the apparatus function. In order to obtain these we subtract from each of the mixture spectra the respective contributions of $CH_4$, as known from data runs on pure $CH_4$. Fitting can be done below the He excitation energies, i.e. in the region of 10 to 19 eV. We then find $\eta_i(E)$ for $CH_4$:

$$\eta_i(E) = F(E)_{CH_4}/F(E)_{He} \tag{2}$$

where all quantities have been measured under identical conditions. Only a few points are measured in this way. The lower limit (25 eV) is set by the I.P. of He and the energy resolving power of the energy loss selector, while the higher limit (30 eV) is set by the maximum energy at which electrons ejected from $CH_4$ can be extracted without discrimination. No correction functions have to be used in this determination of the absolute $\eta_i(E)$. The only assumption made is that the momentum transfer K is small enough to select only dipole transitions, both for absorption and ionization. Using the values for $f^{(1)}(E)$ obtained in this article, we conclude that the contribution of non-dipole terms to the zero degree spectra is at most 1% at an impact energy of 4 keV, at which the ionization efficiency measurements were performed. The absolute ionization efficiency data were used to normalize the relative ionization oscillator strengths on the absorption results.

## 4. RESULTS AND DISCUSSION

### 4.1 *Absorption*

Following the procedure described in 3 the absorption oscillator strength
of $CH_4$ was obtained as shown in figure 4 and Table I. The energy resolution
was 0.5 eV for energy losses up to 25 eV and 1 eV for energies higher than
25 eV. Because a compilation of the extensive photoabsorption data of
$CH_4$ was available (Berkowitz and Inokuti), we normalized the spectrum by
putting:

$$\int_0^{100} \frac{df}{dE} \cdot dE = 8.2$$

However, it is of interest to note that in principle our method of measuring
a relative spectrum over a broad energy range enables us to obtain an
independent absolute scale of quite good accuracy, using the T.R.K. -
sum rule (Fano and Cooper 1968):

$$\int_0^{\infty} \frac{df}{dE} \ dE = \text{number of electrons}.$$

The oscillator strength for the inner shell equals two, minus a correction
for transitions to the valence orbitals already occupied. Taking 1.74
for the K-shell, as calculated by Bearden and Wheeler 1934 for Ne
(isoelectronic with $CH_4$), we arrive at 8.26 for the valence shell.
Allowing for an estimated contribution of 4% at energies above 100 eV,
we end up with an integrated oscillator strength of 7.93 for the spectrum
of fig. 4, a result which differs only 3% from the compilation of absolute
absorption measurements. This kind of procedure makes it possible to obtain
a good normalization when no absolute data are present. There is quite
a scatter in the photon impact results of other authors (see figure 4).
The agreement with the results of Ditchburn (1955) is excellent, while
the discrepancy with the work of DeReilhac and Damany (1970) is not
understood. The broad bump they find around 30 eV is presumably not due
to ionization of electrons from the $2a_1$ orbital, as these authors
suggest, because the photoionization cross section is very low for this
process (see next article).
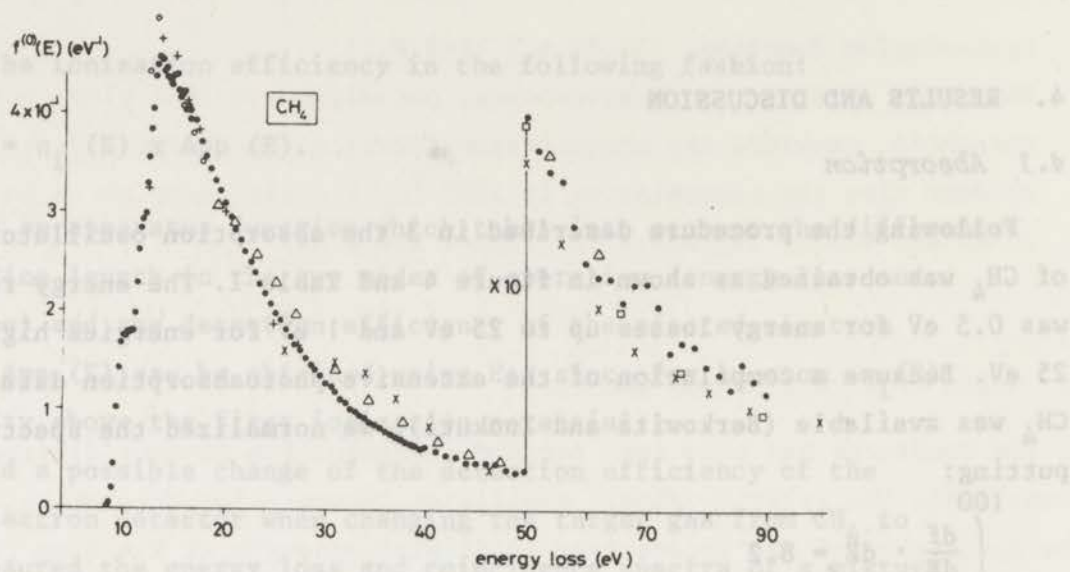
Fig. 4 - Absorption oscillator strength of $CH_4$. ● - this work (for normalization procedure see section 4.1); ○ - Metzger and Cook (1964); + - Ditchburn (1955); △ - Lee et al. (1973); X - DeReilhac and Damany (1970); □ - Lukirskii et al. (1964).
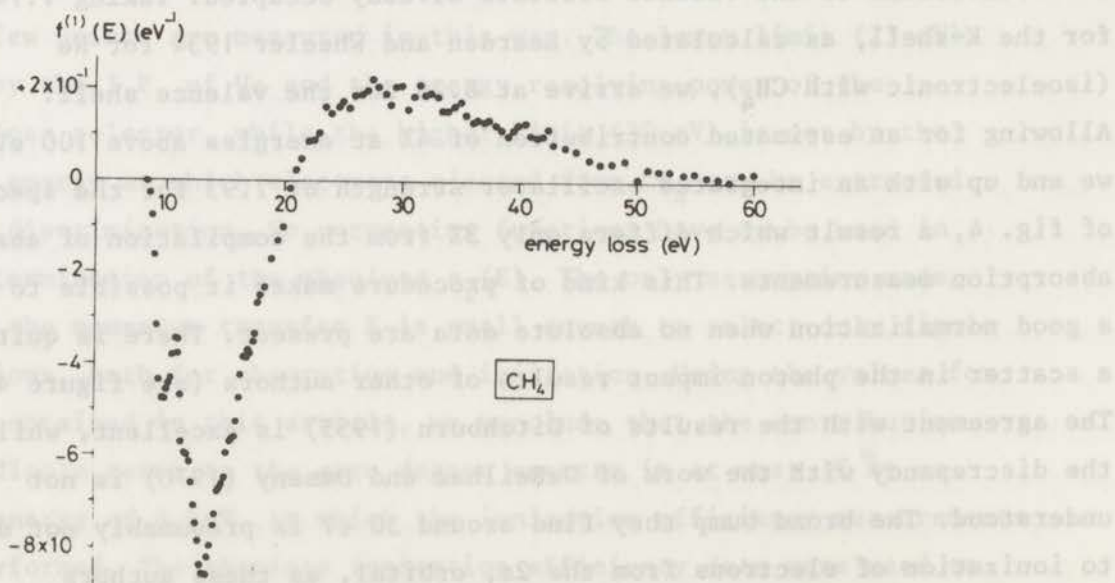


Fig. 5 - Derivative to $K^2$(a.u.) of the generalized oscillator strength of $CH_4$ at K = 0.

The results for $f^{(1)}(E)$ are given in figure 5. This is the first determination of this quantity for $CH_4$. The reliability of our procedure used to derive $f^{(1)}(E)$ from scattering intensities has been earlier demonstrated for He (Backx et al. 1975). The systematic error in $f^{(1)}(E)$ due to the neglect of higher terms was estimated to be $\sim 20\%$ for the discrete transitions. The present spectrum of $f^{(1)}(E)$ for $CH_4$ is in satisfactory agreement with what is to be expected for the quantity on the basis of a sum rule (Inokuti, 1971):

$$\int_0^\infty f^{(1)}(E)dE = 0.$$

For the part of the integral from 0 to 60 eV (i.e. only considering the valence shell) we obtain a value of -1.99, which may be compared with the analogous integral of $|f^{(1)}(E)|$ which yields 10.8.

Although a calculation of generalized oscillator strengths for a molecule like $CH_4$ still does not appear feasible, a measurement of $f^{(1)}(E)$ is still of use for other experiments, in which optical data are derived from small angle electron scattering intensities. For instance, for the experimental arrangement as used by Huebner et al. (1973) where $E_o = 100$ eV and $0 < \theta < 2 \times 10^{-2}$, it is expected on the basis of the present $f^{(1)}(E)$ data that in a measurement on $CH_4$ the apparent oscillator strength would be $\sim 4\%$ too low at 13 eV energy loss and $\sim 4\%$ too high at 30 eV. Although the Born approximation may not be valid at an impact energy of 100 eV our estimation still holds, because it has been shown for a variety of cases that the apparent generalized oscillator strength is not a function of the impact energy for sufficiently small momentum transfers. A theoretical analysis of this phenomenon has been given by Lassettre et al. (1969).

## TABLE I

Optical Oscillator Strengths of $CH_4$ ($10^{-2}$ eV)

| E(eV) | f(E) | E(eV) | f(E) | E(eV) | f(E) |
|-------|------|-------|------|-------|------|
| 8.6   | .57  | 14    | 44.6 | 25    | 19.9 |
| 8.8   | 2.12 | 14.2  | 43.7 | 26    | 18.3 |
| 9.0   | 4.62 | 14.4  | 43.4 | 27    | 16.8 |
| 9.2   | 10.2 | 14.6  | 42.9 | 28    | 15.4 |
| 9.4   | 14.3 | 14.8  | 43.9 | 29    | 14.1 |
| 9.6   | 16.8 | 15    | 44.0 | 30    | 12.9 |
| 9.8   | 17.5 | 15.2  | 42.4 | 32    | 10.7 |
| 10    | 17.4 | 15.4  | 41.6 | 34    | 9.2  |
| 10.2  | 17.9 | 15.6  | 42.0 | 36    | 7.9  |
| 10.4  | 17.9 | 15.8  | 42.2 | 38    | 6.8  |
| 10.6  | 18.1 | 16    | 40.4 | 40    | 5.9  |
| 10.8  | 18.1 | 16.5  | 39.4 | 42    | 5.5  |
| 11    | 19.8 | 17    | 38.3 | 44    | 4.9  |
| 11.2  | 23.1 | 17.5  | 37.2 | 46    | 4.7  |
| 11.4  | 26.3 | 18    | 35.7 | 48    | 4.2  |
| 11.6  | 28.4 | 18.5  | 34.4 | 50    | 4.0  |
| 11.8  | 29.3 | 19    | 33.4 | 55    | 3.4  |
| 12    | 30.0 | 19.5  | 32.3 | 60    | 2.6  |
| 12.2  | 32.9 | 20    | 31.0 | 65    | 2.2  |
| 12.4  | 35.5 | 20.5  | 29.6 | 70    | 2.2  |
| 12.6  | 38.4 | 21    | 28.3 | 75    | 1.6  |
| 12.8  | 40.5 | 21.5  | 27.3 | 80    | 1.5  |
| 13    | 43.8 | 22    | 26.1 | 85    | 1.4  |
| 13.2  | 45.0 | 22.5  | 25.1 | 90    | 1.4  |
| 13.4  | 45.6 | 23    | 24.0 |       |      |
| 13.6  | 45.4 | 23.5  | 22.8 |       |      |
| 13.8  | 44.3 | 24    | 21.8 |       |      |

## 4.2 Ionization efficiency

The absolute ionization efficiency was obtained by normalizing the quotient of the relative oscillator strength for ionization and absorption on a few absolute points obtained in the region of 25 to 27.5 eV energy loss, as described in 3. This ionization efficiency curve is plotted in figure 6. In view of the number of fits and subtractions involved in our procedure, we estimate the accuracy of the absolute determination at $\pm$ 4%, i.e. larger than the statistical scatter of the points in the region of normalization.

Earlier work on $\eta_i(E)$ for $CH_4$ was performed using the technique of photon impact and electron-electron coincidence at low impact energy. Rebbert and Ausloos (1971) reported precise values of the photoionization efficiency, using Ne and He resonance light sources. They obtained values of 1.00 and 0.96 at photon energies of 16.7 - 21.2 eV respectively, which is in excellent agreement with our results. The data of Metzger and Cook (1964) show a lower ionization efficiency over the whole energy interval and even start decreasing at 17 eV, where we still find a plateau of 1.0. The ionization efficiency curve for 70 eV electron impact, presented by Ehrhardt and Linder (1967), has the same shape as ours but a slightly lower plateau value, although the error bars overlap. The slow rise of the ionization efficiency curve to unity is due to the existence of superexcited states, i.e. discrete states above the lowest ionization potential (Platzman 1960, 1961, 1962). As regards the nature of the superexcited states involved, Nishikawa and Watanabe (1973) showed that these are high vibrationally excited Rydberg states converging to the vibrationally excited ground state of $CH_4^+, (1t_2)^{-1}$.[*] They also give arguments that no superexcited states are expected in the region between 17 and 20 eV, which is confirmed by our results. The ionization efficiency curve reported by Nishikawa and Watanabe agrees well with our results which were obtained with an energy resolution of 0.5 eV (see figure 6); however, their assumption that the electronic matrix element $M(\varepsilon)$ for ejection of $1t_2$-electrons with a kinetic energy $\varepsilon$, varies only

[*] Only the change in the electron configuration of the groundstate, $(1a_1)^2(2a_1)^2(1t_2)^6$, is given in the designation of the ion.
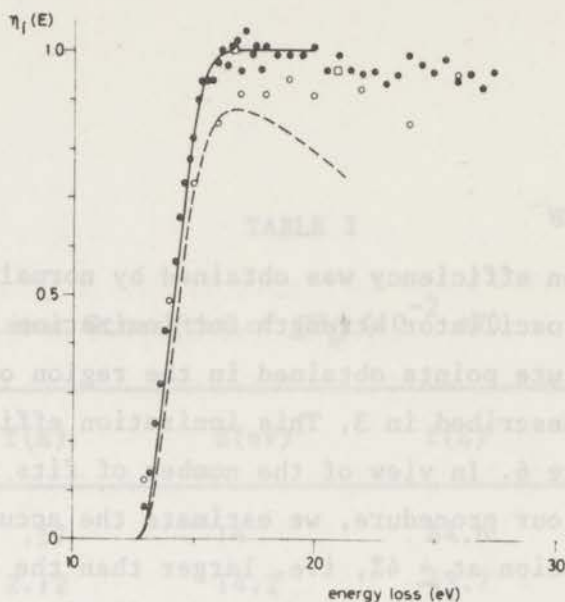
Fig. 6 - Ionization efficiency of $CH_4$. ● - this work; solid curve-theory
Nishikawa and Watanabe (1973); dashed curve - photoionization,
Metzger and Cook (1964); □ - photoionization, Rebbert and
Ausloos (1971); O - low-energy electron-electron coincidence,
Ehrhardt and Linder (1967).
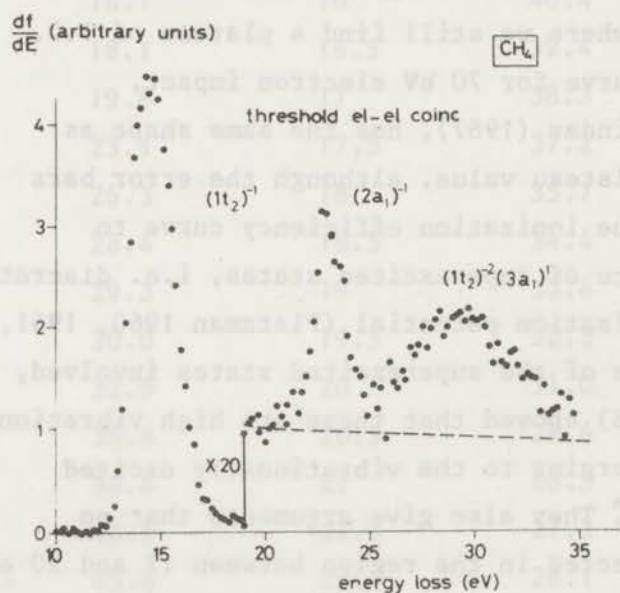


Fig. 8 - Dipole oscillator strengths for the formation of threshold
electrons from $CH_4$, leaving the molecular ion behind in
three configurations: $(1t_2)^{-1}$, $(2a_1)^{-1}$ and $(1t_2)^{-2} (3a_1)^{1}$.
Dashed line - Background from the $(1t_2)^{-1}$ configuration as
obtained by a threshold measurement on He over this range,
taking into account the difference in oscillator strength
distribution of He and the $(1t_2)^{-1}$ configuration.

by 3% for $5 < \varepsilon < 9$ eV is not valid. We find a variation of 25% over
this range (see section 4.3).

In the region between 22 and 24 eV, i.e. the F.C. region of the
second ionic state, $(2a_1)^{-1}$, the ionization efficiency is slightly lower
than unity. Additional evidence for such superexcitation is provided
by our electron-ion coincidence measurements (see next article).
A more detailed discussion of this region is given in section 4.3.

## 4.3 Threshold electrons

The conventional way of studying photoelectric properties of
molecules is to record the energy spectrum of electrons, ejected
from a molecule by a constant energy photon. The relative
Franck-Condon factors for the ionizing transitions are often
derived from the vibrational envelope of a band in such a spectrum,
ignoring the variation of the electronic transition moment,
$M_e^2(\varepsilon)$, over the band, where $\varepsilon$ is the energy of the ejected electron.
If, however, the ejected electron energy is kept fixed while the
energy of the incident photon is varied, the spectrum is uniquely
determined by the Franck-Condon factors, when the dependence of $M_e^2(\varepsilon)$
on the nuclear coordinates is neglected. An example of such a measure-
ment for zero energy electrons, i.e. threshold photoelectron spectroscopy,
is the work of Stockbauer and Inghram (1971).

We were able to perform the electron impact analogue of this
experiment by lowering the extraction field across the collision
chamber such, that essentially only zero energy electrons are
transmitted to the detector. Detection of these "zero energy"
electrons is than made in coincidence with the energy loss electrons;
the discrimination against non-zero energy electrons and photons
from the collision centre being enhanced by setting a narrow time
window so as to pass only the slowest electrons. The conversion
of intensity into oscillator strength is done in the same fashion
as for the ionization measurement (see section 3). From a scan of the
He threshold peak at 24.6 energy loss the measured resolving power is
0.4 eV (inset of fig. 7). Fig. 7 shows the relative oscillator strength
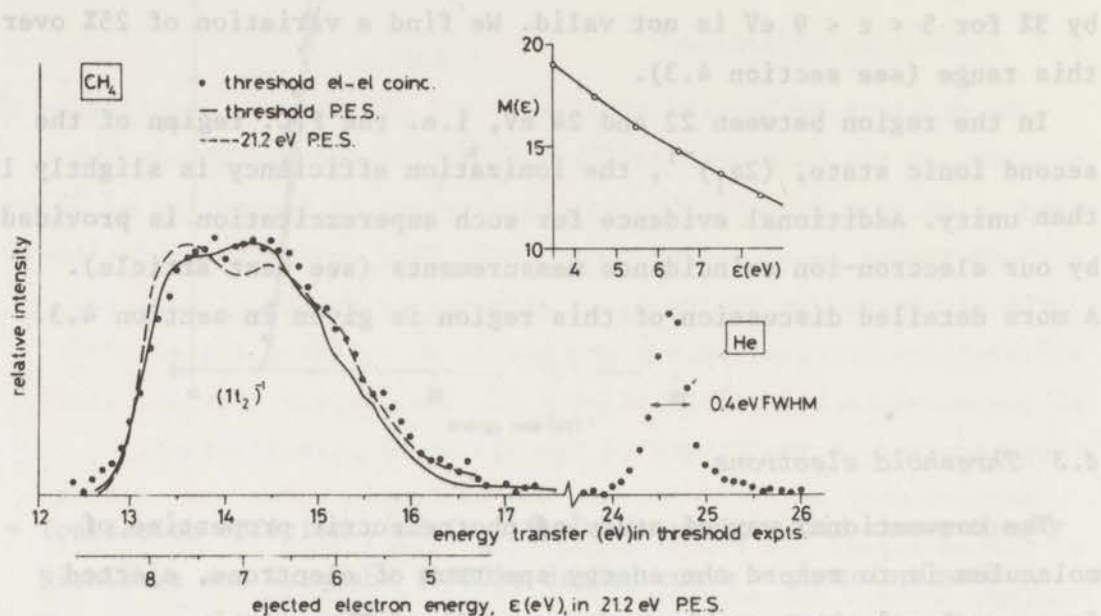
Fig. 7 - Comparison of the dipole oscillator strength for the formation
of threshold electrons from the $1t_2$-orbital with the 21.2 eV
photoelectron spectrum of $CH_4$, corrected for the variation
of the electronic transition moment $M(\varepsilon)$ with the energy
of ejected electrons, $\varepsilon$. Both spectra are expected to give
the Franck-Condon envelope for ejection of a $1t_2$-electron.
● - this work, threshold electron-electron coincidence
measurement. The threshold spectrum of He is plotted in the
same figure to show the energy resolution. In the inset the
variation of $M(\varepsilon)$ is plotted, obtained by measuring scattered
electrons in coincidence with $CH_4^+$ (see section 4.3).
solid line- Stockbauer and Inghram (1971), threshold electron
photoionization.
dashed curve - Baker et al. (1968) and Pullen et al. (1970),
21.2 eV photoelectron spectrum. The spectra of both groups
have been averaged, visually smoothed and corrected for the
analyzer transmission and variation of $M(\varepsilon)$ over the band.

for ejection of threshold electrons (a quantity proportional to the Franck-Condon factor) from the $1t_2$-orbital of $CH_4$. For comparison we have included a photon impact threshold scan of this band by Stockbauer and Inghram; a satisfactory agreement exists between the two scans, apart from a slight difference in width due to the difference in energy resolving power.

It is interesting to investigate whether the shape of the $(1t_2)^{-1}$ threshold spectrum is reproduced when the corresponding 21.2 eV photoelectron band is corrected for the variation of $M_e^2(\varepsilon)$. In this analysis, which leads to the dashed curve in fig. 7, we have made the following steps:

- Two high resolution photoelectron spectra (Pullen et al. 1970; Baker et al. 1968) were visually smoothed, corrected for analyzer transmission as indicated by the authors, and an average of the two was taken.
- $M_e^2(\varepsilon)$ was assumed to have a spectral behaviour (inset of fig. 7) identical to that of the optical oscillator strength, $f(E)$, for production of $CH_4^+$, as we obtained in the same instrument through an electron-ion coincidence measurement (see our subsequent aricle on ionic fragmentation of $CH_4$). The relation between E and $\varepsilon$ is given by: $\varepsilon = E - 13.5$ eV, the last number being the average energy of that part of the $(1t_2)^{-1}$ band (12.6 – 14.4 eV) over which $CH_4^+$ ions are produced. The boundaries are taken from the threshold electron-ion coincidence work of Stockbauer (1973).
- Division of the average photoelectron spectrum by $M_e^2(\varepsilon)$ leads to the pure FC envelope for 21.2 eV excitation (solid curve in fig. 7).

In both the threshold spectrum and in the corrected 21.2 eV spectrum the Jahn-Teller splitting of the $(1t_2)^{-1}$ state shows up as a weak dip in the broad maximum of the band. However, the relative magnitude of the two Jahn-Teller components appears to be inverted for the two cases. A reason for this difference could be a redistribution of the FC overlap due to interference from autoionizing states, either in the threshold case or, more likely, in the case of 21.2 eV photon excitation.

Autoionization is more likely to occur in the latter case, since two conditions are fulfilled. First, 21.2 eV is only 1 eV below the $(2a_1)^{-1}$ onset, so excited states can be expected in that region. Second, such states are too low in energy to be qualified as high Rydberg states, i.e. there is still sufficient overlap between the Rydberg electron and the core for a rapid autoionization.

In conjunction with our findings on the behaviour of $\eta_i$ in the F.C. regions of the two lower ionic states, the following picture emerges. Neutrals are formed from excited states above the lowest I.P. in two cases: either when autoionization is slow because of the necessary conversion of vibrational into electronic energy (the $(1t_2)^{-1}$ F.C. region); or when autoionization is allowed electronically, but we are dealing with such high Rydberg states that the energy exchange between the Rydberg electron and those in the core is slower than dissociation of the ionic core (the ionic dissociation fragment is then neutralized by capture of the Rydberg electron). In all other cases autoionization seems to dominate.

Alternately, the two Jahn-Teller components could have a different behaviour of $M_e^2(\varepsilon)$, which would invalidate our procedure of deriving $M_e^2(\varepsilon)$. It should be pointed out here, than an earlier analysis by Stockbauer and Inghram (1971), along roughly similar lines, led to an apparent variation of $M_e^2(\varepsilon)$ over the band by a factor of 7. This unrealistic result should presumably be ascribed to a slight mismatch of the energy scales in the two experimental spectra.

Fig. 8 shows the results of a threshold scan over an energy loss range up to 35 eV, which includes the $(2a_1)^{-1}$ and a third band centered at 29 eV. The position of this third band agrees well with the value quoted by Appell (1972) in an investigation of appearance potentials of $H^+$ from $CH_4$ and was assigned to the $(1t_2)^{-2}(3a_1)^1$ configuration of $CH_4^+$. A band has also been found by Weigold (1975) at this energy in an electron-electron coincidence experiment at high momentum transfers.

The intensity ratio of the three bands amounts to 1 : 0.023 : 0.014.

The ratio of the first two is significantly lower than the value of 0.14 reported by Brundle et al. (1970) for 40.8 eV photon impact. The conclusion is that the oscillator strength for $(2a_1)^{-1}$ ionization rises slowly at threshold and peaks far beyond threshold. This conclusion is supported by our fragmentation work.

## 5.  CONCLUSION

Using keV electron impact, the absorption oscillator strength of $CH_4$ has been measured over the energy region of 90 eV, with higher accuracy than usually obtained in photoabsorption experiments. Moreover, an estimate of the derivative of the generalized oscillator strength at K = 0 resulted from extraction of the optical oscillator strength from the scattering intensities. With regard to the coincidence measurements, the essential part of the instrument used in this work is the extraction system for charged particles formed in an ionization process. This article describes a novel method for testing its transmission as a function of the 'transverse' energy of the particles. It is found that the system is capable of complete transmission up to energies of 20 eV. Use of this system for electron-electron coincidence measurements confirms earlier data on the absolute ionization efficiency of $CH_4$ in the region up to 20 eV and suggest the occurrence of superexcitation in the region of 22 - 24 eV.

A first result has been presented on the detection of threshold ejected electrons, in coincidence with scattered projectiles. This technique provides new information on the vibrational overlap of the ground state with the states involved in ionization. It is also useful in the detection of high-lying electronic states of ions.

In a subsequent article electron-ion coincidence measurements on $CH_4$ will be presented for energy transfers from the I.P. up to 80 eV.

## ACKNOWLEDGEMENTS

## REFERENCES

- A. Adams and F.H. Read, 1972, J.Phys.E, 5 150.

- J. Appell, 1972, Thesis Université Paris Sud, Orsay (unpublished).

- C. Backx, R.R. Tol, G.R. Wight and M.J. Van der Wiel, 1975, to be published J.Phys.B.

- A.D. Baker, C. Baker, C.R. Brundle and D.W. Turner, 1968, J.Mass Spectrometry and Ion Physics, 1 285.

- J.A. Bearden and J.A. Wheeler, 1934, Phys.Rev. 46 755.

- J. Berkowitz and M. Inokuti, private communication.

- R.S. Berry, 1966, J.Chem.Phys. 45 1228.

- G.R. Branton and C.E. Brion, 1974, J.Electr.Spectr., 3 192.

- C.R. Brundle, M.B. Robin and Basch, 1970, J.Chem.Phys. 53 2196.

- L. De Reilhac and N. Damany, 1970, Spectrochemica Acta, 26A 801.

- R.W. Dichburn, 1955, Proc.Roy.Soc., A229 44.

- H. Ehrhardt and F. Linder, 1967, Z.Naturforschung, 22A 444.

- U. Fano and J.W. Cooper, 1968, Rev.Mod.Phys., 40 441.

- R.H. Huebner, R.J. Celotta, S.R. Mielczarek and C.E. Kuyatt, 1973, Abstracts of VIII ICPEAC, Eds. B.C. Cobic and M.V. Kurepa, (Beograd), p.435.

- M. Inokuti, 1971, Rev.Mod.Phys., 43 297.

- E.N. Lassettre, E. Skerbele and M.A. Dillon, 1969, J.Chem.Phys., 50 1829.

- L.C. Lee, R.W. Carlson, D.L. Judge and M. Ogawa, 1973,
  J.Quant.Spectrosc.Rad.Transfer, 13 1023.
- A.P. Lukirskii, I.A. Brytov and T.M. Zimkina, 1964,
  Opt. i Spektroskopeia, 17 438.
- P.H. Metzger and G.R. Cook, 1964, J.Chem.Phys., 41 642.
- S. Nishikawa and T. Watanabe, 1973, Chem.Phys. 22 95.
- R.L. Platzman, 1960, J. de Phys. et de Rad., 21 853.
- R.L. Platzman, 1961, Intern.J.Appl.Rad.& Isotopes, 10 116.
- R.L. Platzman, 1962, The Vortex, Vol. XXII 8.
- B.P. Pullen, T.A. Carlson, W.E. Moddeman, G.K. Schweitzer,
  W.E. Bull and F.A. Grimm, (1970), J.Chem.Phys., 53 768.
- F.H. Read, A. Adams and J.R. Soto-Montiel, 1970, J.Phys.E, 4 625.
- R.E. Rebbert and P. Ausloos, 1971, J.Res.Natl.Bur.Std. US 75A 481.
- J.A.R. Samson, 1966, Adv. in Atomic and Molec.Phys., 2 Academic
  Press (New York) 177.
- R. Stockbauer and M.G. Inghram, 1971, J.Chem.Phys., 54 2242.
- R. Stockbauer, 1973, J.Chem.Phys., 58 3800.
- E. Weigold, private communication.
- M.J. Van der Wiel, 1973, The Physics of Electronic and Atomic
  Collisions, Invited Lectures and Progress Reports, VIII ICPEAC
  (Beograd) Edts. B.C. Cobic and M.V. Kurepa, 417.
- M.J. Van der Wiel and C.E. Brion, 1973 a, J.Electr.Spectr., 1 309.
- M.J. Van der Wiel and C.E. Brion, 1973 b, J.Electr.Spectr. 1 443.

# C H A P T E R   III

# ELECTRON-ION COINCIDENCE MEASUREMENTS IN $CH_4$

C. Backx and M.J. Van der Wiel

*Measurements are reported of 10 keV electron scattering in $CH_4$ at low momentum transfers, in coincidence with the various ionic products. Ion mass separation was performed in a time-of-flight system with total transmission for fragments with dissociation energies up to 20 eV. Results have been obtained on the oscillator strengths for formation of all ionic products for energy losses from the I.P. up to 80 eV. The present results confirm our earlier electron-electron coincidence measurements of the photoionization efficiency and extend them to higher energy. The oscillator strengths of the $(1t_2)^{-1}$, $(2a_1)^{-1}$ and higher initial states of $CH_4^+$ could be extracted from the data. An autocoincidence technique applied to the ion detector signal makes it possible to obtain the relative abundances of ions formed by dissociation of the unstable $CH_4^{++}$ at 10 keV electron impact.*

## 1. INTRODUCTION

In a previous article (Backx et al. 1975 a, further referred to as I) we reported energy loss measurements of keV electrons, inelastically scattered by $CH_4$. Dipole oscillator strengths both for absorption and for ionization were obtained by that technique, the latter by detecting the scattered projectile electrons in coincidence with the ejected electrons. We now report a study of ionic products of $CH_4$ in coincidence with inelastically scattered electrons again under conditions under which the dipole approximation is valid. The purpose of these further measure-ments was twofold. First, to investigate the possibility of separating the partial oscillator strengths for the various fragments into contri-butions from different electronic states. Second, to check, over a

wide energy range, the usual assumption that electronic superexcitation followed by neutral formation is so improbable, that the photoionization efficiency does not differ measurably from unity.

## 2. EXPERIMENTAL

The apparatus has already been described elsewhere (Backx et al. 1975 b, I). In a quantitative study of dissociative ionization of molecules it is essential that a mass spectrometer is used with a transmission that is independent of the recoil energy of the ionic fragments. We have used a time-of-flight arrangement, consisting of a high extraction field (400 V/cm) across the interaction region, a series of wide cylinder lenses and a flight tube, which has been shown to transmit completely charged particles with recoil energies up to 20 eV, independent of the initial direction of dissociation (see I for details). The limit of 20 eV, beyond which the transmission slowly decreases is not a severe limitation for a study of $CH_4$, since the great majority of fragments is known to have considerably less energy (Appell and Kubach 1971).

Mass analysis is performed in four different modes. First, for a measurement of the mass spectrum produced by 10 keV electron impact the electron gun is pulses (10 nsec, 100 KHz) and the ions are detected in the usual scheme of time-to-amplitude conversion plus multichannel analyser (fig. 1a). Second, in case we want to detect unstable, doubly charged ions, that lead to two ionic fragments with a well-defined time correlation, we made an autocoincidence analysis of the ion signal. This is done by feeding the pulses of the ion detector into both the start and stop input of a T.A.C., with a proper delay (fig. 1b). Third, we have the option of measuring the ions in coincidence with the energy loss electrons (fig. 2a). In that case the T.A.C. is started by the scattered electron pulse, and the mass spectrum obtained is directly equivalent to a photoionization mass spectrum at a photon impact energy equal to the energy loss (section 4.1). Fourth, for measurement of the energy loss spectrum

mass spectrum a

double ionization b

Fig. 1



a

true + random

random b

Fig. 2
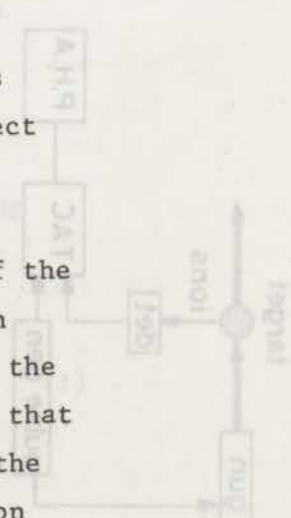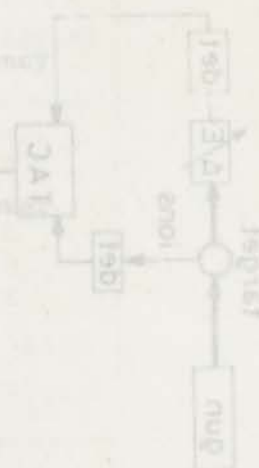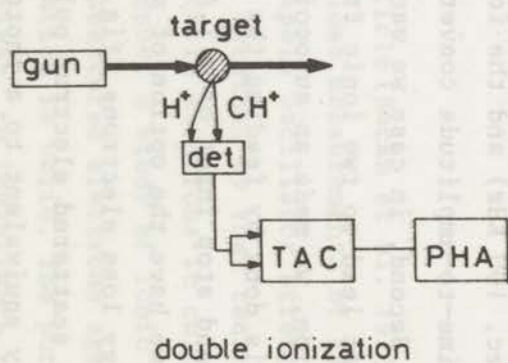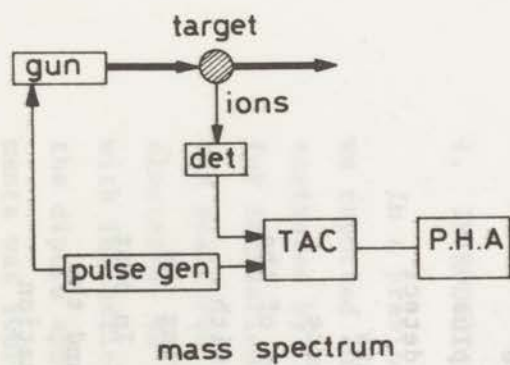
- Detection system for recording time-of-flight mass spectra
  produced by electron impact.
  a. Single ionization: the time-to-amplitude converter is
     started synchronously with the electron beam pulses.
  b. Ion pairs from double ionization of $CH_4$: the faster
     fragment of a pair (i.e. $H^+$, $H_2^+$) starts the T.A.C.;
     the slower stops it. One-particle correlations are
     avoided by inserting a small delay in the start-signal
     line.
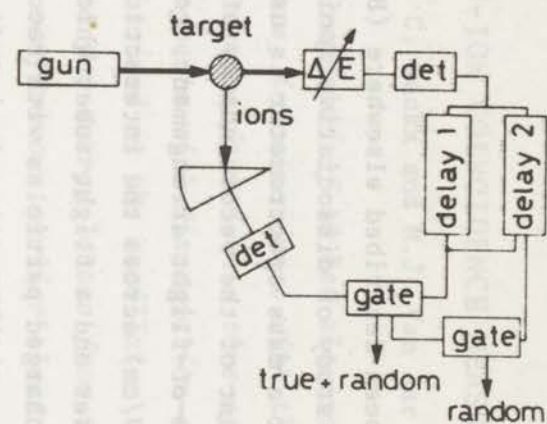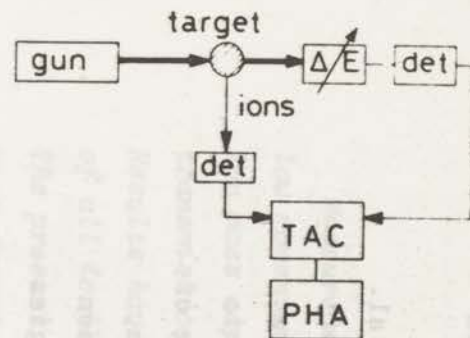
- Circuit for detection of energy loss selected electrons
  in coincidence with mass selected ions.
  a. Energetic fragments: Mass spectra at fixed energy losses
     are recorded as time-of-flight spectra in a high-
     transmission T.O.F. spectrometer.
  b. Parent ions: Mass selection of these thermal energy
     ions is performed using a magnetic spectrometer. The
     coincidence intensity is recorded as a function of
     energy loss using fast coincidence gates, which
     measures true and accidental coincidences simultaneously.

in coincidence with the parent ion $CH_4^+$, which is an ion with only
thermal energy, we employ a $30^o$ magnetic analyzer. This arrangement
allows the detector to count only $CH_4$ ions and therefore leads to
the smallest random coincidence count rate, i.e. the smallest statis-
tical error in the $CH_4^+$ spectrum (fig. 2b). The magnetic mass
spectrometer is also used for a calibration of the relative efficiency
of the ion detector (a Johnston MM-1) for the various ions. From a
comparison of DC currents and pulse rates a constant relative
efficiency was obtained for all C-containing fragments and a 10% lower
value for $H^+$.

## 3. MASS SPECTRUM AT 10 keV ELECTRON IMPACT

### 3.1 Single ionization

The ratios of the peak areas in the mass spectrum, measured with a
pulsed 10 keV electron beam as described in the previous section,
are given in Table I, column 1. A straightforward comparison with
previous work is not possible, since no measurements have been made
at this energy. Moreover, many apparatuses used for measurements
of this type suffered from an unknown discrimination against
fragments with recoil energy. However, one group of investigators
(Adamczyk et al. 1966) has reported partial cross section of $CH_4$
at energies between 20 eV and 2 keV, using a cycloidal mass
spectrometer with complete collection of all ions.

We can compare our data with those of Adamczyk et al. by making
use of the Bethe relation for total cross sections at high impact
energies (Bethe 1930, Fano 1954):

$$\sigma_i(E_o) = \frac{4\,a_o^2\,R}{E_o}\,M_i^2\,\ln\frac{C_i E_o}{R}, \tag{1}$$

where $\sigma_i$ is the cross section for ionization at an electron impact
energy $E_o$, $a_o$ is the Bohr radius, $R$ the Rydberg energy, $C_i$ is
a molecular constant dependent on the generalized oscillator strength
and $M_i^2$ is related to the dipole oscillator strength (see 5.3).

TABLE I

| | Mass spectrum of $CH_4$ at 10 keV electron impact | | |
|---|---|---|---|
| Fragment | abundance (this work) | $\int_{I.P.}^{80eV} n_i(E)\frac{R}{E}\frac{df}{dE}\,dE^+$ | abundance (extrapolated)* |
| $CH_4^+$ | 1.00 | 1.85 | 1.00 |
| $CH_3^+$ | 0.86 | 1.58 | 0.83 |
| $CH_2^+$ | 0.11 | 0.17 | 0.11 |
| $CH^+$ | 0.038 | 0.036 | 0.032 |
| $H^+$ | 0.10 | 0.065 | 0.05 |

+   see section 5.3

*   from the data of Adamczyk et al. (1966).

TABLE II

Fragmentation of $CH_4^{++}$.

| Ion pair | Relative abundances | |
|---|---|---|
| | This work 10 keV electron impact | McCulloh et al. (1965) 1 keV electron impact |
| $H^+ + CH_3^+$ | 1.00 | 1.0 |
| $H^+ + CH_2^+$ | 1.42 | 1.0 |
| $H^+ + CH^+$ | 0.97 | 0.5 |
| $H^+ + C^+$ | 0.64 | 0.3 |
| $H_2^+ + CH_2^+$ | 0.32 | 0.2 |
| $\dfrac{\sigma(\text{double ion.})}{\sigma(\text{single ion})}$ | 0.007 | 0.006 |

The procedure of comparison is as follows. We take the results of Adamczyk et al. at 500 eV, the energy at which normalization was performed on the absolute cross section of Schram et al. (1966). This is an energy at which equation 1 should give a fair prediction of the energy behaviour (except for a small contribution from inner shell processes), while also possible disturbances from secondary electrons in the cycloidal mass spectrometer are still relatively unimportant. From these data points at 500 eV we then extrapolate to 10 keV, using values of $M_i^2$ for each fragment (Table I, column 2), as derived from our differential measurements in section 5.1. We finally obtain a series of partial cross sections at 10 keV, with relative magnitudes that should correspond to those in our mass spectrum (Table I, column 1 and 3). The agreement is quite satisfactory except for the $H^+$ fragment. The reason for this discrepancy might be that our differential measurements leading to $M_i^2$ ($H^+$) do not extend to K-shell energy losses. Such inner shell processes lead to doubly ionized states, which are unstable and decay into $H^+$ plus other fragments.

## 3.2 Double ionization

As regards double ionization of $CH_4$, no $CH_4^{++}$ ions nor any doubly charged ions of lower mass are found in the mass spectrum. The conclusion must be that $CH_4^{++}$ dissociates into two singly charged ions in a time much shorter than needed for extraction of the ions from the collision region. Since both fragments pass through the same electric field, they will exhibit a sharply defined time correlation at arrival on the ion detector.

We have made use of this fact by measuring an autocorrelation spectrum of the ion detector signal (section 2). The result is shown in figure 3, where we plot the autocoincidence intensity as a function of the difference in time of flight between a fast fragment, $H^+$ or $H_2^+$, and the slower ions $CH_3^+$, $CH_2^+$, $CH^+$ and $C^+$.

It appears that the dissociation is rather evenly distributed
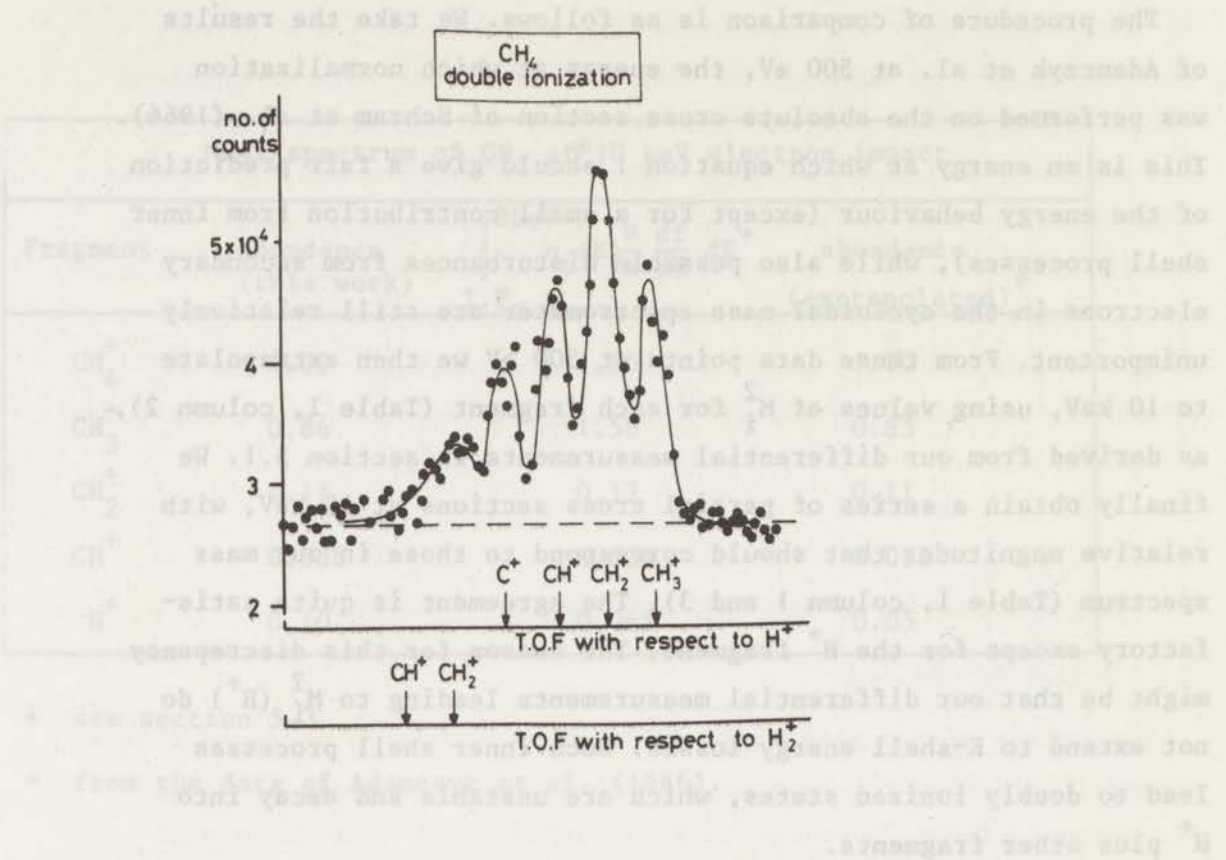
Fig. 3 - Autocorrelation spectrum of ion pairs, produced in the frag-
mentation of $CH_4^{++}$. The horizontal axes display the time-of-
flight of the $C^+$, $CH^+$, $CH_2^+$ and $CH_3^+$ ions with respect to that
of $H^+$ and $H_2^+$.

over all possible exit channels, with the exception of $H_2^+ + H^+ + CH$.
We measured that a fraction of $7.3 \times 10^{-3}$ of the total number of ions
produced at 10 keV impact energy, results from double ionization. The
fact that the multiplier efficiency is 10% lower for $H^+$ than for the
other ionic products has been taken into account in this fraction.
The absolute multiplier efficiency of the carbon containing ions was
assumed to be equal to unity, since the ion impact energy on the
multiplier was 8 keV and the count rate was independent of the voltage
across the multiplier.

In Table II the relative abundances of the various dissociation
routes are given and compared with the data of McCulloh et al. (1964)
using 1 keV electron impact. If both sets of data are normalized by
putting the abundance of the process $H^+ + CH_3^+$ equal to unity, we find
much higher values for the remaining decay routes. If the first step
of the dissociative double ionization process is always production
of a proton, it might be argued that the more kinetic energy the
proton has, the more internal energy there is available for the $CH_3^+$
ion to split off more H-atoms. This would be consistent with the
discrepancy between the two sets of data: McCulloh et al. estimate
a transmission of 30% for protons having a kinetic energy of 7 eV.
Our extraction system is free from discrimination for kinetic energies
up to 20 eV. A detailed discussion of the procedure by which we prove
this was given in I. However, for ion pair formation the situation
is slightly less favorable. The usual argument that, given sufficient
length of the interaction region w.r.t. the (very high) extraction
slit, a representative proportion of the ions is extracted for all
ion energies, does not hold when ion pairs are to be detected. It
can easily be estimated that this effect leads to a slight reduction
of the transmission to about 70% for ion pairs, which share 20 eV
kinetic enery. The agreement of the ratio of double to single
ionization of McCulloh et al. yielding 0.006 with our ratio of
0.007 is only apparent, because ratios normally increase with
decreasing impact energy.

Since by the method described above it is possible to detect the
formation of $CH_4^{++}$, even if the ion is totally unstable it is now
possible to investigate the same aspects of double ionization of
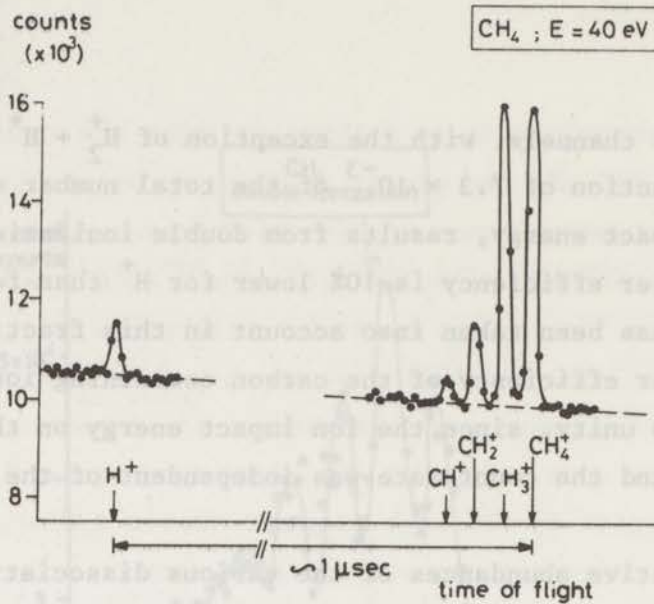
Fig. 4 - Time-of-flight mass spectrum at an energy loss of 40 eV.
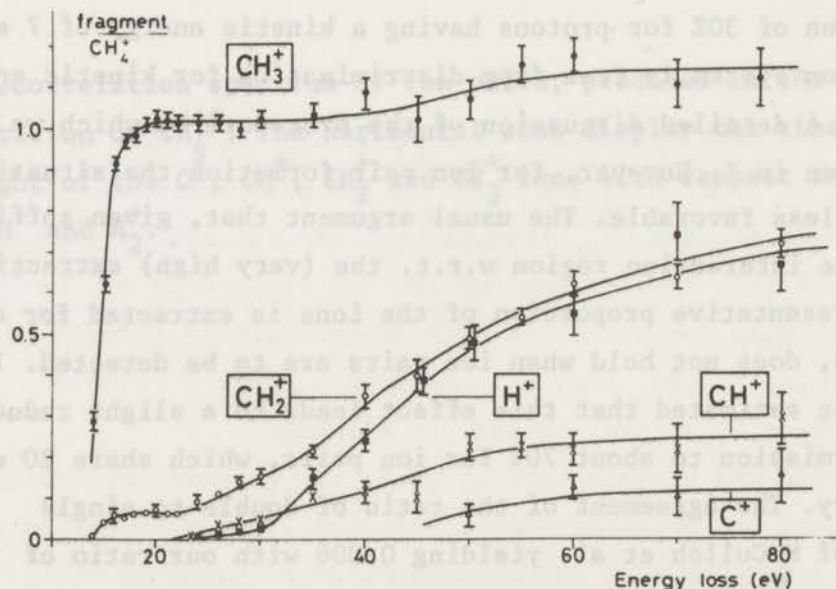


Fig. 5 - The abundances of the various ionic fragments relative to
those of $CH_4^+$ as a function of the electron energy loss. Note
that the ratio of the abundances is constant up to the I.P.
of the $2a_1$-electrons (22 eV).

molecules as previously has been done for the noble gases (Van der Wiel and Wiebes 1971). The most elegant way to realize this, would be low-resolution magnetic separation of the $H^+$ and $H_2^+$ ions from the heavier ions, and detection of both groups of ions in triple coincidence with the energy loss of the projectile electorn. In this case the required mass resolution can be so low (1 : 3), that magnetic separation is feasible without affecting the transmission of recoiling fragments. The $CH_3^+$, $CH_2^+$, $CH^+$ and $C^+$ ions may than be separated by their time of flight.

## 4. MASS SPECTRA AS A FUNCTION OF THE ENERGY LOSS

### 4.1 *Relative ion abundances*

Mass spectra at a particular energy loss have been obtained over a range from the IP up to 80 eV, using the arrangement of fig. 2a and at a resolution of 2 eV. Figure 4 gives an example of such a spectrum at 40 eV. In I it was concluded from a measurement of the derivative of the generalized oscillator strength of $CH_4$, that under our experimental conditions of forward scattering the dipole approximation is valid to a high degree of accuracy. The ratios of the peak areas in the mass spectrum at a selected energy loss, after appropriate correction for the multiplier efficiency, give therefore the ratios of the oscillator strengths for the ionic fragments, i.e. spectra like figure 4 are equivalent to photoionization mass spectra. In figure 5 the measured ratios have been plotted.

When more than one ion originates from the same ionization process, as in the case of dissociative double ionization, e.g. $CH_4^{++} \rightarrow CH_3^+ + H^+$, the time-to-amplitude converter (fig. 2a) is stopped by the fastest fragment, in this case $H^+$, while the slower fragment remains undetected. This means that in our arrangement double ionization only contributes to the $H^+$ ion intensity. At energy transfers where double ionization is energetically allowed, the intensity of fragments containing the C-atom will be measured too low. At an energy transfer of 60 eV the relative abundances of the $CH_3^+$, $CH_2^+$ and $CH^+$ ions with respect to

TABLE III

| E(eV) | $CH_3^+/CH_4^+$ | | | $CH_2^+/CH_4^+$ | | |
|---|---|---|---|---|---|---|
| | This work | Sieck and Gordon | Dibeler | This work | Sieck and Gordon | Dibeler |
| 16.8 | 0.97+0.02 | 1.09 | 0.80 | 0.05+0.01 | 0.047 | 0.30 |
| 21.2 | 1.02+0.02 | 1.04 | – | 0.06+0.01 | 0.048 | – |

Relative abundances of $CH_4^+$, $CH_3^+$ and $CH_2^+$ ions

TABLE IV

| Ion | $(1t_2)^{-1}$ | $(2a_1)^{-1}$ |
|---|---|---|
| $CH_4^+$ | 0.48 | – |
| $CH_3^+$ | 0.49 | – |
| $CH_2^+$ | 0.03 | 0.58 |
| $CH^+$ | – | 0.28 |
| $H^+$ | – | 0.14 |

Relative abundance of ions from the $(1t_2)^{-1}$ and $(2a_1)^{-1}$ state

$CH_4^+$ as given in figure 5 are therefore estimated to be about 10% too low.

Data on fragmentation patterns as a function of photon impact energy are very scarce. Dibeler et al. (1965) measured the relative photoionization cross sections of $CH_4^+$, $CH_3^+$ and $CH_2^+$ at high resolution over a continuous range of energies, while Sieck and Gordon (1973) measured the abundance ratio of these three ions with a resonance light source using Ne (16.7 - 16.9 eV) and He (21.2 eV). The ratios at 16.8 and 21.2 eV of Dibeler et al. and Sieck and Gordon are compared with the present results in Table III. The ratios of Sieck and Gordon are in excellent agreement with the present data. Our $CH_4^+/CH_3^+$ ratio at 16.8 eV which is near the $CH_3^+$ onset, is somewhat lower than theirs, because we worked at energy resolution of 2 eV. There is a large discrepancy with the value of Dibeler et al.; however, the aim of their measurements was not to achieve accurate ratios but rather to obtain the spectral behaviour of the fragments separately.

## 4.2 Contribution of different electronic states

The electronic configuration of $CH_4$ in the ground state in the notation of the symmetry group $T_d$ is $(1a_1)^2(2a_1)^2(1t_2)^6$. The lowest two ionization potentials, which correspond to the ejection of an electron from the $1t_2$ and $2a_1$ orbitals lie at 12.6 and 22 eV respectively (Pullen et al. 1970, Brehm 1966, Brundle et al. 1970). Higher states of $CH_4^+$ formed by two-electron transitions set in at $\sim$ 30 eV (Appell 1972, Weigold 1975, I), while double ionization starts at around 40 eV (Appell 1972, Spohr et al. 1970). Given the relative simplicity of this term scheme of $CH_4^+$, it is possible to derive from the data of section 4.1 the relative ion abundances formed by the $(1t_2)^{-1}$ and $(2a_1)^{-1}$ states separately. In order to do this we need to make three assumptions. First, the vibrational population of a $CH_4^+$ ion in a specific electronic state, and therefore the relative abundance of the ions formed by that state, is independent of the continuum energy of the ejected electron. This is a direct
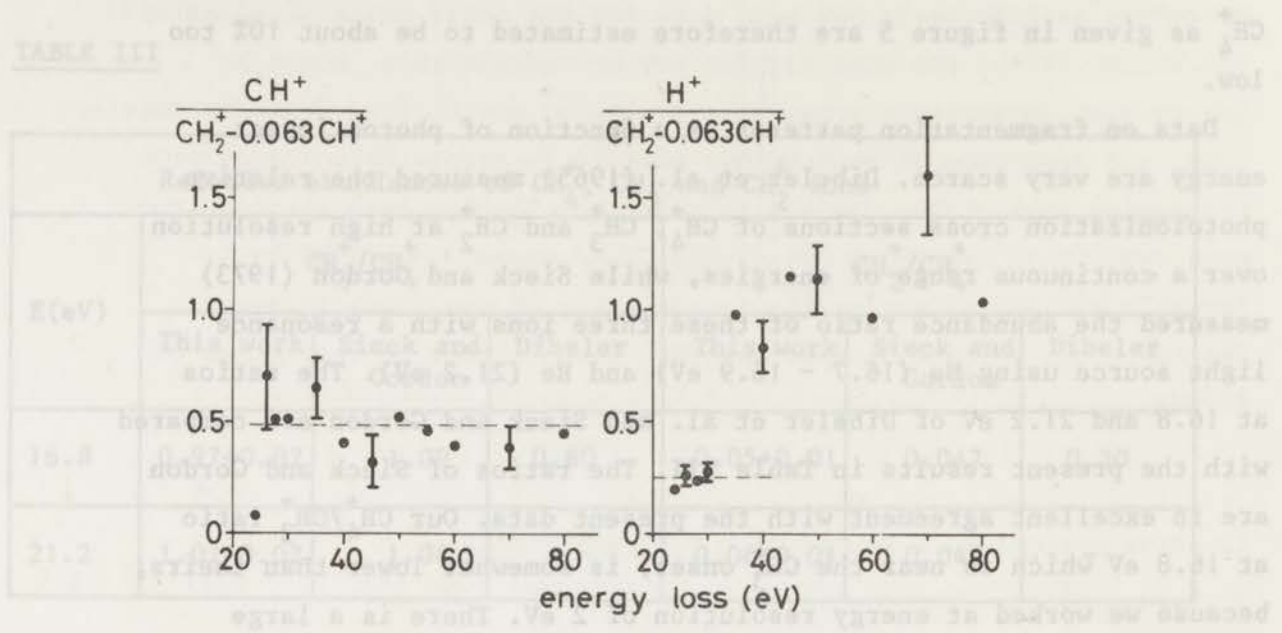
Fig. 6 – Fragmentation of the $(2a_1)^{-1}$ state (I.P. = 22 eV) into $CH_2^+$, $CH^+$ and $H^+$.

    a. Ratio of $CH^+$ and $CH_2^+$ abundances, the latter being corrected for the production of $CH_2^+$ from the $(1t_2)^{-1}$ state (i.e. 0.063 $*$ $CH_4^+$ intensity). Error bars are displayed only for a few data points.

    b. Same for $H^+$ and $CH_2^+$; the rise of the ratio above 30 eV indicates the existence of (a) higher excited ionic state (s) of $CH_4$ around 30 eV, essentially decaying by the formation of protons.

consequence of the Franck Condon principle and will of course apply
only to energy transfers at which the whole Franck Condon region is
energetically allowed. The resolution in the present measurements
is insufficient to observe variations of the relative abundances
of ionic fragments due to a changing vibrational population when
scanning through the Franck Condon region. The abundances of ions
from selected parts of the Franck Condon region can be obtained
with more detail by measuring electrons ejected by photoionization
in coincidence with the various ionic products (Stockbauer 1973,
Brehm and Puttkamer 1967). Second, the electronic part of the
transition moment varies sufficiently slowly with the energy of the
ejected electron, that the ratio of the electronic transition moments
to the different vibrational levels may be regarded as constant
when the energy loss is varied.

Third, contributions form autoionizing states are small compared to
the direct ionization. On the basis of these assumptions we would
expect the breakdown of the $(1t_2)^{-1}$ state to result in constant
abundance ratios between 17 and 23 eV. This is indeed what we find
(see fig. 5 and Table IV). We can then extrapolate these abundances
to energies beyond 23 eV by assuming that $CH_4^+$ is only formed by the
$(1t_2)^{-1}$ state, which is suggested by the constant ratio of $CH_3^+/CH_4^+$
up to at least 30 eV, while it is very unlikely that stable $CH_4^+$
ions will be formed from transitions to higher states.

With regard to the $(2a_1)^{-1}$ fragmentation, the fragment $CH^+$ does
not appear before the onset of this state at 22 eV. The intensity
ratio of $CH^+/CH_2^+$ after subtraction of the extrapolated contribution
of the $(1t_2)^{-1}$ state to $CH_2^+$, being 0.063 times the $CH_4^+$-intensity,
is plotted in figure 6a. The constant ratio between 25 and 80 eV
gives the relative abundance of $CH_2^+$ and $CH^+$ formed by the $(2a_1)^{-1}$
state. In figure 6b the same procedure has been applied to the case
of $H^+$ ions. From the figure it is clear that up to 30 eV $H^+$ is only
formed by the $(2a_1)^{-1}$ state. The new channel of $H^+$ production that
opens up at approximately 30 eV, was ascribed to an ion state with
the configuration $(2a_1)^2(1t_2)^4(3a_1)$ by Appell (1972) from an
analysis of electron impact production curves for protons as a

Fig. 7 - Ionization efficiency of $CH_4$.

● - This work, obtained by dividing the total oscillator
strength for formation of ionic fragments by that for
absorption (see I).

X - Backx et al., electron-electron coincidence measurements
(see I)

function of the proton kinetic energy. Our threshold electron spectrum (see I), gives direct evidence of such a state, producing a band of 4 eV width centered at 29 eV. So we assign at least the onset of the "higher states" spectrum to this particular state.

Table IV lists the relative abundances of ions formed by the ejection of an electron from the $1t_2$ and $2a_1$ orbitals.

## 5. OSCILLATOR STRENGTH SPECTRA

### 5.1 Fragment spectra and ionization efficiency

The next step is now the measurement of the oscillator strength distribution of one of the ions. Together with the relative abundances we then obtain the spectra for ionization, total and partial with respect to the ions formed. The most logical fragment to choose for this determination is the parent ion, since it has the highest abundance and no kinetic energy of formation, which allows easy separation in a mass spectrometer (fig. 2b). The spectral shape of the oscillator strength distribution of $CH_4^+$ is obtained by measuring the ions in coincidence with the small angle scattered electrons as a function of the energy loss. This coincidence signal is than converted to oscillator strength by means of the procedure discussed in I. It was assumed that for the $CH_4^+$ fragment the appropriate correction for non-dipole terms was equally small as for the absorption measurement (also from I). The sum of all partial spectra was normalized, in the region of 12 to 28 eV, on the absolute electron-electron coincidence results from I, which represent the total ionization oscillator strength. We divided the total ionization by the absorption results from I to obtain the ionization efficiency $\eta_i$ as given in figure 7. For comparison our earlier results of the electron-electron coincidence measurements of I have also been included in the figure. The agreement between our previous (ejected electron) results and the present ones indicates that no metastable ions are formed, since the present ion data represent only integer apparent masses. In the region below 17 eV part of the absorption goes into vibrational

superexcitation of Rydberg states converging to the $(1t_2)^{-1}$ ionic state. From 17 to 22 eV no superexcitation is expected on theoretical grounds. A discussion of this region and a comparison with results from other sources were given in I. Over the region from 22 - 24 eV the ionization efficiency appears to be slightly lower than unity. This is exactly the Franck Condon region of the $(2a_1)^{-1}$ state, i.e. we are dealing with superexcited Rydberg states connected with this ionic state, which dissociate into neutral fragments. In the remainder of the spectrum $\eta_i$ is close to unity. The deviation of $\eta_i$ from a value of unity at energies of 70 and 80 eV is probably not significant. In addition to the large statistical uncertainty, these data points may be systematically too low due to formation of $H^+$ fragments with energies exceeding the limit of 20 eV for full transmission in the TOF spectrometer. Given a dissociation limit of $CH_3 + H^+$ at 18.1 eV (Appell and Kubach 1971), $H^+$ fragments with 20 eV could already be expected at an energy loss of 39 eV in the most extreme case. The dissociative double ionization process, which is known to have a series of onset potentials between 40 and 65 eV (Appell 1972) and is a likely source of highly energetic protons, should however be excluded as a possible explanation. The reason is, that in our TOF detection scheme normally only the fastest of two correlated fragments is detected. If a proton is too fast to be extracted, its slower partner is still detected and the double ionization is still properly accounted for in the ionization efficiency.

As a final remark, it should be pointed out that the ionization efficiency reported in this article refers to detection of only those ionizing processes which are completed within about 2 μsec after the initial energy absorption. It is possible, that through superexcitation fast neutral fragments are formed, which escape from the extraction region before converting their internal energy into ionization.

In Table V the oscillator strength for the various ionic products is given from the I.P. up to 80 eV energy loss. For energy losses higher than 28 eV the ionization efficiency has been taken equal to unity in view of the arguments given above, i.e. the oscillator

strength for total ionization was taken equal to the absorption results, which have a lower statistical uncertainty.

## 5.2 *The $(1t_2)^{-1}$, $(2a_1)^{-1}$ and higher states*

By making use of the results of sections 4.2 and 5.1, we derived the oscillator strength spectra for ionization of $CH_4$ to the $(1t_2)^{-1}$, $(2a_1)^{-1}$ and higher states (fig. 8). The procedure has been summarized in Table VI, while the resulting values are listed in Table V. Information of this kind is usually obtained using photo-electron spectrometry at varying photon energy. The method described here does not suffer from the problems one encounters in P.E.S. concerning photoelectrons angular distributions and energy analyser transmission. The method does require, however, relative simplicity of the term scheme and of the fragmentation pattern. The thresholds of the two outer orbitals correspond to those reported earlier in photoelectron spectroscopy (Brundle et al., 1970). Our onset for excitation to "higher" states at 30 eV confirms the value quoted by Appell (1972) in an investigation of appearance potentials of $H^+$ from $CH_4$.

It is of interest to compare the shapes of the $1t_2$ and $2a_1$ continua with those of the corresponding orbitals in the isoelectronic Ne atom, the 2p and 2s respectively. The $1t_2$ continuum peaks very near threshold and decays much more rapidly than the 2p continuum in Ne (Samson 1966). It should be remembered that ejection of a $1t_2$ electron with high momentum has to occur from parts of coordinate space near one of the nuclei, in view of the necessary momentum transfers to a nucleus. The observed low probability for such a process testifies to the truly molecular nature of the $1t_2$ orbital. The $2a_1$ orbital, on the other hand, appears to be rather more atomic in behaviour. The spectrum peaks far above threshold, while in particular the ratio of I.P. to the energy at the peak oscillator strength corresponds closely to that calculated for the Ne 2s-electrons (Amusia et a. 1972).

The relative intensity of the two continua can only be compared with

68
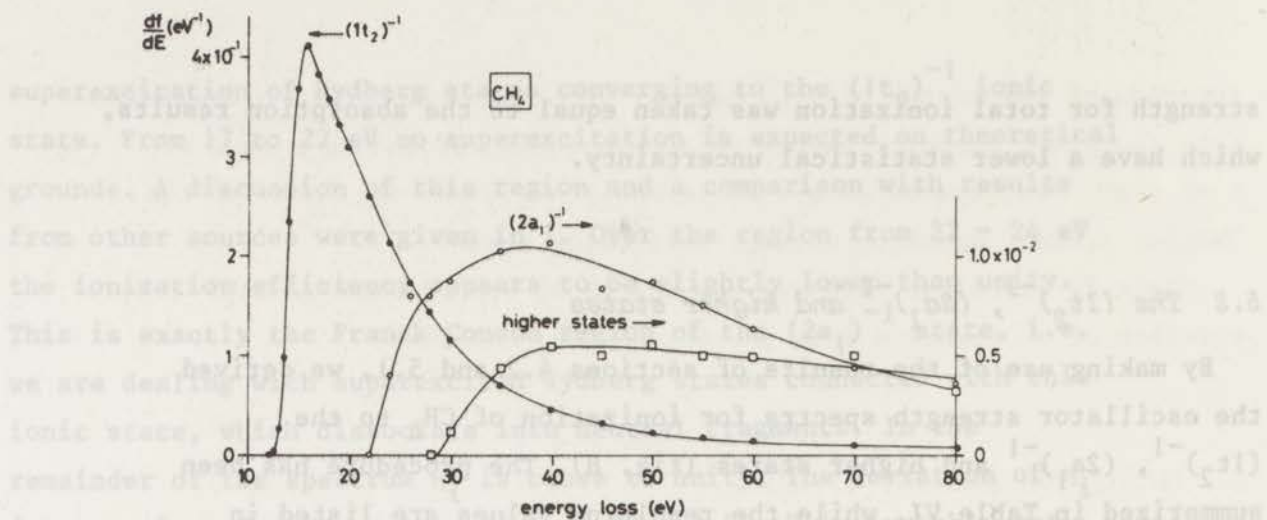


Fig. 8 - Oscillator strengths for the $(1t_2)^{-1}$, $(2a_1)^{-1}$ and higher states of $CH_4^+$. See section 5.2 for the procedure of deriving these spectra from the fragment spectra.

TABLE VI

Summary of procedure used in deriving the electronic state spectra from the fragment spectra (section 4.2)

| State | Energy range | Oscillator strength equal to: |
|---|---|---|
| $(1t_2)^{-1}$ | ≤ 22 eV | total ionization |
| | > 22 eV | $2.08 \times CH_4^+$ * |
| $(2a_1)^{-1}$ | < 30 eV | total ionization$-2.08 \times CH_4^+$ * |
| | ≥ 30 eV | $1.25(CH_2^+ - 0.063\ CH_4^+) + CH^+$ * |
| "Higher states" | ≥ 30 eV | total ionization$-[(1t_2)^{-1} + (2a_1)^{-1}]$ |

* see figs. 5 and 6

one value at 304 Å (40.8 eV). We find a $2a_1/1t_2$ ratio of 0.22, compared to 0.14 as reported by Brundle et al. (1970). The latter value was not corrected for angular distribution of the photoelectrons nor for analyser transmission.

The maximum slope in the onset of each of the spectra in fig. 7 should equal the peak intensity of the corresponding band in the threshold electron scan as has been obtained in I. Such a comparison of relative intensities, though only very approximate in view of the limited resolution, yields the following result for the three states (in order of increasing I.P.):

   1 : 0.018 : 0.010 for the ionization curves;
   1 : 0.023 : 0.014 for the threshold electron scan.

### 5.3 *Oscillator strength sums*

The quantity $M_i^2$, introduced in section 3.1 and defined as

$$M_i^2 = \int_{IP}^{\infty} \eta_i(E)\frac{df}{dE}\frac{R}{E}\,dE,$$

provides a link between our differential measurements and total electron impact cross sections, by means of the Bethe relation (eq. 1). From an analysis of the impact energy dependence of the total cross section, values of $M_i^2$ for $CH_4$ have been obtained by Schram et al. (1966) and by Rieke and Prepejchal (1972). The numbers quoted are $4.28 \pm 0.10$ and $4.23 \pm 0.13$, respectively. In spite of this good agreement, there is a significant discrepancy with the value of 3.84, derived from the oscillator strength distribution presented in table V. This number includes estimated contributions of 0.02 arising from the valence shell spectrum above 80 eV and of 0.06 for the K-shell, using absorption data of Lukirskii et al. (1964). A similar procedure was applied by Berkowitz et al. (1973), who find $M_i^2 = 3.77$, using literature values for the ionization efficiency and taking $\eta_i$ equal to unity above 20 eV.

The discrepancy between the two sets of data is not understood. Trapping of slow ejected electrons in the magnetic field (Gryzinski

TABLE V

| E(eV) | total | CH$_4^+$ | CH$_3^+$ | CH$_2^+$ | CH$^+$ | C$^+$ | H$^+$ | $(1t_2)^{-1}$ | $(2a_1)^{-1}$ | Higher states |
|---|---|---|---|---|---|---|---|---|---|---|
| 14 | 23.5 | 18.3 | 5.2 | | | | | 23.5 | | |
| 15 | 36.8 | 22.2 | 13.7 | 0.89 | | | | 36.8 | | |
| 16 | 41.2 | 20.8 | 19.1 | 1.25 | | | | 41.2 | | |
| 17 | 38.3 | 19.0 | 18.4 | 0.95 | | | | 38.3 | | |
| 18 | 35.8 | 17.5 | 17.2 | 1.05 | | | | 35.8 | | |
| 19 | 33.3 | 16.0 | 16.2 | 1.04 | | | | 33.3 | | |
| 20 | 31.0 | 14.8 | 15.2 | 1.03 | | | | 31.0 | | |
| 22 | 24.5 | 11.8 | 11.9 | 0.71 | | | | 24.5 | | |
| 24 | 20.5 | 9.68 | 9.78 | 0.87 | 0.05 | | 0.06 | 20.1 | 0.4 | |
| 26 | 17.4 | 8.02 | 8.17 | 0.88 | 0.29 | | 0.11 | 16.7 | 0.8 | |
| 28 | 15.3 | 6.95 | 6.95 | 0.97 | 0.29 | | 0.13 | 14.5 | 0.8 | |
| 30 | 12.7 | 5.64 | 5.81 | 0.85 | 0.26 | | 0.14 | 11.7 | 0.88 | 0.12 |
| 35 | 8.6 | 3.43 | 3.53 | 0.75 | 0.36 | | 0.52 | 7.13 | 1.03 | 0.44 |
| 40 | 6.3 | 2.25 | 2.46 | 0.79 | 0.26 | | 0.54 | 4.68 | 1.07 | 0.55 |
| 45 | 4.7 | 1.61 | 1.64 | 0.64 | 0.17 | | 0.63 | 3.35 | 0.84 | 0.51 |
| 50 | 3.8 | 1.14 | 1.22 | 0.56 | 0.26 | 0.08 | 0.56 | 2.37 | 0.87 | 0.56 |
| 55 | 3.2 | 0.93 | 1.08 | 0.50 | 0.21 | | 0.47 | 1.93 | 0.76 | 0.51 |
| 60 | 2.6 | 0.70 | 0.83 | 0.44 | 0.15 | 0.09 | 0.39 | 1.46 | 0.64 | 0.50 |
| 70 | 1.95 | 0.48 | 0.53 | 0.31 | 0.11 | | 0.45 | 1.00 | 0.45 | 0.50 |
| 80 | 1.50 | 0.38 | 0.42 | 0.27 | 0.11 | 0.06 | 0.26 | 0.79 | 0.36 | 0.35 |
| $\int_{0}^{80eV} \frac{R}{E}\frac{df}{dE}\cdot dE$ | 1.85 | 1.58 | 0.17 | 0.036 | | | 0.065 | | | |

1973) in the instrument of Schram et al. is a possible reason for
an enhanced cross section. In the experiment of Rieke and Prepejchal,
as was already pointed out by Berkowitz et al. (1973), the high
pressure could have been responsible for additional ionization, even
in a pure gas, due to collisions of superexcited and ground state
molecules.

The oscillator strength sums for the separate fragments have been
listed below the corresponding columns of Table V. These numbers were
used in section 3.1 in order to compare ion abundances at different
impact energies.

## 6. CONCLUSION

A quantitative study of ionic fragmentation of $CH_4$ has been made
over a range of energy transfers covering most processes of interest
in the valence shell. We have described a method for the study of
double ionization leading to rapid dissociation into two singly charged
fragments. It was also demonstrated that for a molecule like $CH_4$, the
relative simplicity of the fragmentation pattern permits a separation
to be made of the contributions from different electronic states,
without some of the difficulties inherent to photoelectron spectroscopy.
The present results indicate that for energies of 25 eV and upwards
superexcitation leading to neutral fragments is an improbable process.
Further studies of one of the exit channels that remained unobserved,
namely the formation of excited neutrals, are in progress.

72

REFERENCES

- B. Adamczyk, A.J.H. Boerboom, B.L. Schram and J. Kistemaker,
  1966, J.Chem.Phys., 44 12.
- M.Ya. Amusia, V.K. Ivanov, N.A. Cherepkov and L.V. Chernysheva,
  1972, Phys.Letters 40A 361.
- J. Appell and C. Kubach, 1971, Chem.Phys.Letters, 11 486.
- J. Appell, 1972, Thesis Université Paris-Sud, Orsay (unpublished).
- C. Backx, G.R. Wight, R.R. Tol and M.J. Van der Wiel, 1975 a,
  J.Phys.B, to be published.
- C. Backx, R.R. Tol, G.R. Wight and M.J. Van der Wiel, 1975 b,
  J.Phys.B, to be published.
- J. Berkowitz, M. Inokuti and J.C. Person, 1973, Abstracts of VIII
  ICPEAC, Eds. B.C. Cobic and M.V. Kurepa, (Beograd), p. 561.
- C.R. Brundle, M.B. Robin and Basch, 1970, J.Chem.Phys., 53 2196.
- H. Bethe, 1930, Ann.Physik, 5 325.
- B. Brehm and E. Von Puttkamer, 1967, Z.Naturforschung, 22a 8.
- B. Brehm, 1966, Z.Naturforschung, 21a 196.
- V. Dibeler, M. Krauss, R.N. Reese and F.M. Harllee, 1965,
  J.Chem.Phys., 42 11 3791.
- U. Fano, 1954, Phys.Rev., 59 1198.
- M. Gryzinski, 1973, Abstracts VIII ICPEAC, Eds. B.C. Cobic and
  M.V. Kurepa, (Beograd), p. 398.
- A.P. Lukirskii, I.A. Brytov and T.M. Zimkina, 1964, Opt.Spectry.
  (USSR) (English Translation) 17 234.
- K.E. McCulloh, T.E. Sharp, H.M. Rosenstock, 1964, J.ChemPhys., 42
  10 3501.
- B.P. Pullen, T.A. Carlson and W.E. Moddeman, 1970, J.Chem.Phys., 53 2 768.
- F.F. Rieke and W. Prepejchal, 1972, Phys.Rev., A6 4 1507.
- J.A.R. Samson, 1966, Advances in Atomic and Molecular Physics, Vol. 2,
  Academic Press (New York), p. 177.
- B.L. Schram, M.J. Van der Wiel, F.J. De Heer and H.R. Moustafa, 1966,
  J.Chem.Phys., 44 149.
- R. Spohr, T. Bergmark, N. Magnusson, L.O. Werme, C. Nordling and
  K. Siegbahn, 1970, Physics Scripta, 2 31.

- L.W. Sieck and R. Gordon, 1973, Chem.Phys. Letters, 19 509.
- R. Stockbauer, 1973, J.Chem.Phys., 58 3800.
- E. Weigold, private communication.
- M.J. Van der Wiel and G. Wiebes, 1971, Physica, 53 225.

# CHAPTER IV

## ELECTRON-ION COINCIDENCE MEASUREMENTS OF $H_2$, HD AND $D_2$

### C. Backx, G.R. Wight and M.J. Van der Wiel

*The gross spectral behaviour of the dipole oscillator strengths for absorption, ionization and dissociation of $H_2$, HD and $D_2$ has been measured over the energy range of 0 to 70 eV, using the technique of detection of forward scattered 8 keV electrons in delayed coincidence with the ions. A quantitative collection of ionic fragments is ensured up to kinetic energies of 20 eV.*

*The absorption results are in excellent agreement with those of Samson and Cairns. By subtracting the total ionization spectrum from absorption, a 2 eV wide region is found above the ionization potential where part of the oscillator strength goes into neutral formation. No appreciable isotope effect is observed in this region.*

*The measurement of spectra for both $H_2^+$ and $H^+$ (or the corresponding ions of the isotopes) made it possible to separate the effects of vibrational and electronic transition moments on the ratio $H^+/H_2^+$ formed by transitions to the $1s\sigma_g$ state of $H_2^+$ and to test various theoretical predictions. The $H^+$ (or $D^+$) spectrum shows extensive contributions from autoionization, which is discussed in terms of excitation to Rydberg levels converging to the $2p\sigma_u$ and $2p\pi_u$ states of $H_2^+$.*

## 1. INTRODUCTION

Because $H_2$ is the most simple molecule, and therefore theoretically the most accessible it has been studied extensively both by photon and electron impact. Photoionization and absorption studies have been performed for example by Cook and Metzger (1964) and Samson (1965), together covering the energy region up to 60 eV, while Chupka and Berkowitz (1969) reported high resolution (0.04 Å) mass spectroscopic

data in the range from 745 to 810 Å. This high resolution work yielded
a wealth of spectroscopic information and revealed the important role
of autoionization. Mass spectrometric studies of the photoionization
cross section over a wide range of photon impact energies are very
scarce; there are reports of $H_2^+$ by Comes and Lesmann (1964), using
discrete lines, and Dibeler et al. (1964) employing a dispersed rare
gas continuum as photon source, while Browning and Fryar presented
results on the dissociative photoionization of $H_2$ and $D_2$ in terms of
the intensity ratio of $H^+$ to $H_2^+$ and $D^+$ to $D_2^+$ as a function of the
photon impact energy up to 30 eV. Dissociative ionization of $H_2$ ($D_2$)
has been studied to a much greater extent by electron impact; we mention
the work of Dunn and Kieffer (1963), Kieffer and Dunn (1967), Brunt
and Kieffer (1970), McCulloh and Rosenstock (1968), Crowe and McConkey
(1973 a,b) and Stockdale et al. (1975). The subject of these reports
is the energy and angular distribution of protons at various electron
impact energies (but without energy analysis of the scattered electrons),
which gives insight into the validity of the Born Oppenheimer approximation,
the relation between the symmetry of the ionic state and the angular
distribution of the resulting protons and also the contribution of
autoionizing states to the dissociative ionization process.

The present situation, as far as the work presented here is concerned,
can be summarized as follows:
- there is poor agreement between theory and experiment for photoabsorption
- the experimental ratio of $H^+/H_2^+$ produced by excitation to the ground
  state ($1s\sigma_g$) of $H_2^+$ is not yet well predicted by theory.
- Although quite different results have been obtained for the energy
  distribution of fast protons formed by electron impact, they all
  show additional structure due to other states than the first excited
  state of $H_2^+(2p\sigma_u)$
- In connection with this there are no published results of the optical
  oscillator strengths of $H^+$ over a wide enough energy range to clearly
  point out contributions from various ionic states.

In order to improve the experimental situation in these regards, we
now report optical oscillator strengths for absorption, ionization and
fragmentation of $H_2$, $D_2$ and HD at energy transfers of 10 to 70 eV, with

an energy resolution of 0.5 eV. The oscillator strengths for absorption
have been obtained from an analysis of energy loss spectra of 8 keV
electrons, the relative spectra being normalized by application of the
Thomas-Reiche-Kuhn sum rule (Inokuti 1971). The oscillator strengths
for ionization and dissociative ionization have been obtained in a
similar way from measurements of the energy loss selected electrons
in delayed coincidence with the ions. The oscillator strengths for
ionization have been normalized on those for absorption at energy losses
where the ionization efficiency (i.e. the probability that energy
absorption results in ionization) is constant and assumed to be equal
to unity.

## 2. MODES OF OPERATION AND ANALYSIS

The apparatus has already been described in earlier reports on
He and $CH_4$ (Backx et al. 1975 a,b, Backx and Van der Wiel 1975). Briefly,
and 8 keV electron beam traverses a collision chamber containing target
gas at a pressure of $10^{-4}$ - $10^{-5}$ torr. Electrons scattered through a
small angle, adjustable electrostatically over a range of 0 to $2 \times 10^{-2}$
rad, are energy analysed and detected. Ionic fragments formed by the
energy transfer of the primary electron to the target molecules $H_2$, $D_2$ or
HD were extracted from the collision chamber and transported to the ion
detector by an electrostatic lens system, which was proven to be free
of discrimination against the initial kinetic energy of the extracted
particles up to 20 eV initial energy (Backx et al. 1975 b). Since
there are no repulsive states of $H_2^+$ that give rise to protons with more
than 20 eV kinetic energy, the oscillator strength distribution that is
obtained for $H^+$ is free from transmission effects of the ion detection
system. Mass analysis is based on the difference in time of flight of
the different ions with respect to the corresponding scattered projectile
electron, which is measured in delayed coincidence with the ions. Data
were taken in three different ways. First, for absorption measurements
energy loss spectra have been recorded over the range from 10 to 90 eV
energy loss at two different, small scattering angles, i.e. $\theta_1 = 0$

(opening angle $1.4 \times 10^{-4}$ sterad) and $\theta_2 = 2 \times 10^{-2}$ rad. From the scattering intensities two values of the generalized oscillator strength (G.O.S.) or rather average G.O.S. values in two momentum transfer ranges were obtained at each energy loss. We can improve the usual dipole approximation at small momentum transfer (K) by writing the G.O.S. as

$$f(K,E) = f^{(0)}(E) + f^{(1)}(E).K^2, \tag{1}$$

(i.e. only neglecting the contribution of terms of a higher order than $K^2$; E is the energy loss). The two measured values of $f(K,E)$ on the same relative scale and a normalization of $f^{(0)}$, were used to solve the two unknowns, $f^{(0)}$ (the optical oscillator strength for absorption) and $f^{(1)}$, the derivative with respect to $K^2$ of the G.O.S. at zero momentum transfer. This analysis and its reliability has been discussed in more detail in an earlier publication (Backx et al. 1975 a) in particular with regard to the proper integration over all momentum transfers involved at two scattering angles.

In the second mode of operation, the parent ions, i.e. $H_2^+$, $D_2^+$ and $HD^+$, have been measured in coincidence with the electrons scattered only in the forward direction in order to obtain the G.O.S. at the smallest momentum transfer ($\sim 0.01$ a.u.) for the formation of parent ions at energy losses from the I.P. to 80 eV. The fast logic coincidence circuit, which simultaneously selects true and accidental coincidences and stores the true signal in a bidirectional counter, has been described earlier (Van der Wiel and Wiebes 1971).

In the third mode, the contribution of dissociative ionization with respect to the formation of parent ions was obtained by recording mass spectra at various settings of the energy loss of the forward scattered electrons. For this purpose we used a time-to-amplitude converter (T.A.C.) which was started by a scattered electron and stopped by the corresponding ion after a sharply defined time interval (peak halfwidth 20 nsec.). The output pulses of the T.A.C. were stored in an on-line D116 Nova minicomputer, which operated as a pulse height analyser. The time-of-flight spectra were processed in the following way. A smooth background of accidental coincidences was generated by making a least squares fit of a function
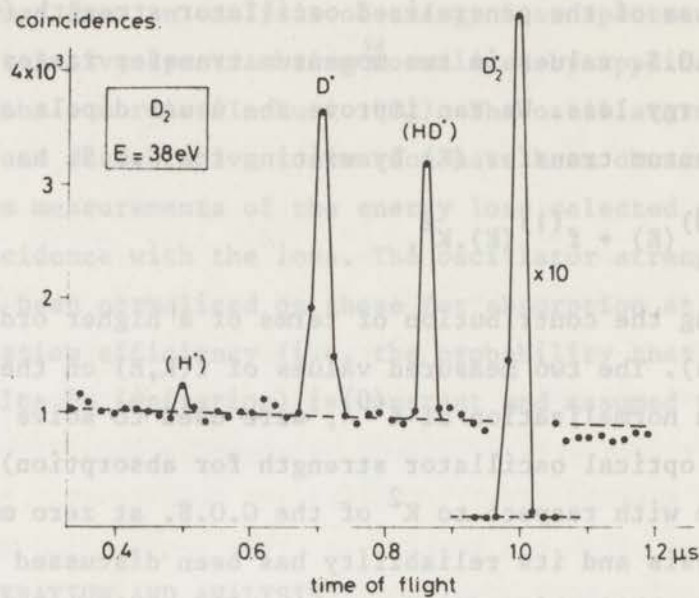
Fig. 1 - Coincidence time-of-flight spectrum of ions formed in $D_2$ by 8 keV

electron impact at an energy loss of 38 eV. The impurity peaks

in the spectrum and the correction for the background of

accidental coincidences are discussed in section 3. The accumulation

time of this spectrum was 15 min.

of the form $Ce^{-\alpha n}$ (in which n is the channel number and $\alpha$ depends on the random countrate of the stop pulses) to the data points in regions where no peaks were present. This accidental background was subtracted from the time-of-flight spectrum and the counts in each of the peak channels were added up. Although the sloping of the background was never more than 4% over the whole spectrum, a dead time correction (which varies with channel number) of the peak intensities was extracted from the slope.

Figure 1 shows a time-of-flight spectrum of $D_2$ at an energy loss of 38 eV. The dashed line is the least-squares fit to the background. The background beyond the $D_2^+$ peak is $\sim$ 10% lower than the fitted background; this effect arises because the ion extraction is so efficient that 10% of the scattered electrons were coincident with $D_2^+$ ions at this energy loss. Therefore, in 10% of the cases that the T.A.C. was started by a scattered electrons, it is stopped at the $D_2^+$ peak. Therefore, 10% of the start pulses did not contribute to the background in the region after the $D_2^+$ peak, and for this reason it has not been used in the background fit.

The purity of the gases was checked by recording mass spectra which showed that $H_2$ was pure, $D_2$ contained 4% HD and HD contained 1% $D_2$ and a small amount of water. Since we measured the fragmentation spectra of all three gases, corrections could easily be made for the small impurities of the isotopes. Although the base pressure in the apparatus was $5 \times 10^{-8}$ Torr, the $H^+$ peak in the $H_2$ measurements had to be corrected for the contribution of water present in the background gas. This correction was known from the $D_2$ spectra and was less than 1% for energy transfers up to 30 eV and gradually rose to 5% at higher energy transfers. A correction for $H^+$ from water present in the HD sample was made using the photoionization data on water of Cairns et al. (1971). The relative detection efficiency of the CuBe (Johnston MM-1) ion detector for the various ions was not calibrated. However, an accurate measurement was made of the $H^+/D^+$ intensity ratio from HD at energy losses of 21, 24 and 30 eV. At these energies one is sufficiently far above the dissociation limits $H^+ + D$ and $D^+ + H$ to expect complete Demkov coupling (Demkov 1964) of the two states involved, $1s\sigma_g^*$ and $2p\sigma_u$, which results in equal intensities for the two fragments.

---

\* For convenience we give the symmetry of the occupied orbital to characterize the electronic state of the molecular ion.
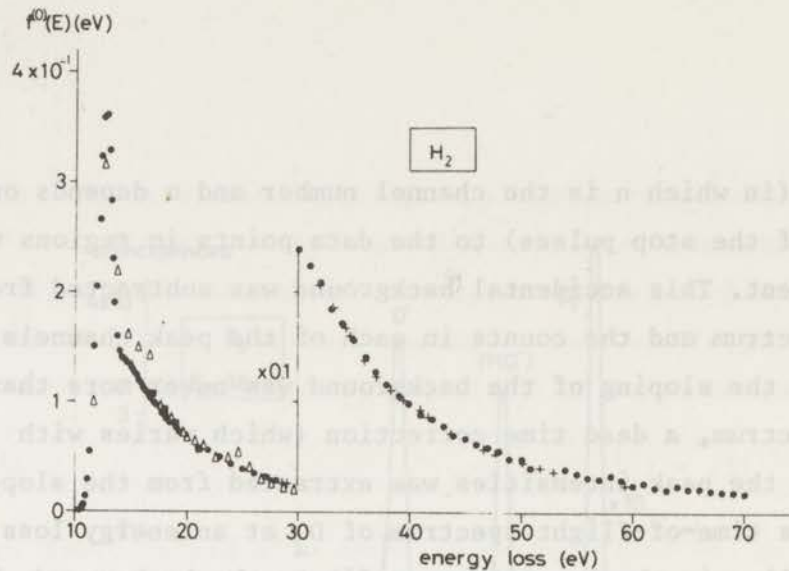
Fig. 2 - Absorption oscillator strength spectrum of $H_2$. ● - this work,

normalized on an integral value of two (T.R.K. sum rule) with

a 1% correction for energies beyond 80 eV; + - photoabsorption,

Samson and Cairns (1965); ■ - Cook and Metzger; Δ - extrapolation

of G.O.S. obtained at 461 eV impact energy, Lassettre and Jones
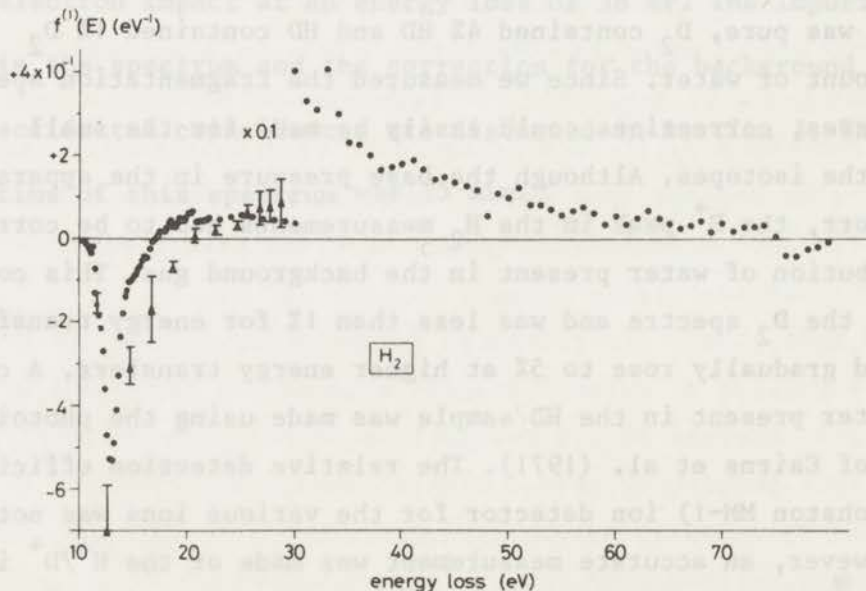
(1964).



Fig. 3 - Derivative of the G.O.S. with respect to $K^2$, at $K^2 = 0$. (K in a.u.)

● - this work (absolute value based on the normalization of the

optical term, fig. 2). Δ - from analysis of the G.O.S. of

Lassettre and Jones (1964) over a range of $K^2$ from 0.05 to 0.2 a.u.

Furthermore the correction for the $H_2O$ impurity is only 4% at these energies. The measured ratios were: $H^+/D^+$ = 1.02 ± 0.06, 1.01 ± 0.06, 1.01 ± 0.05 at 21, 24 and 30 eV respectively. From these ratios we concluded that the efficiency was the same for all ions, at least to an accuracy which cannot easily be improved by doing an actual comparison of DC currents versus ion count rates.

## 3. RESULTS AND DISCUSSION

### 3.1 *Optical Oscillator Strengths for absorption of $H_2$*

Using the procedure described in 2, we obtained the optical oscillator strengths $f^{(0)}(E)$ for absorption of $H_2$ as given in figure 2 and Table I. Normalization was provided by the T.R.K.-sum rule, that is the integrated optical oscillator strength spectrum including an estimated contribution of 1% from energy losses higher than 80 eV, was normalized to 2. Results from photoabsorption experiments by Cook and Metzger (1964) and Samson and Cairns (1965) have also been plotted in the figure. The agreement with the data of Samson and Cairns is within a few percent, which is much better than the 10% accuracy claimed for the optical data. The results of Cook and Metzger deviate more from our spectrum, however the numbers had to be obtained from a logarithmic plot.

Lassettre and Jones (1964) measured the G.O.S. of $H_2$ at four momentum transfers smaller than 0.2 a.u. for energy losses up to 28 eV, using an electron impact energy of 461 eV. The values they found by extrapolating the G.O.S. to $K^2$ = 0 have also been plotted in the figure. The accuracy of their optical values is not high, mainly because of uncertainties in the extrapolation.

### 3.2 *Derivative of the G.O.S. at $K^2 = 0$*

The derivative with respect to $K^2$ of the G.O.S. at $K^2$ = 0, $f^{(1)}$, as obtained by the procedure described in 2, has been plotted in figure 3. The only earlier data pertaining to this subject are those

TABLE I.  Oscillator strengths of $H_2$

| E(eV) | $f^{(0)}(10^{-2}eV^{-1})$ absorpt | $*H_2^+$ | E(eV) | $f^{(0)}(10^{-2}eV^{-1})$ absorpt | $*H_2^+$ | E(eV) | $f^{(0)}(10^{-2}eV^{-1})$ absorpt | $*H_2^+$ |
|---|---|---|---|---|---|---|---|---|
| 10 | 0.08 | | 20 | 6.95 | 6.82 | 40 | 0.99 | 0.89 |
| 10.5 | 0.26 | | 21 | 6.25 | 6.13 | 42 | 0.84 | 0.75 |
| 11 | 1.70 | | 22 | 5.51 | 5.40 | 44 | 0.71 | 0.63 |
| 11.5 | 7.66 | | 23 | 4.92 | 4.82 | 46 | 0.65 | 0.58 |
| 12 | 20.7 | | 24 | 4.38 | 4.30 | 48 | 0.61 | 0.54 |
| 12.5 | 34.1 | | 25 | 3.92 | 3.83 | 50 | 0.48 | 0.42 |
| 13 | 32.5 | | 26 | 3.49 | 3.42 | 52 | 0.41 | 0.36 |
| 13.5 | 21.2 | | 27 | 3.24 | 3.15 | 54 | 0.39 | 0.34 |
| 14 | 14.9 | | 28 | 2.89 | 2.81 | 56 | 0.32 | 0.28 |
| 14.5 | 13.8 | | 29 | 2.68 | 2.58 | 58 | 0.33 | 0.28 |
| 15 | 13.3 | 0.53 | 30 | 2.46 | 2.35 | 60 | 0.24 | 0.20 |
| 15.5 | 12.6 | 4.73 | 31 | 2.27 | 2.15 | 62 | 0.23 | 0.20 |
| 16 | 11.7 | 8.68 | 32 | 2.06 | 1.93 | 64 | 0.23 | 0.20 |
| 16.5 | 10.8 | 9.74 | 33 | 1.90 | 1.76 | 66 | 0.21 | 0.18 |
| 17 | 10.1 | 9.63 | 34 | 1.72 | 1.58 | 68 | 0.19 | 0.17 |
| 17.5 | 9.58 | 9.60 | 35 | 1.55 | 1.36 | 70 | 0.16 | 0.14 |
| 18 | 8.83 | 8.91 | 36 | 1.39 | 1.18 | | | |
| 18.5 | 8.25 | 8.50 | 37 | 1.31 | 1.14 | | | |
| 19 | 7.85 | 7.97 | 38 | 1.29 | 1.04 | | | |
| 19.5 | 7.25 | 7.41 | 39 | 1.10 | 0.94 | | | |

+  In part of the spectrum more data points were measured than given in the table (see fig. 2); for those regions the table lists an average over the interval of the table.

*  $f^{(0)}(H_2^+) = f_{abs}^{(0)} \cdot \eta_i/(1+H^+/H_2^+)$, where for $\eta_i$ the smooth curve through the measured data points of fig. 4 was used and $H^+/H_2^+$ is given in Table II.

of Lassettre and Jones (1964), already referred to in the previous section. A derivative could be obtained from the slope of a straight line drawn through their G.O.S.-values for $K^2 < 0.2$. The results of such an analysis has also been plotted in figure 3. Although the general trend is similar there is an appreciable discrepancy with our results. Partly, this could be due to uncertainties in the straight line fit as indicated by the error bars we assigned to the triangles in figure 3. Apart from that, it could be pointed out that a correlation exists between the deviations of Lassettre and Jones' $f^{(0)}$ from the optical values and that of their $f^{(1)}$ values from ours. A check on our $f^{(1)}$ spectrum is provided by the application of a sum rule (Inokuti 1971):

$$\int_0^\infty f^{(1)}(E)dE = 0 \qquad (2)$$

The part of this integral from 0 to 80 eV energy loss yields $-0.02$, which in order to estimate the accuracy should be compared with the analogous integral of $|f^{(1)}|$ yielding 2.17.

### 3.3 Ionization efficiency and discrete excitation

From our results on $f^{(0)}$ and $f^{(1)}$ for absorption the application of eq. 1 shows that the contribution of the $f^{(1)}$-term to the "forward" scattering intensities is at most 2%. For this reason we did not determine $f^{(1)}$ for ionization separately, but restricted the measurements to forward scattering. The following procedure was adopted to determine $f^{(0)}$ for ionization:

- the G.O.S. of $H_2^+$ was derived from the "forward" energy loss spectrum (15 to 60 eV) recorded in coincidence with $H_2^+$ ions selected by their time-of-flight.
- the intensity ratio of $H^+/H_2^+$ was measured from ion T.O.F. spectra at energy losses over the same range, under the same scattering conditions.
- the total G.O.S. for ionization, i.e., $(1 + H^+/H_2^+)$ times the G.O.S. of $H_2^+$, was devided by the corresponding quantity for absorption to give an ionization efficiency (fig. 4). This relative efficiency $\eta_i$ was
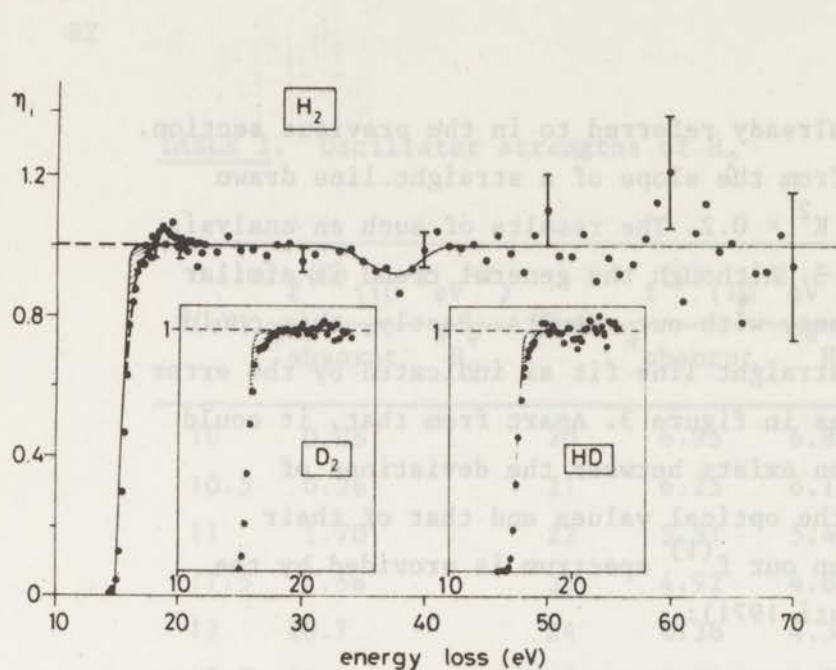
Fig. 4
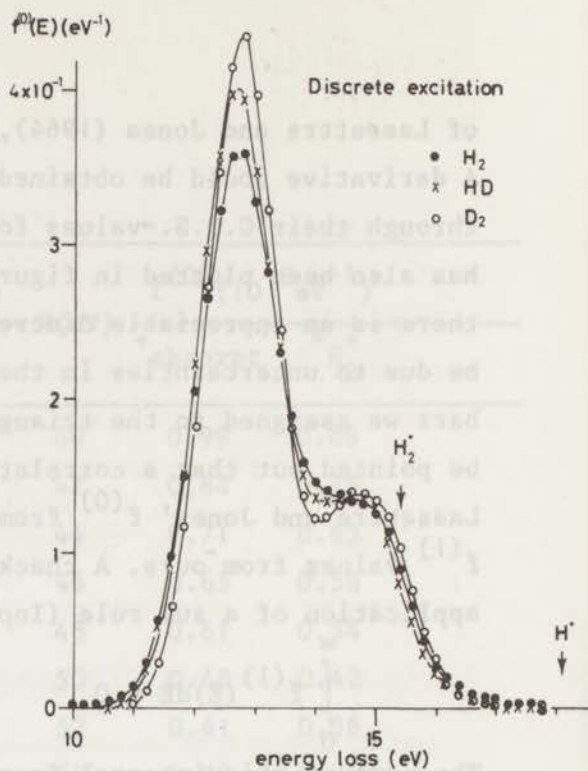
Fig. 5

Fig. 4 - Ratio of the G.O.S. for ionization and absorption of $H_2$ as

obtained from forward scattering intensities ($K^2 \sim 0.01$ a.u.).

The absolute scale is obtained by normalizing the average of

the ratios at energy losses of 18-34 eV and 44-70 eV to unity.

In section 4.2 reasons are given for considering the spectrum as

essentially representing the photoionization efficiency. The

insets show the ionization efficiency of HD and $D_2$ in the

vicinity of the threshold for ionization. The full curves at

threshold represent a step function folded with the energy loss

resolving power (0.5 eV). The shaded areas then represent the

contribution of superexcited states.

Fig. 5 - Difference of absorption and ionization oscillator strengths;

● - $H_2$; x - HD and ○ - $D_2$. The integrated oscillator strengths

below and above the I.P. are quoted in section 4.2

found to be constant above 18 eV, and for that reason was normalized
to unity in that region (except for a few points around 37 eV, which
are lower than the adjacent regions). The spectrum of $\eta_i$ can be
considered to be essentially that for photoionization, since firstly
the $f^{(1)}$ contribution is very small and secondly this contribution
is the same for ionization and aborption if $\eta_i$ is close to
unity.

- Given this $\eta_i$ for photoionization, $f^{(0)}$ $(H^+ + H_2^+)$ was obtained as the
  product of $\eta_i$ (the smooth curve in figure 4) and the $f^{(0)}$ for
  absorption (section 3.1).

The same procedure has been employed for $D_2$ and HD with the restriction
that the G.O.S. derived from "forward" scattering for $HD^+$ and $D_2^+$ has
been measured only up to 20 eV energy loss. Above this energy the
oscillator strengths for total ionization were taken to be equal to
that of $H_2$.

There are two regions in the ionization efficiency curve where
$\eta_i$ (E) (figure 4), is lower than unity (below 18 eV and around 37 eV).
Below 18 eV the oscillator strength for total ionization has been
subtracted from that for absorption to obtain spectra of excitation of
$H_2$, HD and $D_2$ as plotted in figure 5. The absorption and ionization
spectra of $D_2$ and HD have only been measured up to 20 eV, since above
this energy these spectra are expected to be identical to the
corresponding spectra of $H_2$ and were normalized on the $H_2$ spectra at 20 eV.
The integrated oscillator strengths of the $H_2$, HD and $D_2$ neutral
excitation spectra in figure 5 are essentially equal and amount to
$8.6 \times 10^{-1}$, $8.8 \times 10^{-1}$ and $8.8 \times 10^{-1}$ for $H_2$, HD and $D_2$ respectively.
The differences in the spectral distribution of the different isotopes
must therefore be attributed to a change in Franck-Condon factors of
the various excited states, which in emission give rise to the Lyman,
Werner and higher band systems, while the electronic transition
matrix elements remain the same. Since the heavier isotopes have a
smaller zero point vibrational energy in the ground state, the excitations
will take place over a smaller range of internuclear distances, resulting
in more sharply peaked Franck-Condon envelopes. This effect has been

TABLE II. Fragmentation ratios of $H_2$ and $D_2$ [*].

| E(eV) | $H^+/H_2^+$ ($\times 10^{-2}$) | $D^+/D_2^+$ ($\times 10^{-2}$) | E(eV) | $H^+/H_2^+$ ($\times 10^{-2}$) | $D^+/D_2^+$ ($\times 10^{-2}$) | E(eV) | $H^+/H_2^+$ ($\times 10^{-2}$) | $D^+/D_2^+$ ($\times 10^{-2}$) |
|---|---|---|---|---|---|---|---|---|
| 18 | 0.33 | 0.20 | 22 | 2.04 | 0.66 | 30 | 4.44 | 2.15 |
| 18.2 | 0.72 | 0.29 | 22.2 | 1.96 | 0.65 | 31 | 5.36 | 3.21 |
| 18.4 | 1.17 | 0.31 | 22.4 | 1.87 | 0.76 | 32 | 6.96 | 4.38 |
| 18.6 | 1.08 | 0.53 | 22.6 | 1.97 | 0.55 | 33 | 7.95 | 6.92 |
| 18.8 | 1.43 | 0.53 | 22.8 | 1.92 | 0.58 | 34 | 8.65 | 8.40 |
| 19 | 1.52 | 0.52 | 23 | 1.97 | 0.78 | 35 | 9.49 | 8.68 |
| 19.2 | 1.57 | 0.65 | 23.2 | 1.85 | 0.52 | 36 | 9.29 | 8.25 |
| 19.4 | 1.59 | 0.48 | 23.4 | 2.08 | 0.84 | 37 | 7.96 | 7.32 |
| 19.6 | 1.70 | 0.60 | 23.6 | 2.21 | 0.79 | 38 | 7.78 | 7.07 |
| 19.8 | 1.86 | 0.48 | 23.8 | 2.03 | 0.76 | 39 | 8.74 | 8.04 |
| 20 | 1.72 | 0.70 | 24 | 2.00 | 0.67 | 40 | 9.94 | 9.21 |
| 20.2 | 1.90 | 0.64 | 24.2 | 1.98 | 0.88 | 45 | 12.1 | 11.4 |
| 20.4 | 1.94 | 0.74 | 24.4 | 2.04 | 0.60 | 50 | 13.6 | 11.7 |
| 20.6 | 1.79 | 0.60 | 24.6 | 2.12 | 0.89 | 55 | 15.4 | 12.8 |
| 20.8 | 1.88 | 0.75 | 24.8 | 2.23 | 0.56 | 60 | 16.8 | 13.4 |
| 21 | 1.86 | 0.62 | 25 | 2.04 | 0.85 | 65 | 14.4 | 13.8 |
| 21.2 | 1.88 | 0.64 | 26 | 2.21 | 0.94 | 70 | 17.6 | 14.8 |
| 21.4 | 1.94 | 0.63 | 27 | 2.46 | 1.12 | | | |
| 21.6 | 1.92 | 0.76 | 28 | 3.22 | 1.56 | | | |
| 21.8 | 1.92 | 0.77 | 29 | 3.92 | 1.85 | | | |

[*] Ratios above 40 eV are three-point averages of the actual data points (fig. 9).

also demonstrated by high resolution electron energy loss measurements
of these band systems made by Geiger and Schmoranzer (1969), which
provide the Franck-Condon factors for the various bands separately.

Above the ionization potential, which is approximately 15.4 eV for
all isotopes, the oscillator strengths for discrete excitation do not
drop to zero with the halfwidth of the energy resolution of these spectra
(0.5 eV). This gives evidence for the existance of superexcited states,
that is Rydberg states converging to highly vibrationally excited states
of $H_2^+$. Chupka and Berkowitz (1969) reported high resolution (0.04 Å)
photon impact mass spectrometric data of $H_2^+$ from 15.3 to 16.6 eV, which
unambiguously showed the important role of autoionization in this
energy range. In the decay of these superexcited states three exit
channels are in competition: autoionization, fluorescence and predisso-
ciation. Since a predissociation time depends on the reduced mass of
the molecule, an important contribution of predissociation to the
decay of the superexicted states might lead to a smaller oscillator
strength for neutral excitation for the heavier isotopes. However,
no such systematic behaviour appears from the present neutral
oscillator strengths, which integrated from 15.4 to 18 eV, lead to
values of $4.8 \times 10^{-2}$, $4.1 \times 10^{-2}$ and $5.4 \times 10^{-2}$ for $H_2$, HD and $D_2$
respectively. That no appreciable isotope effect is seen, may be partly
due to the limited accuracy of the oscillator strength for discrete
excitation, which is the small difference of two spectra, and partly
to a compensating change of Franck-Condon factors in the excitation
process. Fluorescence from superexcited states of $H_2$ has been reported
by Guyon (1974).

Within the accuracy of the ionization efficiency spectrum (figure 4)
the only other energy range giving evidence for the production of neutral
dissociation fragments from $H_2$ is that around 37 eV energy loss. A
doubly excited state has been reported by Misakian and Zorn (1972),
who measured the energy and angular distributions of H(2s) atoms as
a function of electron impact energy. The state was designed to be a
$^1\Pi_u$ state with an appearance potential of 32 eV, having the dissociation
limit H(2s) + H(2p). The evidence from this work for the production of
neutrals around 37 eV is presumably connected with this state.
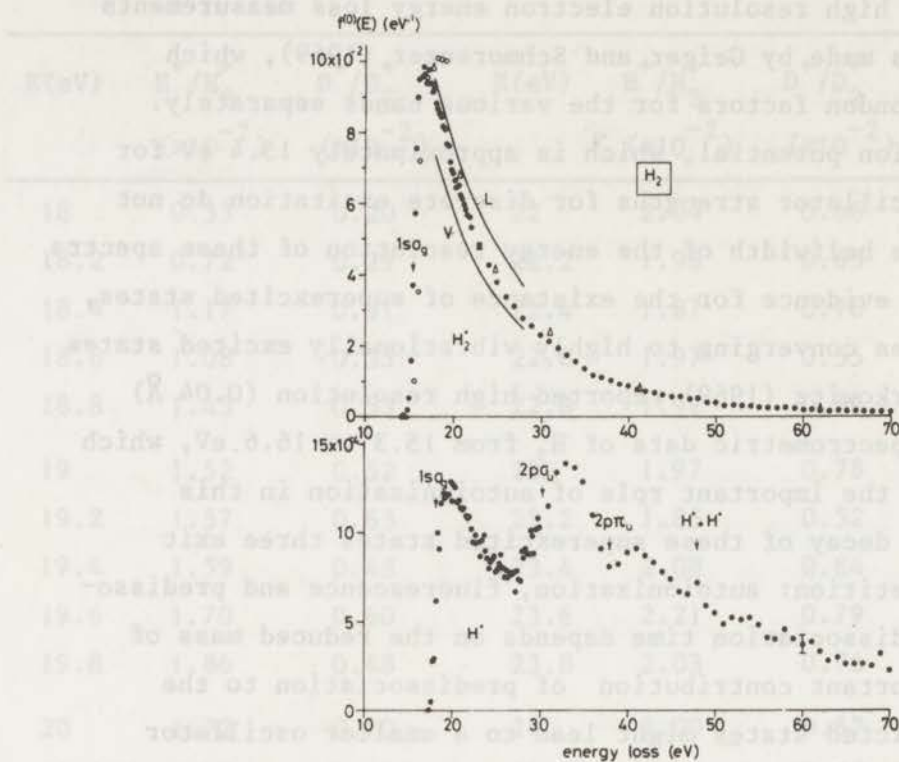
Fig. 6 - a. Oscillator strength of $H_2^+$. • - this work; $\Delta$ - photoionization,

Samson et al. (1974); $\bigcirc$ - theory total ionization, Flannery

and Öpik (1965); solid curve - theory total ionization, Kelly

(1973) (L=dipole length); (V=dipole velocity)

b. Oscillator strength of $H^+$. The spectrum is free from

discrimination against fast fragments, since no states of $H_2^+$

are known that produce fragments of more than 20 eV kinetic

energy. The onsets of the various excited ion states are

indicated at the minimum energies required for a vertical

transition from the outer classical turning point of the $H_2$

ground state (see figure 7).

## 3.4 Oscillator strengths of $H_2^+$ and $H^+$

The $H^+/H_2^+$ ($D^+/D_2^+$) fragmentation ratios were used to redistribute the total optical oscillator strengths for ionization obtained in 3.3 over the two ionic channels. This procedure leads to a $f^{(0)}$ spectrum for $H_2^+(D_2^+)$ with better statistical accuracy than the G.O.S. spectrum from the coincidence measurement at forward scattering, while also the error due to non-dipole terms is much smaller than 2%. For $H^+(D^+)$ the restriction has to be made that our analysis does not guarantee the $f^{(1)}$ contribution to be small also for a fragment of such low abundance. It should be noted however, that the ratios of $H^+$ to $H_2^+$ and $D^+$ to $D_2^+$ reported by Browning and Fryar (1973) at a number of photon impact energies below 30 eV are in excellent agreement with our fragment ratios plotted in figure 9.

The $H_2^+$ and $H^+$ spectra are presented in figure 6 and tables I and II. The only photoionization measurements that have been performed over a large continuous energy range are those of Samson et al. (1975), who reported absolute values for total ionization. A few points of their curve are plotted in figure 6; the points are about 4% higher than the sum of our $H_2^+$ and $H^+$ results (note the different scales for $H_2^+$ and $H^+$). Calculations on total photoionization have been made by Flannery and Öpik (1965) up to 18 eV and Kelly (1973) up to 30 eV energy loss, and these results have also been plotted in the figure. The $H_2^+$ spectrum (I.P. = 15.4 eV) has a large scale behaviour rather similar to that of atomic hydrogen, that is a maximum value at threshold and a smooth decrease towards higher energy (except for considerable structure in the first 2 eV above threshold, Chupka and Berkowitz 1969), without showing any structure from ionic states higher than the $1s\sigma_g$. Since all higher ionic states known are repulsive, more structure appears in the $H^+$ spectrum (figure 6). The arrows in this spectrum indicate the onsets of higher ionic states obtained by drawing vertical lines in the potential energy diagram of $H_2$ (Sharp 1971) from the "right hand" classical turning point of the ground state up to the repulsive curves of $H_2^+$ (see figure 7 for the most important states).
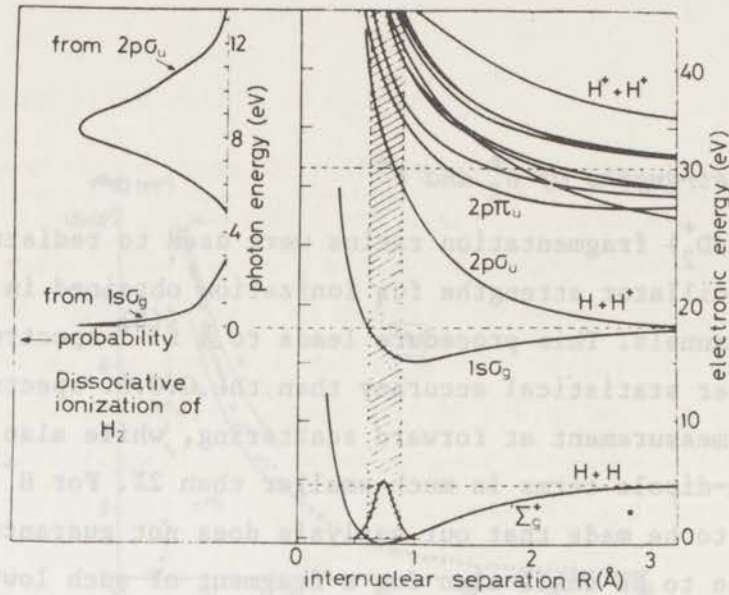
Fig. 7 - Potential energy diagram for the ground state of $H_2$, some

of the states of $H_2^+$, and $H_2^{++}$ (taken from Dunn (1963)). The

energy scale is relative to the ground vibrational level

of $H_2$. On the left is indicated the expected energy distri-

bution of protons from the $1s\sigma_g$ and $2p\sigma_u$ states of $H_2^+$. The

relative heights of these two curves are not to be compared.
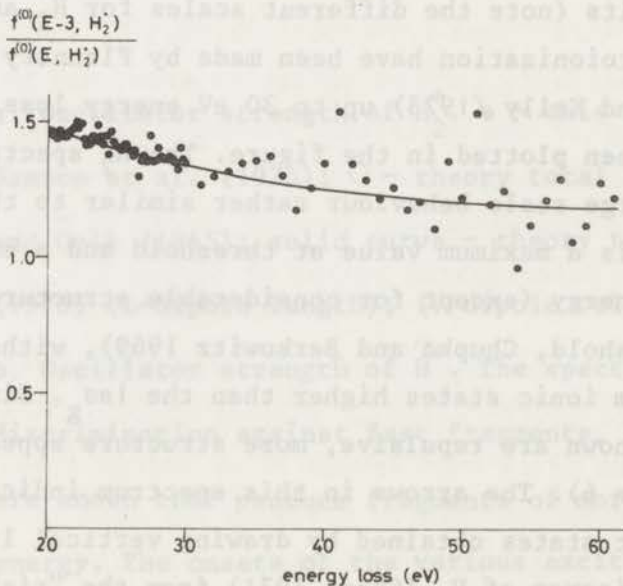


Fig. 8 - Ratio of $f^{(0)}(H_2^+)$ at the endpoints of 3 eV intervals (E = energy

loss). This ratio represents an estimate of the ratio of

electronic transition matrix elements for excitation to the

repulsive and bound part of the $1s\sigma_g$ state of $H_2^+$ as a function

of energy loss (see section 4.5).

## 3.5 Ratio of $H^+$ and $H_2^+$ formed by the $1s\sigma_g$ state

Close above threshold (18.1 eV) $H^+$ is only formed by excitation to the repulsive part of the $1s\sigma_g$ state having a small vibrational overlap with the ground state of $H_2$. There has been some discussion about the discrepancy between experiment and theory as regards the amount of $H^+$ with respect to $H_2^+$ that is formed from the $1s\sigma_g$ state of $H_2^+$ (Dunn 1966, Browning and Fryar 1973). This will be shown to be caused mainly by the variation of the electronic transition matrix element as a function of the energy of the ejected electron. Since our experiment yields accurate ratios for $H_2$ and its two isotopes, we shall deal with this problem in some detail. In the Born-Oppenheimer approximation the ratio of oscillator strengths of $H^+$ and $H_2^+$ from the $1s\sigma_g$ state can be written as:

$$\frac{f^{(0)}(E,H^+)}{f^{(0)}(E,H_2^+)} = \frac{\int\limits_{u=18.1}^{E} M_e^2(E-u,\overline{R})\ q(u)\ du}{\sum\limits_{u=15.4}^{18.1} M_e^2(E-u,\overline{R})\ q(u)} , \qquad (3)$$

where $q(u)$ is the Franck-Condon factor for excitation to the vibrational state or continuum with ionization potential $u$ and $M_e(E-u,\overline{R})$ is the electronic transition matrix element for excitation to the $1s\sigma_g$ state as a function of the energy of the ejected electron (the difference of the energy loss $E$ and the ionization potential $u$) and of the internuclear distance $R$. This internuclear distance has been taken equal to the average $R$ over which the transition takes place, $\overline{R}$ (which was assumed to be the same for excitation to the bound and the repulsive part). In order to make a comparison of calculated Franck-Condon factors with the results of this experiment we have to make the following approximation. Since $M_e^2(\epsilon,\overline{R})$ (see fig. 6) is a smooth function of $\epsilon = E-u$ and $q(u)$ has only a value over a small range of $u$, we may write for eq. (3),

$$\frac{f^{(0)}(E,H^+)}{f^{(0)}(E,H_2^+)} = \frac{M_e^2(E-\overline{u}(rep),\overline{R})}{M_e^2(E-\overline{u}(bound),\overline{R})} \cdot \frac{\int\limits_{u=18.1}^{E} q(u)\ du}{\sum\limits_{u=15.4}^{18.1} q(u)} \qquad (4)$$

92
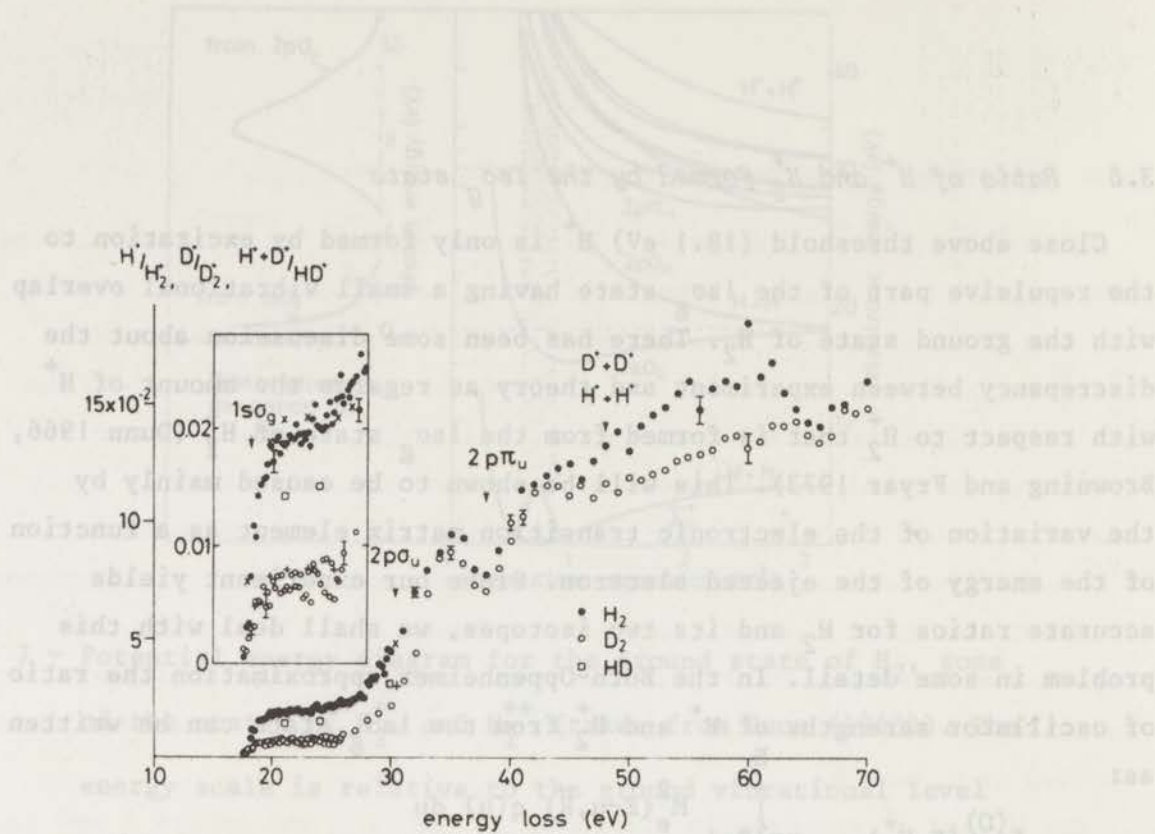


Fig. 9 - Ratio of fragment-to-parent ion production in $H_2$, HD and $D_2$.

● - $H_2$, □ - HD, ○ - $D_2$, this work; x - $H_2$, + - $D_2$, Browning and Fryar (1973). The "plateau" values for $1s\sigma_g$ ionization, evaluated over the energy range 23-24 eV, amount to (in percents) 2.02±0.11, 1.51±0.10 and 0.73±0.11 for $H_2$, HD and $D_2$ respectively.

where $\bar{u}$(bound) is the average of the ionization potentials of the bound vibrational levels of $H_2^+$ weighted by the Franck-Condon factors and $\bar{u}$(rep) the same for the repulsive part. $\bar{u}$(bound) has been obtained from the Franck-Condon factors calculated by Dunn (1966) and is equal to 16.1 eV. For $\bar{u}$(rep) a value of 19.1 eV has been estimated from a graph by Dunn and Kieffer (1963) (see figure 7). If E is high enough, the ratio of the integrals of the Franck-Condon factors in eq. 4 becomes independent of E and can be replaced by:

$$\frac{\int\limits_{u=18.1}^{E} q(u)\, du}{\sum\limits_{u=15.4}^{18.1} q(u)} = \frac{1 - \sum\limits_{u=15.4}^{18.1} q(u)}{\sum\limits_{u=15.4}^{18.1} q(u)} \tag{5}$$

The variation of $M_e^2(\varepsilon,\bar{R})$ with $\varepsilon$ can be derived from the $H_2^+$ oscillator strength spectrum (figure 6) using the same approximation as in the denominator of eq. 4:

$$M_e^2(\varepsilon,\bar{R}) \sim f^{(0)}(\varepsilon + \bar{u}(\text{bound}), H_2^+) \tag{6}$$

The ratio of the electronic transition moments in eq. 4 is then obtained by substitution of eq. 6:

$$\frac{M_e^2(E-\bar{u}(\text{rep}),\ \bar{R})}{M_e^2(E-\bar{u}(\text{bound}),\ \bar{R})} = \frac{f^{(0)}(E-3, H_2^+)}{f^{(0)}(E, H_2^+)} \tag{7}$$

This ratio plotted in figure 8, makes it possible to derive the ratio of summed Franck-Condon factors (eq. 5) from the ratio of $H^+$ and $H_2^+$ given in figure 9. Only the six data points from 23 to 24 eV were used in the calculation. This energy range was chosen such that it was above the Franck-Condon region of the repulsive part and low enough to avoid contribution of Rydberg states converging to the $2p\sigma_u$ state of $H_2^+$. The ratio of Franck-Condon factors derived yields $0.0142 \pm 0.008$ for the $H_2$ molecule. This value may be used to check the accuracy of calculated Franck-Condon factors to the discrete vibrational states. The sum over all these states may be substituted in equation 5 to reproduce our ratio, which is a sensitive test
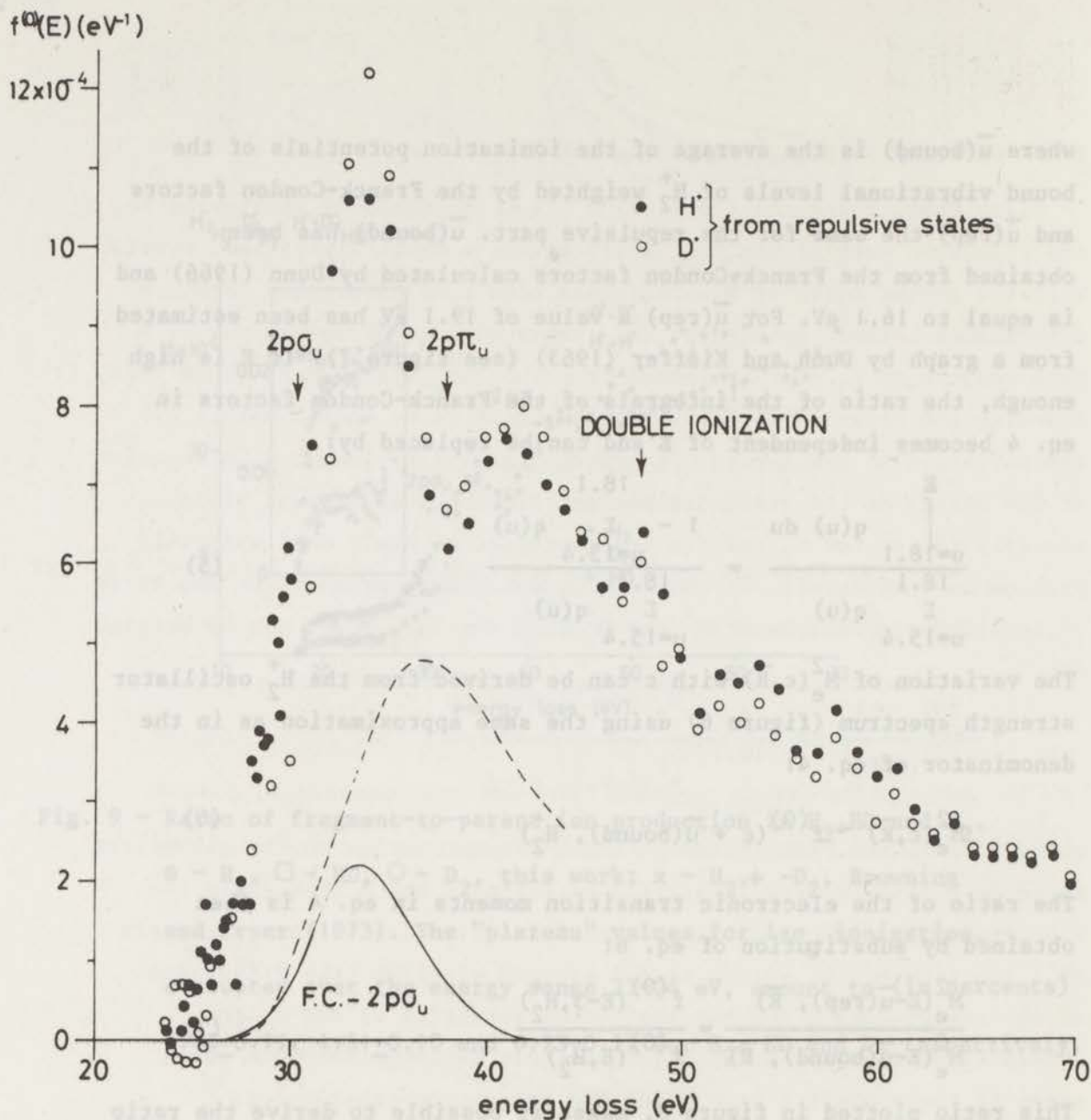
Fig. 10- Oscillator strengths for $H^+$ from $H_2$ and $D^+$ from $D_2$, formed by excitation to ionic states above the $1s\sigma_g$. The spectra are obtained by subtracting from the total $H^+$ and $D^+$ spectrum (fig. 6b) the contribution of the $1s\sigma_g$ state, using $f^{(0)}(E, H^+, 1s\sigma_g) = 0.0142 \times f^{(0)}(E-3, H_2^+)$ (see section 4.6).

Full curve: Franck-Condon envelop for excitation to the $2p\sigma_u$ state of $H_2^+$ (arbitrary scale).

Dashed curve: Expected oscillator strength distribution of $H^+$ produced by excitation to the $2p\sigma_u$ state of $H_2^+$ when it is estimated that $M_e^2(\varepsilon, 2p\sigma_u) = M_e^2(\varepsilon, 1s\sigma_g)$ (see section 4.6).

because the numerator is small. The Franck-Condon factors caculated by Dunn (1966) lead to a ratio of $2.8 \times 10^{-2}$, while the calculations of Villarejo (1968) predict a ratio of $1.47 \times 10^{-2}$. Browning and Fryar (1973), using the reflection approximation and data of Flannery and Öpik (1965), calculated a ratio of $1.34 \times 10^{-2}$. Our ratio of $D^+$ and $D_2^+$ from $D_2$, also plotted in figure 9, has been used in the same way as for $H_2$ to obtain the ratio in eq. 5, which yielded $0.0073 \pm 0.0008$. For HD one accurate ratio of $H^+ + D^+$ and $HD^+$ at 24 eV was used, which yielded a value of $0.0106 \pm 0.0008$. In table III the numbers are compared with calculations of the Franck-Condon factors.

## 3.6  $H^+$ ($D^+$) oscillator strengths above 25 eV

With the exception of the $1s\sigma_g$ state, no other ionic states of $H_2$ are known to be bound (around the equilibrium internuclear distance of the groundstate). From section 3.5 (eq. 4 and 7) it then follows that the oscillator strength for formation of $H^+$ by direct ionization into the $1s\sigma_g$ continuum is given by

$$f^{(0)}(E,H^+,1s\sigma_g) = 0.0142 \times f^{(0)}(E-3,H_2^+) \tag{8}$$

This estimated contribution of the $1s\sigma_g$ state to the formation of $H^+$ has been subtracted from the oscillator strength spectrum of $H^+$ (figure 6) to obtain the $H^+$ spectrum from states higher than the $1s\sigma_g$, as plotted together with the analogous spectrum of $D^+$ from $D_2$ in figure 10. The spectra of $H^+$ and $D^+$ are nearly identical, which is to be expected because the potential energy curves of $H_2$ and $D_2$ are the same and the difference in Franck-Condon envelopes is very minor (see e.g. Kieffer and Dunn 1967 for the $2p\sigma_u$ state). The Franck-Condon envelope for ionization of $H_2$ ($D_2$) to the $2p\sigma_u$ continuum as calculated by Kieffer and Dunn, has been drawn on an arbitrary scale in the figure (solid curve). Already at 25 eV there is a contribution to $H^+$ ($D^+$) formation from states higher than the $1s\sigma_g$, while the next state ($2p\sigma_u$) is not expected to set in below 28 eV. This onset at 25 eV must therefore be due to autoionizing states, presumably Rydberg states

TABLE III. Ratio of integrated Franck-Condon factors for excitation to the repulsive and bound parts of the $1s\sigma_g$ state of $H_2^+$.

$$1 - \sum_{u=15.4}^{18.1} q(u) \Big/ \sum_{u=15.4}^{18.1} q(u) \quad \text{of } 1s\sigma_g \text{ state}$$

| Isotope | Experiment | | Theory | | |
| | this work | Browning and Fryar * | Dunn | Villarejo | Browning and Fryar |
|---|---|---|---|---|---|
| $H_2$ | $(1.42\pm0.08)\times10^{-2}$ | $(1.45\pm0.12)\times10^{-2}$ | $2.8\times10^{-2}$ | $1.45\times10^{-2}$ | $1.34\times10^{-2}$ |
| HD | $(1.06\pm0.08)\times10^{-2}$ | - | - | - | - |
| $D_2$ | $(0.51\pm0.08)\times10^{-2}$ | $(0.57\pm0.06)\times10^{-2}$ | $0.63\times10^{-2}$ | $0.52\times10^{-2}$ | - |

* We used the ratio of $M_e^2$ values for excitation to the bound and repulsive part of the $1s\sigma_g$ state as given in figure 8 to convert the $H^+/H_2^+$ ($D^+/D_2^+$) intensity ratio of Browning and Fryar to the ratio of integrated F.C.-factors.

converging to the $2p\sigma_u$ state of $H_2^+$ ($D_2^+$). Energies of such states were calculated by Hazi (1973) and Bottcher (1974). A considerable amount of evidence for the importance of autoionizing states in the formation of $H^+$ in the energy range around 30 eV is available from measurements of the energy and angular distribution of $H^+$ ($D^+$) formed by electron impact. By measuring the angular distribution of protons formed by 33 eV electron impact, Brunt and Kieffer (1970) showed that at least two processes contributed to the formation of protons: a process which results in a $\cos^2\theta$ angular distribution (which is characteristic for a $^1\Sigma_g^+(1s\sigma_g) \rightarrow {}^2\Sigma_u^+(2p\sigma_u)$ transition) and a process leading to an isotropic $H^+$ distribution. They attributed the latter process to autoionization. Moreover, the autoionizing process was presumed to occur near the threshold of the $^1\Sigma_g^+ \rightarrow {}^2\Sigma_u^+$ ionizing transition, because the two contributions were quite insensitive to the electron impact energy. Prominent structure in the energy distribution of protons formed by electron impact has been reported by Crowe and McConkey (1973) and Stockdale et al. (1975). A discussion of the superexcited states involved has been given by Hazi (1973).

At first sight, the shoulder around 40 eV in the spectrum of figure 10 might only be attributed to the onset of the $2p\pi_u$ repulsive state of $H_2^+$ ($D_2^+$) on the tail of the $2p\sigma_u$ continuum. However this would require the oscillator strength of the $2p\sigma_u$ to drop much faster from 34 to 38 eV than might reasonably be expected, eg. by assuming that the electronic transition moment has a shape similar to that of the $1s\sigma_g$ state (dashed curve, arbitrary scale). The latter curve was obtained by integrating $M_e^2(\epsilon, 1s\sigma_g)$ over the Franck-Condon region of the $2p\sigma_u$ state (Kieffer and Dunn 1967): $f^{(0)}(E, H^+, 2p\sigma_u) =$
$= \int_u M_e^2(E-u, 1s\sigma_g) \cdot q(u, 2p\sigma_u)$. Therefore, the observed behaviour suggests either of two possibilities; first, there is a large contribution of autoionizing states in the vicinity of threshold of the $2p\sigma_u$ state (producing a peak with essentially the shape of the $2p\sigma_u$ F.C.-envelope) and second, there is a vibrationally broadened window resonance at 38 eV. The first suggestion is consistent with the experimental work quoted above on the energy and angular distribution of protons. The second suggestion should be considered in conjunction with the ionization

efficiency data (figure 4), which show that around 37 eV some neutral formation occurs. This would require the existence of a discrete state, which partly autoionizes and partly dissociates into excited neutrals. Such a state was reported by Misakian and Zorn (1972). They measured the formation of fast H(2s) atoms from $H_2$ by electron impact excitation and proved that these fast H(2s) atoms were originating from a $^1\Pi_u$ doubly excited state having the dissociation limit H(2s) + H(2p) and an appearance potential of 32 eV. The excitation function had the form expected for an optically allowed transition, while the angular distribution of the H(2s) atoms was according to a $^1\Sigma_g^+ \to {}^1\Pi_u$ excitation, That this $^1\Pi_u$ state also partially autoionizes has been discussed by Hazi (1973), who calculated the energies and lifetimes for autoionization of Rydberg states converging to the $2p\Pi_u$ state of $H_2^+$.

## 4. CONCLUSION

From a differential electron scattering experiment we have generated a set of optical oscillator strengths for absorption, ionization and dissociative ionization, which:

- are not based on the dipole approximation but contain an accurate correction for non-dipole terms of the generalized oscillator strength
- cover a sufficient energy range to allow normalization on the T.R.K. sum rule
- represent all dissociative ionization processes without discrimination against fragment energy.

In a 2 eV region immediately above the first I.P. superexcitation is observed. An isotope effect of the ionization efficiency in this region was not observed. Transitions to the $1s\sigma_g$ state of $H_2^+$ ($HD^+$, $D_2^+$) have been discussed in terms of the ratio $H^+/H_2^+$ ($H^+ + D^+/HD^+$, $D^+/D_2^+$). Since the variation of the electronic transition moment is known to a good approximation from the $H_2^+$ oscillator strength distribution, the pure vibrational overlap of the ground state with the bound and repulsive part of the $1s\sigma_g$ states of $H_2^+$, $HD^+$ and $D_2^+$ could be derived from these ratios.

From the spectral distribution of $H^+$ it is concluded that autoionization plays a significant role in the dissociative ionization of $H_2$ $(D_2)$. The autoionizing states are discussed in terms of Rydberg states converging to the $2p\sigma_u$ and $2p\pi_u$ states of $H_2^+$ $(D_2^+)$. Evidence has been given for the existence of a partially non-autoionizing state at 37 eV, which has been reported earlier and designated to be a $^1\Pi_u$ state.

## ACKNOWLEDGEMENTS

## REFERENCES

- C. Backx, R.R. Tol, G.R. Wight and M.J. Van der Wiel, 1975 a J.Phys.B. accepted for publication.
- C. Backx, G.R. Wight, R.R. Tol and M.J. Van der Wiel, 1975 b J.Phys.B to be published.
- C. Backx and M.J. Van der Wiel, 1975 J.Phys.B to be published.
- C. Bottcher, 1974 J.Phys.B., $\underline{7}$ L 352.
- R. Browning and J. Fryar, 1973 J.Phys.B, $\underline{6}$ 364.
- R.B. Cairns, H. Harrison and R.I. Schoen, 1971 J.Chem.Phys., $\underline{55}$ 4886.

- W.A. Chupka and J. Berkowitz, 1969 J.Chem.Phys., $\underline{51}$ 4244.

- F.J. Comes and W. Lessman, 1964 Z. Naturforsch. $\underline{19a}$ 508.

- G.R. Cook and P.H. Metzger, 1964 J.Opt.Soc.Am., $\underline{54}$ 968.

- A. Crowe and J.W. McConkey, 1973 a J.Phys.B., $\underline{6}$ 2088.

- A. Crowe and J.W. McConkey, 1973 b Phys.Rev.Letters, $\underline{31}$ 192.

- Yu.N. Demkov, 1964 Soviet Physics JETP, $\underline{18}$ 138.

- V.H. Dibeler, R.M. Reese and M. Kraus, 1965 J.Chem.Phys., $\underline{42}$ 2045.

- G.H. Dunn and L.J. Kieffer, 1963 Phys.Rev., $\underline{132}$ 2109.

- G.H. Dunn, 1966 J.Chem.Phys., $\underline{44}$ 2592.

- M.R. Flannery and U. Öpik, 1965 Proc.Phys.Soc., $\underline{86}$ 491.

- J. Geiger and H. Schmoranzer, 1969 J.Mol.Spectr., $\underline{32}$ 39.

- P.M. Guyon, 1974, private communication.

- A.U. Hazi, 1973 Abstracts of VIII ICPEAC Beograd, Edts. B.C. Cobić and M.V. Kurepa, p. 542.

- M.Inokuti, 1971 Rev.Mod.Phys., $\underline{43}$ 297.

- H.P. Kelly, 1973 Chem.Phys.Letters, $\underline{20}$ 547.

- E.N. Lassettre and A.E. Jones, 1964 J.Chem.Phys., $\underline{40}$ 1222.

- K.E. McCulloh and H.M. Rosenstock, 1968 J.Chem.Phys., $\underline{48}$ 2084.

- M. Misakian and J.C. Zorn, 1972 Phys.Rev., $A\underline{6}$ 2180.

- J.A.R. Samson and R.B. Cairns, 1965 J.Opt.Soc.Am., $\underline{55}$ 1035.

- J.A.R. Samson, G.N. Hadded and J.L. Gardner, 1974 VUV.Rad.Phys. Edts. E.E. Koch, R. Haensel and C. Kunz, p.157.

- T.E. Sharp, 1971 Atomic Data $\underline{2}$ 119-169.

- S.M. Silvermann and E.N. Lassettre, 1964 J.Chem.Phys., $\underline{40}$ 1265.

- J.A.D. Stockdale, V.E. Andersen, A.E. Carter and L. Deleanu, 1975 J.Chem.Phys., to be published.

- R.J. Van Brunt and L.J. Kieffer, 1970 Phys.Rev., $A\underline{2}$ 1293.

- M.J. Van der Wiel and G. Wiebes, 1971 Physica, $\underline{54}$ 411.

- D. Villarejo, 1968 J.Chem.Phys., $\underline{49}$ 2523.

# SUMMARY

This thesis describes a number of experiments determining oscillator-strengths for dipole excitation by making use of the characteristics of the scattering of fast electrons. The oscillatorstrengths for absorption are obtained from the cross section for inelastic scattering at small angles. The probability for ionization and dissociative ionization are determined by measuring the scattered electrons in coincidence with the ions formed or electrons ejected.

In Chapter I measurements on He are presented and the derivation of dipole oscillatorstrengths from the differential scattering cross section is demonstrated. By taking energy loss spectra at two scattering angles, a good approximation is obtained for the derivative to the momentum transfer of the generalized oscillatorstrength at momentum transfer zero. This quantity gives information about the probability for quadrupole and hexapole excitation. The results are in excellent agreement with recent theoretical calculations.

In Chapter II $CH_4$ is studied. The oscillatorstrength distributions for the following processes have been determined:
- absorption
- ionization
- formation of low energy electrons

One of the purposes of these measurements is to establish the contribution of 'super excited' states (i.e. discrete states with an energy higher than the lowest ionization potential) to the formation of neutral fragments. The absorption and ionization spectra lead to the conclusion that the decay of super excited states by dissociation in neutral fragments is only probably a few eV above the lowest ionization potential and closely below the higher ionization potentials. The energy loss spectra for the formation of electrons ejected with low kinetic energy provide the ionization potentials and Franck-Condon envelopes of the various ion states.

In Chapter III ionization and dissociative ionization of $CH_4$ has been studied by measuring scattered electrons in coincidence with ions and ionic fragments formed. The ions have been mass selected by the difference

in time of flight. The ion extraction system has been designed such that
it is free of energy discrimination for ions with recoil energy of less
than 20 eV. The oscillatorstrength distributions for the formation of
$CH_4^+$ in the various initial states have been derived from the fragment
spectra, by assuming the validity of the Born-Oppenheimer approximation.

Information about the probability for double ionization has been
provided by measuring the two ionic fragments, resulting from the
dissociation of the unstable $CH_4^{++}$ ion, in coincidence with each other.
The difference in time of flight of the two fragment ions indicates
in which ions the doubly charged ion dissociated.

In Chapter IV measurements of the spectral behaviour of the oscillator-
strengths for absorption, ionization and dissociative ionization of $H_2$,
HD and $D_2$ are presented. The absorption spectrum is in excellent agree-
ment with the results of photoabsorption measurements. The spectra of
$H_2^+$ and $H^+$ (and the isotopes) give enough information to permit a
separation to be made of the effect of vibrational and electronic
transition moments on the ratio of $H^+/H_2^+$ for ions formed by the $1s\sigma_g$
state of $H_2^+$ ($HD^+$, $D_2^+$). The $H^+$ ($D^+$) spectra show important contributions
from autoionization, which has been discussed in terms of Rydberg
levels converging to the $2p\sigma_u$ and $2p\pi_u$ states of $H_2^+$.

# SAMENVATTING

Dit proefschrift beschrijft een aantal experimenten ter bepaling van oscillator sterkten voor dipool excitatie van molekulen door middel van de verstrooiing van snelle elektronen. De oscillator sterkte voor absorptie wordt verkregen uit de werkzame doorsnede voor inelastische verstrooiing onder kleine hoeken. De waarschijnlijkheid voor ionisatie en dissociatieve ionisatie wordt bepaald door de verstrooide elektronen in coincidentie te meten met de gevormde ionen of uitgestoten elektronen.

In hoofdstuk I worden metingen aan He beschreven en gedemonstreerd op welke wijze dipool oscillator sterkte spektra worden afgeleid uit de werkzame doorsnede. Doordat de energie verlies spektra bij twee hoeken gemeten worden kan ook een goede benadering voor de afgeleide naar de impulsoverdracht van de gegeneraliseerde oscillator sterkte bij impuls-overdracht nul verkregen worden. Deze grootheid geeft informatie over de waarschijnlijkheid voor kwadrupool en hexapool excitatie. De resultaten zijn in uitstekende overeenstemming met theoretische berekeningen.

In hoofdstuk II wordt $CH_4$ bestudeerd. Hiertoe worden de oscillator sterkte verdelingen voor de volgende processen bepaald:

- absorptie
- ionisatie
- vorming van laag energetische elektronen

Deze metingen hebben o.a. tot doel vast te stellen in hoeverre 'super geëxciteerde' toestanden (diskrete toestanden boven de laagste ionisatie potentiaal) bijdragen tot de vorming van neutrale fragmenten. Uit de absorptie en ionisatie spektra blijkt dat het verval van super geëxciteerde toestanden in neutrale fragmenten alleen waarschijnlijk is binnen enkele eV boven de laagste ionisatie potentiaal en dicht onder de ionisatie potentialen voor de vorming van aangeslagen iontoestanden. De energie verlies spektra voor de vorming van elektronen uitgestoten met lage energie (< 0,2 eV) verschaffen de ionisatie potentialen en Franck-Condon verdelingen van de verschillende iontoestanden.

In hoofdstuk III worden ionisatie en dissociative ionisatie van $CH_4$ bestudeerd door de verstrooide elektronen in coincidentie te meten

met de gevormde ionen en ion-fragmenten. De ionen worden op massa
gescheiden door hun looptijdverschil. Speciale aandacht is besteed
aan het ionen ekstraktie systeem opdat het vrij is van energie
diskriminatie voor ion fragmenten met een dissociatie energie van
minder dan 20 eV. De oscillator sterkte verdelingen voor de vorming
van $CH_4^+$ in de verschillende initieel aangeslagen toestanden kunnen
onder aanname van de Born-Oppenheimer benadering worden afgeleid
uit de spektra van de fragment-ionen. Informatie over de waarschijn-
lijkheid voor dubbele ionisatie van $CH_4$ is verkregen door de twee
fragment-ionen, die ontstaan door dissociatie van het $CH_4^{++}$ ion, met
elkaar in coincidentie te meten. Het verschil in looptijd van de
twee fragment ionen geeft aan in welke brokstukken het dubbel geladen
ion is gedissocieerd.

In hoofdstuk IV worden de metingen van het spektrale gedrag van
de dipool oscillator sterkten voor absorptie, ionisatie en disso-
ciatieve ionisatie van $H_2$, HD, en $D_2$ beschreven. Het absorptie
spektrum is in uitstekende overeenstemming met het resultaat van
fotoabsorptie metingen. De spektra van $H_2^+$ en $H^+$ geven voldoende
informatie om het effect van de vibratie en elektronen overgangs-
momenten op de verhouding $H^+/H_2^+$ te scheiden voor ionisatie naar de
$1s\sigma_g$ toestand van $H_2^+$ ($D_2^+$, $HD^+$). Uit de spektra van $H^+$ ($D^+$) blijkt dat
autoionisatie een belangrijke rol speelt bij de vorming van dit ion.
Deze processen worden bediscussieerd in relatie met de Rydberg-
toestanden die convergeren naar de $2p\sigma_u$ en $2p\pi_u$ toestanden van $H_2^+$.

# CURRICULUM VITAE EN DANKBETUIGINGEN

Na het behalen van het einddiploma HBS-B aan het St-Franciscus College te Rotterdam begon ik in september 1964 mijn studie aan de Rijksuniversiteit te Leiden. Het candidaatsexamen in de Natuur- en Wiskunde met bijvak Scheikunde legde ik in juni 1969 af. Mijn studie werd voortgezet bij de afdeling theoretisch organische chemie van wijlen Prof.Dr. L.J. Oosterhoff. In dienst van deze afdeling bestudeerde ik samen met Dr. F.W.E. Knoop optisch verboden aangeslagen toestanden van molekulen door middel van de verstrooiing van laag energetische elektronen. Dit onderzoek werd verricht onder leiding van Dr. A.J.H. Boerboom op het F.O.M.-Instituut te Amsterdam. Het doctoraalexamen in de experimentele natuurkunde met bijvakken klassieke mechanica en theoretisch organische chemie legde ik in september 1971 af. Hierna begon ik in dienst van het F.O.M.-Instituut onder leiding van Dr. M.J. Van der Wiel aan het onderzoek dat resulteerde in dit proefschrift. Sedert mei 1975 ben ik verbonden aan het European Space Research and Technology Centre te Noordwijk.

een uitstekend stuk werk geleverd. H. ten Horst en T. Van der Houw
nagen altijd kans elektronische problemen binnen korte tijd op te
lossen. De bereiding van dit proefschrift was in goede handen bij
mevrouw M. Veldhuizen, die het typewerk verrichte, F.L. Monteria
en Th. van Dijk, die het fotografisch werk verzorgden, mevrouw
M.M. Turhana-Cabanas, die de figuren tekende en M.A. Okhuizen die
dit proefschrift drukte.

I

S T E L L I N G E N

*bij het proefschrift*

DIPOLE EXCITATION

AND

FRAGMENTATION

OF

$H_2$, HD, $D_2$, and $CH_4$.

*door*

*C. Backx*

*Leiden, 12 november 1975.*

# I

De bewering van Lichte en Skogerboe, dat het micro-
golf geïnduceerde plasma een minder gevoelige methode
is dan het inductief gekoppelde plasma voor optische
detectie van spoorelementen in het geval van metalen
die stabiele monoxides vormen, lijkt voorbarig.

*B. Rosen, "Spectroscopic data relative to dia-
tomic molecules", Pergamon Press (1970).
F.E. Lichte en R.K. Skogerboe, Anal. Chem. 45,
2 (1973).*

# II

De in dit proefschrift beschreven methode voor het
meten van optische oscillator sterkten voor ionisatie
kan ook toegepast worden op dubbele ionizatie van mole-
kulen, waarvan het dubbel geladen ion instabiel is.
Daartoe kan het resulterende ionenpaar in drievoudige
coïncidentie worden gemeten met het verstrooide primaire
elektron.

*Dit proefschrift, hoofdstuk 3.*

# III

In de literatuur is onvoldoende vermeld dat de ener-
gie-resolutie van een "Retarding Potential Difference"
(R.P.D.) elektronenkanon bedreven in een axiaal magneet-
veld, zoals gebruikelijk in de "Trapped Electron Method"
(T.E.M.) beperkt wordt door de temperatuur van de gloei-
draad.

*R.E. Fox, W.M. Hickam, D.J. Grove en T. Kjeldaas,
Rev. Sci. Instr. 26, 1101 (1955).
G.J. Schulz, Phys. Rev. 112, 150 (1958).*

# IV

De experimentele resultaten waaruit Hartfuss conclu-
deert dat het inductieve effect op intersystem-crossing
belangrijker is dan het verschil in spin-baan koppeling

in $C_6H_5Cl$ en $C_6H_5F$ zijn aanvechtbaar.

*H.J. Hartfuss, Z. Naturforschung 29a, 1489 (1974).*
*R.W.B. Pearse and A.G. Gaydon, "The Identification*
*of Molecular Spectra", Chapman and Hall Ltd.,*
*London (1965).*

V

De suggestie van Dance en Walker om het meest in-
tense signaal in het drempel elektron-impact exci-
tatie spectrum van acetyleen toe te schrijven aan
directe aanslag van een triplet-toestand ($\check{c}\ {}^3\Pi$) is
aan bedenkingen onderhevig.

*D.F. Dance en I.C. Walker, Chem. Phys. Letters 18,*
*601 (1973).*
*G.J. Schulz, Rev. Mod. Phys. 45, 378 (1973).*

VI

Metingen van de "Giant Glory" in het Na-J systeem
zal bijzonder veel informatie verschaffen over de
exacte vorm van de adiabatische potentiaal rond het
kruisingspunt.

*Yu.N. Demkov en J. Los, Phys. Letters 46A, 1 (1973)*

VII

Dat aanslag naar de ${}^3B_2$ toestand in pyridine wel en
naar de overeenkomstige ${}^3B_{2u}$ toestand van benzeen
(5.4 eV) niet wordt waargenomen in drempel elektron-
impact spectra, kan verklaard worden door de aanwezig-
heid van een "shape"-resonantie in pyridine bij 5.5 eV.

*E.H. van Veen en F.L. Plantenga, Chem. Phys. Letters*
*30, 28 (1975).*
*R. Azria en G.J. Schulz, J. Chem. Phys. 62, 573*
*(1975)*

# VIII

Voor een kwantitatieve detectie van ionen afkomstig van een dissociatief ionisatieproces, verdient de "time of flight" massaspectrometer de voorkeur boven de conventionele magnetische massaspectrometer.

*Dit proefschrift, hoofdstuk II, III.*

*C. Backx*        *Leiden, 12 november 1975.*

Errata:

page 78    .... are discussed in section 3 ......... Read: section 2

  "   84    .... In section 4.2 reasons are given ... Read: section 3.3

  "   84    .... are quoted in section 4.2  ......... Read: section 3.3

  "   90    .... (see section 4.5) .................. Read: section 3.5

  "   94    .... (see section 4.6) .................. Read: section 3.6